2015

Autonomous Small Scale Data-logger for Temperature Mapping

Ahmed Gamal Eldin Tawfik

Autonomous Small Scale Data-logger for Temperature Mapping

by

Ahmed G. Tawfik

A thesis submitted to the School of Engineering

in partial fulfillment of the requirements for the degree of

Master of Science in Electrical Engineering

UNIVERSITY OF NORTH FLORIDA

COLLEGE OF COMPUTING, ENGINEERING AND CONSTRUCTION

July 2015

The Thesis of Ahmed Tawfik is approved: (Date)

_____ _____
Dr. Juan Aceros

_____ _____
Dr. Brian Kopp

_____ _____
Dr. Patrick Kreidl

_____ _____
Dr. John Nuszkowski

Accepted for the School of Engineering:

_____ _____
Dr. Murat Tiryakioglu
Director of the School of Engineering

Accepted for the College of Computing, Engineering and Construction:

_____ _____
Dr. Mark A. Tumeo
Dean of the College of Computing, Engineering and Construction

Accepted for the University:

_____ _____
Dr. John Kantner
Dean of the Graduate School

ACKNOWLEDGMENTS

I would like to thank my committee members, Dr. Kopp, Dr. Kreidl, and Dr. Nuszkowski for their continuous support and guidance through the entire duration of my masters. I wouldn't have been able to reach this achievement without their insight and experience.

A special thanks to the committee chair and my supervisor, Dr. Aceros. He has been a true support and a great assistance for every step I have taken. I was able to proceed and succeed in this work because of his great support and wide experience.

I would like to thank Olga Kostrubsky and Chuck Hood at Vistakon (a division of Johnson & Johnson Vision Care, Inc) for their support and assistance towards the success of this work.

TABLE OF CONTENTS

LIST OF FIGURES

LIST OF TABLES

ABSTRACT

Modern manufacturing processes require minimal human intervention and a high degree of automation to meet industry demands. Due to variability in industrial process conditions, custom systems are often sought for these applications. These systems must be compact, economical, and capable of operating under different environmental conditions. This work presents the development, fabrication, testing, and validation of a low cost small scale temperature data-logger used as a monitoring system for automated applications. The proposed system is battery powered and packaged in a manner able to operate in temperatures up to 100^{o}C, with exposure to chemicals such as Isopropyl Alcohol, Propylene Glycol, and De-Ionized water for a period of 2 hours with accuracy of ±0.5^{o}C. The hydration process used for contact lens manufacturing is proposed as a target application for the developed system.

The developed system was bench top tested and validated using a convection oven and the three chemicals Propylene Glycol, Isopropyl Alcohol, and De-ionized Water. In addition, the system was tested “in-situ” in the hydration lines of a contact lens manufacturing process. The development process illustrated in this work including the system design, fabrication, and testing can be used as a base to develop the “best fit” monitoring system for multiple other applications.

Chapter 1: Introduction

Advanced manufacturing processes rely on minimum human intervention and a high degree of process automation. These processes require continuous accurate monitoring to ensure meeting industry standards and achieving the desired goals. The nature of these processes includes operation in heated environments, pressure exposure, or exposure to hazardous chemicals, all of which affect the operation and the accuracy of the monitoring systems. In addition, the high precision and spatial resolution of these processes require that the monitoring systems be compact and economical. Accurate, reliable, repeatable, and reproducible sensors to operate in these particular environments are required.

Temperature monitoring presents an example of a key parameter for most manufacturing processes. The ability of the monitoring system to operate in heated environments is an important aspect for manufacturing process monitoring. In this work, the development of a monitoring system for an automated manufacturing process is presented, with the temperature measurement of the hydration process in contact lens manufacturing as the target application. This chapter discusses the background on monitoring systems in automated manufacturing, specific objectives and requirements of this research, and the target application in this work.

1-1- Importance of this Work

Monitoring automated process ensures the preservation of materials and the energy efficiency of the process. Temperature is considered one of the most important conditions affecting automated processes. Accurate temperature monitoring can confirm design predictions and operating performance, improve energy efficiency, and increase the lifespan of both the materials and the components [1]. Different technologies and techniques can be used in monitoring applications involving unusual conditions. These technologies and techniques are chosen based on their attractive features, extended range of operating temperature, low power, high speed and low sensitivity to the surrounding environment. The monitoring systems must meet stringent conditions specific to the target application such as heated surroundings, humidity exposure, limited size, or hazardous surrounding environment.

The economic advantage of a new technology added to an industry is considered as one of the main criteria for implementing this specific technology into operation [2]. The implementing of the advanced monitoring systems into the manufacturing process is limited by their economic advantage to certain industries due to the unique conditions of these industries. The monitoring system implemented in a production process should meet the stringent operation conditions, while ensuring technical and economic benefits.

This project focuses on developing a platform for automated systems monitoring. The platform should be small in size for suitable implementation in different industries, economical to meet the stringent requirements and conditions of different industries, and characterized by a high degree of accuracy to ensure reliable monitoring. The

system is engineered to operate in any domestic applications or in compliance with most common industries such as petrochemical, pharmaceutical, beverages, or consumer products.

1-2- Literature Review

Manufacturing techniques are changing dramatically due to continuous competition in the industry and rapid advancements in automation and robotics. Manufacturing industries integrate advanced technologies and automation into the production process to improve the effectiveness of the manufacturing personnel, which improves the effectiveness of the overall operation. Process automation reduces the workers' focus on simple and time consuming tasks, to increase their focus on achieving higher levels of productivity [3]. Temperature is one of the most essential parameters to sense in any automated manufacturing process [4]. Early detection of temperatures higher than safe values is important to prevent system or product failure, while lack of temperature control can ultimately lead to production loss [4],[5]. The use of temperature monitoring systems in unusual environmental conditions, such as heated or humid environments or hazardous chemicals exposure, is limited to a high degree by the temperature constraints of the electronics that must accompany the sensing element [6]. The monitoring systems and its associated electronics must be robust and protected from the surrounding environment's effects to be able to operate properly [7].

Monitoring environmental parameters, which is essential for the success of any industry, is a tedious process. The monitoring process of these parameters should be automated to improve its reliability and accuracy [4]. Autonomous sensors and effectors which are

used in any industry help in monitoring the process for control purposes, and preventative maintenance and repair. Automation technologies applied to any industry must be selected for their ease in transferring to the industry environment, offering the greatest return for the least effort, improving the system's capability, and integrating well with the system [3]. Advanced process control aims to achieve technology leadership and cost effectiveness [8]. Most of the work conducted on monitoring environmental conditions to improve the performance of advanced processes had less consideration and focus on the application side and implementation in industrial environment [4].

Multiple monitoring systems have been developed using different approaches which are capable of operating in environmental conditions specific to their target application. Tortissier et al., 2011, developed a wireless chemical detection platform capable of operating inside heated environments using an acoustic device and radio frequency linkage. In their work, Tortissier et al, reported the challenges faced during developing the chemical detection platform as choosing suitable target temperature compatible materials, designing the proper transducing part, designing safe packaging, designing a wireless link for real-time remote sensing, and designing a dedicated experimental setup which often requires bulky and costly equipment. These challenges are considered as the common challenges faced in developing a monitoring system for heated environments. The first repeatability and stability investigation of the system demonstrated the reproducibility of the developed system [9]. In the work conducted by Boufouss et al., 2013, a CMOS voltage reference circuit was designed to handle the heated environments present in biomedical applications. The voltage reference circuit was designed using partially-depleted (PD) Silicon-on-Insulator (SOI) technology. This

technology is suitable for harsh environments applications due to its extended range of operating temperature and low sensitivity to surrounding environment [10].

In another work, Tangirala et al, 2008, developed a battery powered hand-held programmable-logic-device (PLD) based temperature and Relative Humidity (RH) sensing platform. The platform served as a universal platform for sensing temperature and RH in multiple applications to reduce product defects and improve worker productivity and efficiency. The developed platform was composed of commercially available temperature and RH sensors combined with PLD technology Integrated Circuit (IC) chip. The PLD technology was chosen for this platform to develop a universal platform that could be used for multiple applications. The platform design focused on reducing power consumption and the area occupied by reducing the amount of hardware used. Sensing the equilibrium moisture content of wood was chosen as an illustrative application for the developed platform to validate its operation. The developed system was powered by a 5V battery [11].

Another autonomous sensor system was developed by Dalola et al, 2009, which focused on contactless initializing, and utilizing the locally available energy for powering. The developed system was composed of low-power electronics for radio frequency (RF) communication and power-harvesting. The system contained an external unit which was responsible for reading the data previously monitored by the system. Measuring the temperature of the walled-in pipes was chosen as a target application for the developed system. The system had a data rate of one reading every two seconds with accuracy of $\pm 1.5^{o}C$. The developed system is a useful instrument for domestic and industrial temperature measuring for efficiency evaluation [12]. In an effort to achieve a small

volume temperature and humidity monitoring system, Jingwei et al., 2009, discussed the design of a temperature and humidity real-time detector. The detector had a simple circuit which utilized a digital temperature sensor to monitor temperature range from -55^{o}C to +125^{o}C with resolution ±0.1^{o}C. The simulated results showed the monitoring and alarming capabilities of the detector with error less than ±0.3% [13].

The process of developing an accurate and reliable temperature monitoring system requires choosing an applicable temperature sensing technique. There are multiple approaches to measure temperature based on the physical phenomena being sensed. Different temperature sensing instruments were reported by Doebelin, 1990, such as bimetallic thermometers which sense the thermal expansion phenomenon, thermocouples which are thermoelectric sensors sensing voltage difference between two junctions as an indicator of temperature change, resistance thermometers which sense electrical resistance, and digital thermometers which combines the thermometers' phenomenon with advancements in technology. The Resistance Temperature Detector (RTD) and thermocouple are among the most widely used temperature measurement instruments. With the recent development in digital signal processing, many applications are relying on digital sensors for temperature measurements. The digital thermometers are less time-consuming and less prone to errors due to the reduction of the external conversions required [14]. Each of these devices has its own advantages which make it suitable for certain applications.

1-3- Problem Statement

Due to the expansion of automated systems, a monitoring system platform able to operate in different environments and conditions is required. The new platform should be able to meet different industries' unique requirements including size, accuracy, and economical advantage to be suitable for implementation in different applications.

1-4- Target Application

The hydration process as a stage of contact lens manufacturing is chosen as the target application for testing and validating the developed system. The system requirements and specifications were identified based on this application. Contact lenses are manufactured in an initial hard form, which goes through a hydration stage to reach its final soft form before packaging. The product is hydrated using one or more of three different chemicals based on the material used in manufacturing and the type of contact lens produced. The product goes through three hydration stages inside three different towers, using different chemicals heated at different temperatures in each tower. The three chemicals used during the hydration process are propylene glycol (PG), isopropyl alcohol (IPA), and de-ionized water heated at temperature 85-90^{o}C, 63-67^{o}C, and 88-92^{o}C respectively.

The contact lenses are manufactured inside a special tray to convey the product through different stages of the production process. Each tray consists of a number of contact lens holders which can carry four contact lenses. Figure 1 shows the contact lens holder composed of four cavities to carry the contact lens inside each cavity; figure 2 shows a holder tray composed of two contact lens holders.

When the contact lens tray reaches the hydration stage, it goes through the three hydration towers consecutively. In each tower the tray moves up the tower for duration of about 20-30 minutes before it is transported to the bottom of the following tower. Figure 3 shows an illustrative diagram of the movement of the contact lens tray between the three towers through the hydration process. The contact lenses are exposed to certain chemicals which are dispensed from the dispensing nozzles inside each tower for its entire duration. The dispensing nozzle heads are located at the top of each tower to distribute the chemicals inside the tower. The nozzle heads are designed to fit over each cavity inside the tray at the top of the hydration tower to ensure the complete hydration of each contact lens. Figure 4 shows the chemicals' dispensing nozzle and its orientation with the contact lens tray. The hydration process lasts for a period of about one and a half hours, which might slightly increase due to emergency or inspection stops.

The temperature inside the hydration towers should stay within the allowed limits to ensure the quality of the product and its compliance with industry standards. Currently, the temperature inside the hydration tower is monitored based on each chemical's temperature at the insertion head into the towers. Mapping the hydration tower's temperature at different locations from the bottom to the top of the tower will help in the standardization process for the tower's set up, as well as provide opportunities for improvements [15]. Standard commercial temperature data-loggers are not suitable for this application due to the size limitations and the surrounding environment effects. A small size temperature data-logger is required to monitor the temperature inside the hydration towers without affecting the hydration process. The data-logger should be

battery powered and able to operate in heated environments while exposed to certain chemicals.

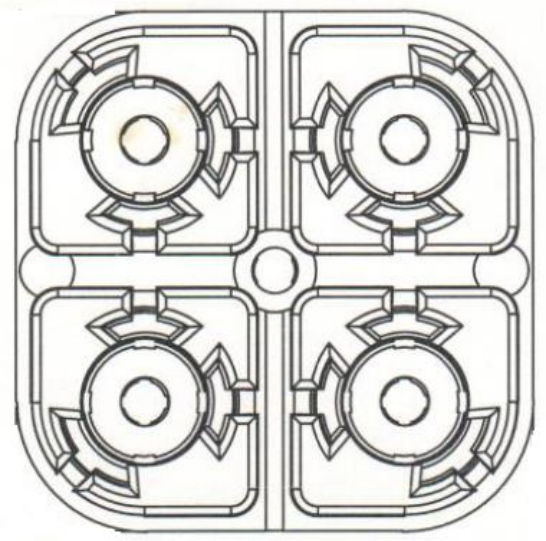

Figure 1: Contact Lens Holder [15]

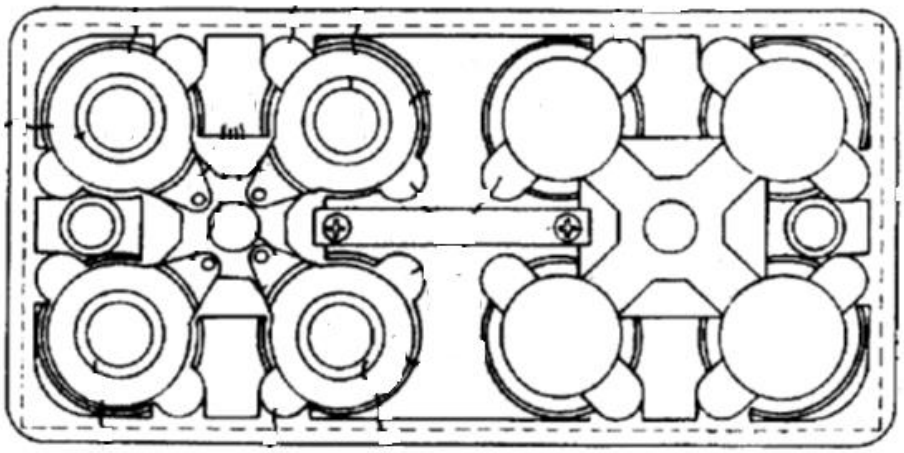

Figure 2: Contact Lens Holder Tray [16]

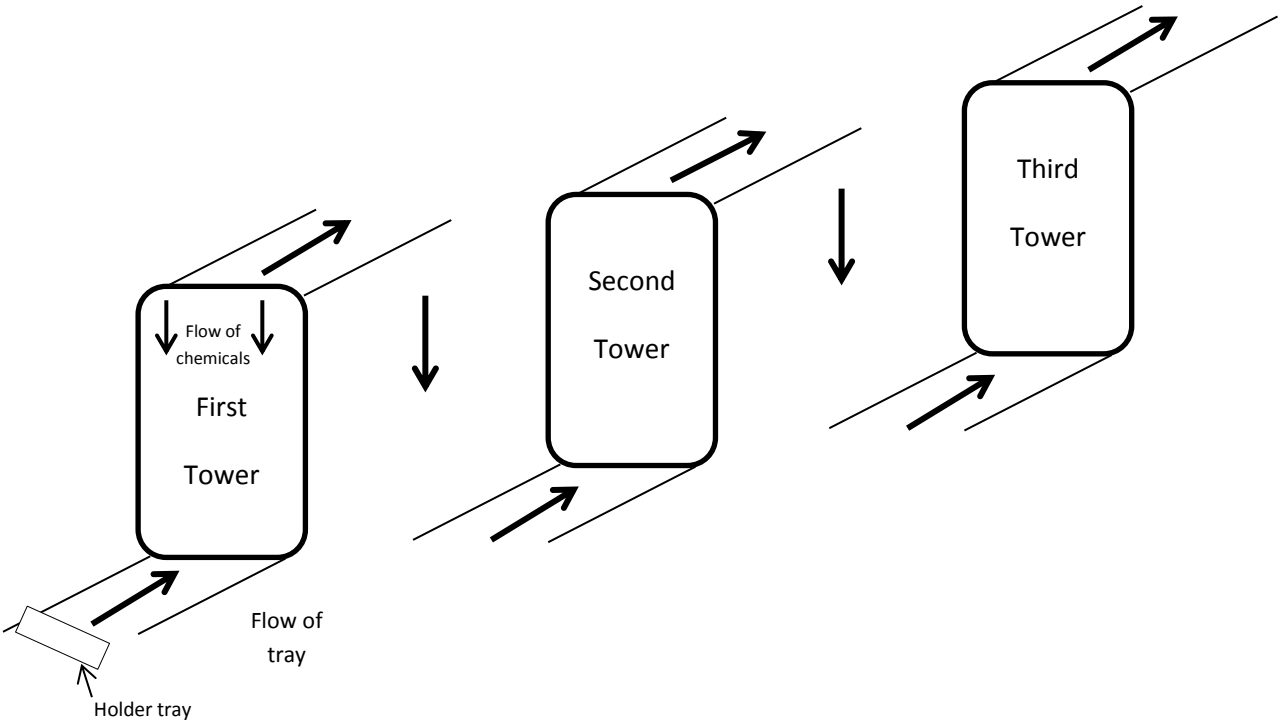

Figure 3: Hydration Process

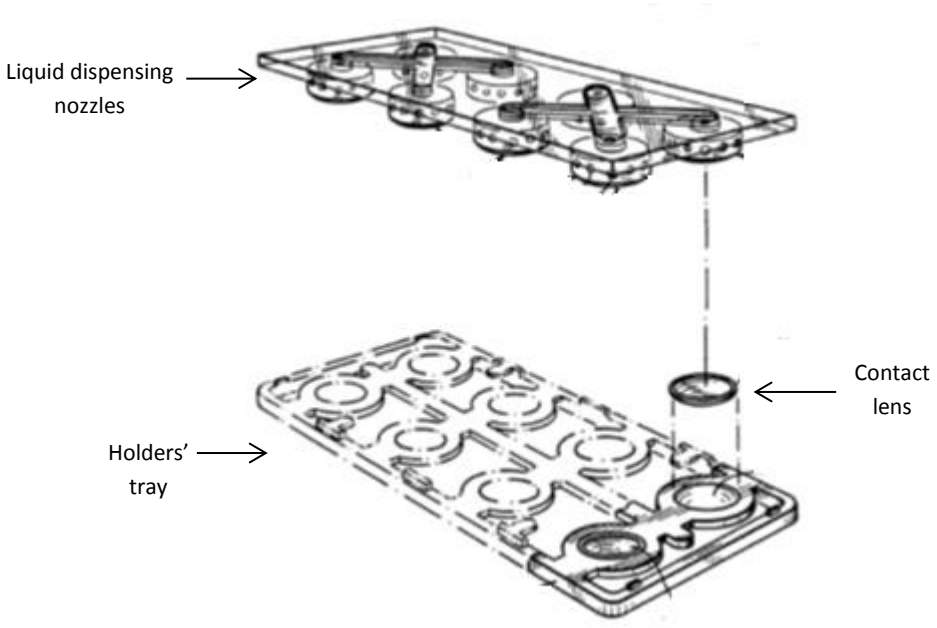

Figure 4: Dispensing Liquid Nozzle Head Orientation with Holders Tray [17]

1-5- Requirements

The requirements of the system are based on the operation of the hydration process of contact lens manufacturing. The requirements are:

1- Size: The overall size of the data-logger represents the main requirement of the system. The size of the data-logger should be suitable for its implementation into the production line without affecting its operation. In order for the developed system to be implemented inside the holder tray and to observe the temperature accurately, the system must be applied inside the contact lens holder. Only one suitable location for implementing the system was allowed to avoid its effect on the contact lenses inside the holder or the operation of the hydration tower, especially the liquid dispensing nozzle. The location allowed is at the middle of the holder, which requires the machining of the holder by milling the center to allow the implementation of the system. The size of the system must be 16x16x6mm to allow its implementation inside the contact lens holder. Figure 5 shows the location of the data-logger inside the contact lens holder.

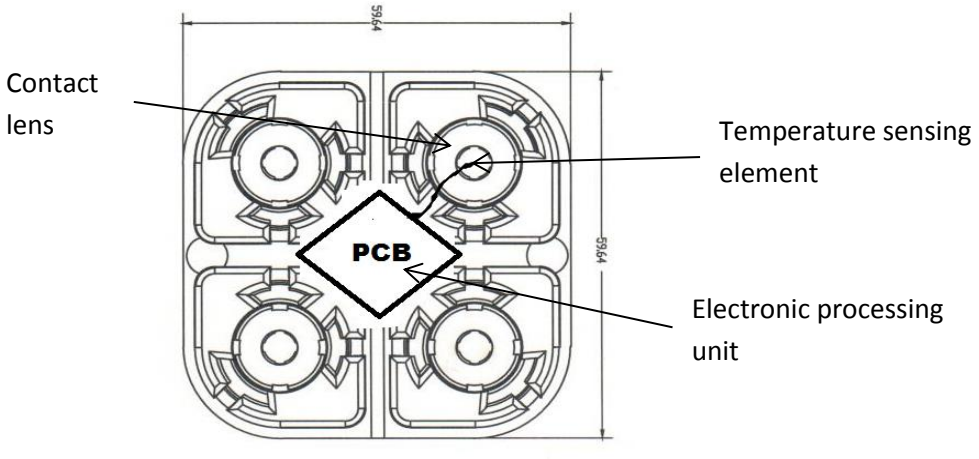

Figure 5: Data-logger Orientation inside Contact Lens Holder

2- Economical: The overall cost of the system is considered a high priority requirement for the system. The system should be cost effective to be easily duplicated for several uses at different locations. The system should be developed entirely from off-the-shelf, available commercial electronics and components. The estimated overall cost of the system should be less than $50.

3- Temperature range: The data-logger should be able to monitor temperature above the highest temperature inside the tower to ensure monitoring the entire temperature range. Since de-ionized water has the highest temperature inside the towers, among all the other chemicals, which reaches 92^{o}C, the system should be able to record temperature over this value. The developed data-logger temperature range must extend from room temperature (23^{o}C) up to 100^{o}C to be able to monitor the entire temperature range inside the hydration tower.

4- Duration: The data-logger should be able to operate for the duration of two hours to ensure monitoring the temperature during the entire hydration process including any emergency or maintenance stops.

5- Chemical exposure: The data-logger should be able to operate in exposure to the chemicals and liquids used inside the hydration towers (propylene glycol, isopropyl alcohol, and de-ionized water). The data-logger operation should not be altered due to the exposure to these chemicals and liquids, and its readings should stay consistent and reliable.

6- Power efficient: The data-logger should be self-powered to be able to operate reliably inside the hydration towers without any external connections. The data-

logger design should ensure enough power supply for the system to provide accurate readings for the entire duration of two hours.

7- Accuracy and data rate: The data-logger should be able to monitor and record the changes in temperature accurately. To ensure the accurate monitoring of temperature inside the hydration towers, the data rate for temperature readings should be one reading per second (1 Hz). The accuracy of the data-logger should be as low as ±0.1^{o}C to reflect the difference in temperature between different locations inside the hydration tower.

Table 1 summarizes the requirements of the developed system arranged in their order of priority in the system design and their weight in affecting the components choice.

Table 1: Developed Data-logger Requirements

Parameter	Requirement
Size	16x16x6mm
Overall cost	Less than $50
Readings range	23^{o}C – 100^{o}C
Duration	2 hours
Exposure	Heated chemicals such as PG, IPA, and de-ionized water
Power	Battery powered
Data rate / Accuracy	One reading per second / ±0.1^{o}C

1-6- Thesis Objective

Design, fabricate and test an economical, autonomous small-scale temperature data-logger capable of working in temperatures from 23^{o}C up to 100^{o}C with ±0.1^{o}C accuracy in exposure to different chemicals for a period up to 2 hours. The system should be easy to implement and simple to duplicate.

Chapter 2: System Design and Testing Protocol

This chapter discusses the steps taken to develop the system, which are the subsystems' design, selection of system operation mechanism, signal processing techniques, and system packaging. The system design is focused on developing, integrating, and fabricating the required functional blocks, which form the system, in addition to choosing the components and electronics to achieve the parameters required for the developed system. The characterization of the system, and the setup used for the system's testing and verification are discussed in this chapter.

The design of the temperature monitoring system included several challenging steps:

1- Designing the required functional blocks and choosing suitable compatible electronics and components to achieve the size and cost required
2- Choosing a suitable power source for the system
3- Configuring the interface between the system and the end user
4- Developing the system's operation concepts for reliable performance
5- Designing the system's circuit to achieve the required size
6- Designing the correct packaging which enables safe and accurate operation
7- Achieving the required accuracy of the system
8- Designing a dedicated experimental setup for testing and validation

2-1- System Description

The system is composed of a number of functional blocks responsible for different operations which ensures meeting the requirements of the system. The system is composed of two subsystems, the data-logger and the external unit, each is responsible for a specific process. The data-logger, which is referred to as the “device” in the rest of this document, is responsible for monitoring and recording the temperature. The external unit is responsible for providing the required interface between the device and the end user for data retrieving and displaying. Figure 6 shows the required functional blocks of the system and their integration.

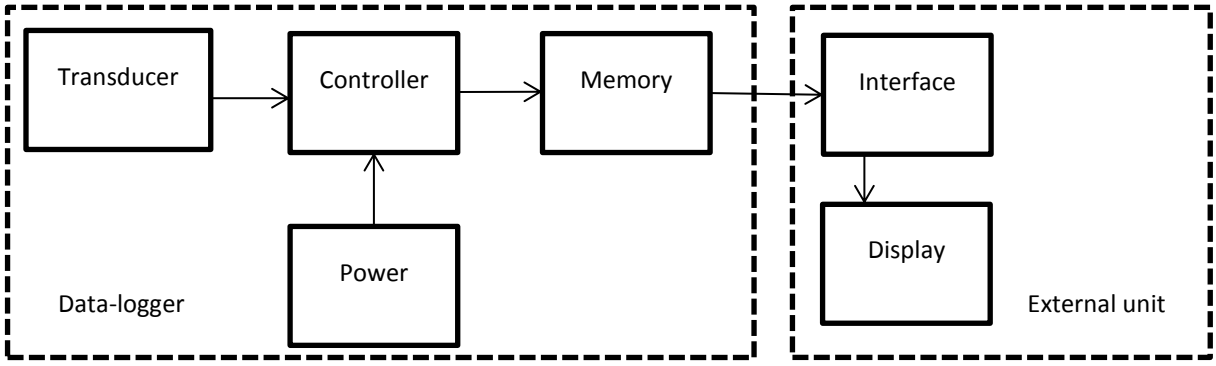

Figure 6: System’s Functional Blocks Diagram

The required functional blocks of the system are:

1- Controller: The main block of the system responsible for establishing the proper communication and synchronization between the different system components. The controller’s main function is collecting the data from the sensing element, applying the required conversions to the data, and sending the data to the memory.

2- Transducer: The sensing element of the system which is able to sense change in a physical phenomenon that represents the change in temperature.
3- Memory: The storage unit where the readings can be stored during the operation of the data-logger until retrieved by the end user at the end of its cycle.
4- Power: The power source which is able to provide the required power supply for accurate and reliable operation of the system during its intended duration.
5- Interface: The external unit which is able to provide the linkage between the system and the end user. The interface unit should be responsible for controlling the system during the retrieval of the readings from the system.
6- Display: The final stage of the system's operation where the data can be represented to the end user. The data representation should be user friendly and easy to interpret.

Selecting suitable electronics for the system is considered a significant challenge to ensure the required parameters are met, in particular the size and the temperature requirements. Components required for each functional block are chosen based on the factors affecting their function on the system. The required electronics are selected based on the following criteria:

1. Controller unit: Many factors affect the operation of the microcontroller and its suitability for the requirements of the system. The microcontroller selection is affected by the high priority requirements of the system, which are the size, economical advantage, temperature range, and power consumption. The microcontroller temperature rating must be higher than the maximum temperature rating of the system to guarantee proper operation during the entire

temperature range. The microcontroller chosen should have a low price to reduce the overall cost of the system. The overall power consumption of the microcontroller to perform the required operations should be as low as possible to ensure the ability of the system to operate accurately through its entire duration. The data rate and accuracy requirements don't effect the microcontroller selection due to its lower priority, while chemical exposure, and operation duration requirements don't play a significant role in the selection process of the microcontroller, due to the small effect of the microcontroller on these requirements. Multiple microcontrollers were considered for the system due to the combination of its size, which is less than 16x16mm, its temperature rating, which is higher than or close to 100^{o}C, and its power consumption. Table 2 shows the list of all the considered controllers.

Table 2: Controller Selection

Name	Size (mm)	Temperature rating (^{o}C)	Voltage (V)	Memory (KB)	Price ($)	Power consumption (mW)
MSP430F2012	4x4	105	1.8 – 3.6	0.256	2.7	0.4
C8051F931	4x4	85	1.8 – 3.6	64	1.6	6.3
ADuC7019	6x6	125	2.7 – 3.6	62	12.71	120
ADuC841	8x8	85	2.7 – 3.6	62	19.33	13.5
ADuc7128	9x9	125	3 – 3.6	162	13.92	135
MSP430F249	9x9	105	1.8 – 3.6	60	9.22	0.49

The ADuC7128 and the MSP430F249 ranked at the bottom of the decision matrix due to their bigger size compared to the other microcontrollers. The ADuC841 and ADuC70190 were chosen due to their relatively small size and high temperature ratings, but didn't rank at the top of the matrix due to their higher price. The C8051F391 has the smallest size among all the chosen microcontrollers, but it has a lower temperature rating than the required temperature, which affects the operation of the entire system in heated environments. The MSP430F2012 ranked at the top of the decision matrix and was chosen as the Microcontroller Unit (MCU) for the system due to its small size, high temperature rating, low power consumption, and low price.

MSP430F2012 is a Texas Instruments (TI) ultra-low power microcontroller. The architecture of the microcontroller and the five low-power modes increase the controller optimization to extend its battery life. The MSP430F2012 is suitable for sensor systems applications in which analog data is converted to digital values for storage or transfer to a host system, which is used in portable measurement applications. The device features a powerful 16-bit reduced instruction set computer (RISC)[1] controller, 16-bit memory registers, built-in communication capability using synchronous protocols - Inter-Integrated Circuit (I^2C) and Serial Peripheral Interface (SPI)[2], and a 10-bit Analog to Digital Converter (ADC). The MSP430F2012 is 4x4mm in size, has rated supply voltage between 1.8 Volts (V) and 3.6V, and an active mode current of 0.1microAmpere (μA) at 1Mega Hertz (MHz) [18].

[1] RISC is a microcontroller that can perform fewer numbers of instructions so that it can operate at a faster speed
[2] I^2C and SPI are synchronous protocols used for communication between integrated circuits

2. Temperature sensing element: The multiple approaches to measuring temperature reported by Doebelin, 1990, are studied in the temperature sensing element selection. The resistance temperature detector (RTD), thermocouples, and digital thermometers are considered for this application. The differences which played an important role in the selection decision between the RTD, thermocouple, and digital thermometer are stated in Table 3.

Table 3: Temperature Sensing Elements Comparison

Resistance Temperature Detector (RTD) [19]	Thermocouple [19]	Digital thermometer [20]
- Accurate - Linear - Stable - Repeatable - Resistance to noise - Expensive	- Fast response - Wide temperature range - Low stable	- Less off chip components - No ADC required - Fixed accuracy and resolution - High power consumption

For its stability and linearity, the RTD is the most suitable sensing element for applications which require accurate readings in low temperature ranges. A Wheatstone bridge circuit is used with the RTD to achieve higher accuracy and linear relation between resistance change and temperature change. A Wheatstone bridge circuit schematic is shown in figure 7. The relation between the bridge circuit input and output voltages, resistance, and temperature are shown in equations 1 and 2 [14].

$$E_o = (R_T/(R_T+R_4) - R_2/(R_2+R_3)) * E_{ex} \quad (1)$$

E_o is the output voltage, E_{ex} is the source voltage, R_T is the RTD resistance, R_2, R_3, and R_4 are the bridge resistors values

$$R_T = R_o * (1+ AT + BT^2) \quad (2)$$

R_T is RTD resistance, R_o is resistance at 0^oC, T is temperature, A and B are equation's constants,

for 1000Ω RTD, A= $3.81*10^{-3}$, B = $-6.02*10^{-7}$

for 100Ω RTD, A= $3.9083*10^{-3}$, B = $-5.775*10^{-7}$

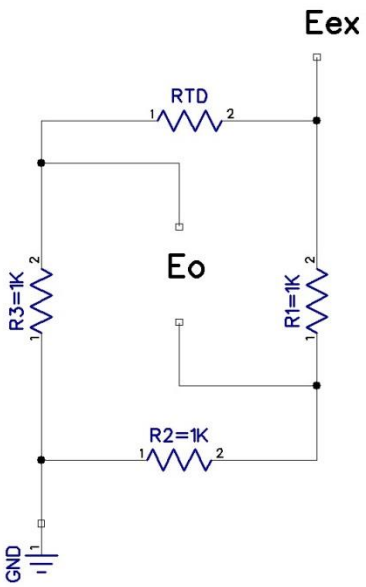

Figure 7: Wheatstone Bridge Connection

The Honeywell 700 series RTD with 1000Ω was chosen as the temperature sensing element for the developed system. The selection of this RTD was based on its small size of 2x2mm, low cost of $11, and low power consumption [21]. The RTD with a higher resistance value (1000 Ω) was chosen to decrease the

current drawn by the Wheatstone bridge which was measured to be 1.3 mA at 1.5V source voltage.

3. Memory: An external memory chip was added to the system to ensure the availability of enough memory to store the readings during the entire operation of the hydration tower. The memory chip was chosen based on its storage capabilities in addition to its temperature rating. The memory block should be able to store readings for the entire duration of two hours (total duration = 7200 seconds) with a data rate of 1 Hz. The MCU has a 10-bit ADC which stores each reading into two bytes of memory (storage per reading = 2 bytes). The minimum amount of storage required to save the temperature readings for the duration required with the required data rate is 116 kilobit (Kbit) based on the following equation:

   Total required capacity = data rate * total duration * storage per reading (3)

   Temperature strongly affects the capabilities of the memory chips. The increased temperature affects the ability of the memory register to store the data correctly, which decreases its longevity. The temperature effect is more significant on the memory chip with higher storage capacity. The capacity of memory storage should be increased to allow more temperature readings for proper signal processing, better representations of the temperature readings, and higher accuracy. The number of the samples recorded is chosen as two samples per second, which is averaged using signal processing to present one reading per second to reduce the noise effect and purify the output without violating the temperature rating of the memory chip. The minimum required

storage capacity is 2*116k bit which is 230k bit. By considering the available memory chips, the memory chip's minimum storage capacity is 256k bit. The Microchip 24AA256 memory was selected for the system due to its small size of 5x7mm with 256k bit of storage. The 24AA256 has a voltage range from 1.7V to 5.5V. This memory chip has been developed for low-power applications such as data acquisition systems. The 24AA256 has the advantage of page write[3] for up to 64 bytes of data, which allows less communication cycles and less power consumptions. The Microchip 24AA256 can be accessed through I^2C communication protocol [22].

4. Power: The power source is responsible for providing the required power for the entire duration of the system's operation. The power budget of the system was calculated based on the power requirements of each functional block and the required duration of operation of the system. The voltage required for the operation of the electronics in the system should be 2.2V with a minimum allowed voltage of 1.8V. The overall current required by the system is 1.8mA. The overall energy required by the system is 8mWh. The power for each component and the overall power requirements are presented in table 4.

[3] Page write allows sending multiple bytes of data in one cycle for faster operation

Table 4: Power Budget

	Voltage Required	Current Required
Microcontroller	2.2V	0.06mA
Memory	1.8V	0.4mA
Wheatstone Bridge	1.5V	1.3mA
Total current		1.8mA
Minimum charge		2*1.8 ≈ 4mAh
Required power	2.2V * 1.8mA = 4mW	
Minimum Energy	2 * 4mW = 8mWh	

The selection of the power source was focused on three criteria, size, power delivered, and charging capabilities. Two kinds of power sources were investigated, super capacitor and coin battery. Table 5 summarizes the differences between the considered super capacitors and coin batteries. The super capacitors are characterized by small size and high power capabilities, but low temperature rating, which is lower than the required temperature for system monitoring. The super capacitors with higher temperature rating, as in the case of the Panasonic super capacitor, have a bigger size not suitable for the required size of the system. The coin batteries are characterized by low temperature ratings similar to the super capacitors. After further consideration and discussion with the manufacturers of each component, the coin batteries proved to have higher tolerance to higher temperatures compared to the super capacitors. There are two kinds of coin batteries available, rechargeable and non-rechargeable. One battery from each kind was chosen for further testing and investigation. The

Panasonic ML series ML920 was chosen as a rechargeable coin battery due to its small size and high power capabilities. The Panasonic CR series CR1025 was chosen as a non-rechargeable battery due to its small size and high power capabilities.

Table 5: Power Source Selection

Name	Max. temperature (^{o}C)	Size (mm)	Voltage (V)	Current (mA)	Type	Price ($)
CR1025	60	10 (Diameter) 2.5 (Height)	3	30	Non-rechargeable battery	1.10
ML920	60	9 (Diameter) 2 (Height)	3	11	Rechargeable battery	2.25
RG0V244V Panasonic	85	10.5 (Diameter) 5 (Height)	3.6	20	Capacitor (0.22 F)	1.86
XH414HG SEIKO	60	4.8 (Diameter) 1.4 (Height)	3.3	33	Capacitor (0.08 F)	1.67
CPH3225A SEIKO	60	3.2x2.5	3.3	20	Capacitor chip (0.011 F)	1.76

5. Interface: The available interfaces for the communication between the memory chip and the end user are I^2C (inter-integrated circuit) and SPI (serial peripheral interface). The I^2C links more than one device on one line without a need for a selection line, requires two connection lines, provides less noise, is

inexpensively implemented, and has a communication check. The SPI cannot support more than one device on the same bus without a selection line, it requires four connection lines for the interface, provides high speed interface, and requires less power. For this application, I^2C has more advantages over SPI due to its ability to communicate using two connection lines which reduces the size of the interface subsystem. The size reduction capability of the I^2C is more important than the power reduction capabilities of the SPI due to the higher priority of the size requirement over the power requirement for this application. I^2C was chosen as the communication protocol for the system; the protocol was implemented to the communication between MCU and memory, and between the system and the end user for graphical display of the readings. Table 6 presents the comparison between the I^2C and SPI interface. The interface choice affected the final design of the system to include the required connections for the chosen interface.

Table 6: Interface Comparison

I^2C	SPI
- 2 wires connections - Can support multiple devices - Less noise - Cheaper - Message received check	- 4 wires connections - Less power - High speed

2-2- Power Source Selection

The power source represents one of the most significant functional blocks in the system. The correct choice of the power source guarantees the accurate operation of the data-logger during its entire intended duration without any disturbance or discontinuity. Two different power sources were considered for the system, rechargeable coin battery and non-rechargeable coin battery. The rechargeable battery which is Panasonic ML920, is a magnesium lithium coin battery, while the non-rechargeable battery is Panasonic CR1025, which is a magnesium dioxide lithium coin battery. The two options were studied and investigated to determine the more suitable power source for the system. The power testing for the two considered sources was conducted by connecting each battery to a load drawing power equivalent to the power drawn by the device. The two batteries were placed in a heated environment to resemble the target environment of the system. The two batteries were placed in 100^{o}C environment for duration of over four hours representing two cycles of the system's operation. The voltage delivered by each battery was recorded and plotted for the entire duration. Figure 8 shows the graphs representing the voltage curve of the two batteries over time.

The blue (lower) curve presents the voltage from the rechargeable battery. The curve showed the battery supplying initial voltage at 2.3V; the voltage increased slightly at the beginning of the first cycle due to the temperature effect on the chemistry of the battery to reach 2.4V. At the end of the first cycle, the voltage dropped to 2.3V. During the second cycle, the voltage dropped to 1.9V, which is close to the minimum voltage required by the system. The battery output voltage dropped lower than the minimum

allowed voltage after duration of about two and half cycles. The battery was charged using the settings advised by its manufacturer for duration of two hours, which increased the voltage supply of the battery to 2.2V. The battery was unable to restore its full capacity due to the effect of the temperature on its chemistry. The battery was unable to provide enough voltage higher than the threshold voltage to handle more cycles inside the system.

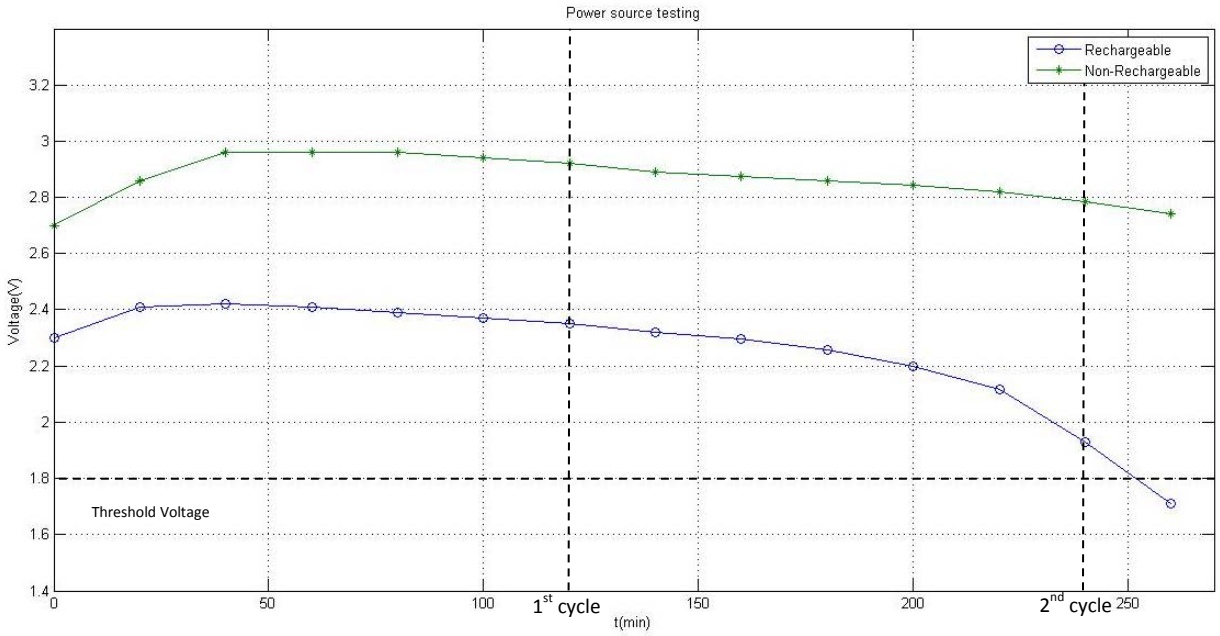

Figure 8: Testing Results for Power Source Selection

The green (higher) curve presents the voltage from the non-rechargeable battery. The curve showed the battery supplying initial voltage at 2.7V; the voltage increased slightly at the beginning of the first cycle due to the temperature effect on the chemistry of the battery to reach 2.95V. At the end of the first cycle, the voltage dropped to 2.9V. During the second cycle, the voltage dropped to 2.8V, which is much higher than the minimum voltage required by the system.

The non-rechargeable battery showed better performance than the rechargeable battery as a power source for the device. The non-rechargeable battery was able to operate the system for two complete cycles while providing a high voltage margin over the required voltage. The high voltage margin ensures the proper operation of the system and improves the consistency in the reference voltage provided to the ADC and the Wheatstone bridge, and guarantees accurate readings. The rechargeable battery was able to operate the system for two full cycles but with voltage dropping to a level close to the minimum required voltage, which affects the reference voltage in the system. The reference voltage provides a constant voltage to the Wheatstone bridge and the ADC to reduce the noise effects and improves its accuracy. The recharging capability of the rechargeable battery didn't perform as an added advantage over the non-rechargeable battery due to the operation in a heated environment, which affects the chemistry of the battery. The non-rechargeable battery was chosen as the power source for the developed system due to the better performance and the lower cost.

2-3- User Interface

A communication subsystem and power switching subsystem were added to the system for better interfacing between the system and the end user. The communication subsystem was added to provide the correct communication lines and ensure reliable interface between the data-logger and the external unit. The I^2C interface requires two communication lines, which are Serial Clock Line (SCL) and Serial Data Line (SDA)[4]. To avoid the interference between the writing process by the microcontroller and the reading process by the external unit, and to avoid overwriting the data during the data

[4] SCL is used to provide the synchronization clock, SDA is used to transfer the data

retrieving, the power source for the microcontroller was isolated from the power source from the external unit.

The I^2C communication interface is initialized by sending a control signal from the master device to the slave device. The control signal is composed of a sequence of 0 and 1 bits to synchronize the communication between the two devices followed by the address of the slave device and the type of the operation (0 for read, 1 for write). The slave device responds to the control signal by sending an acknowledgement byte to the master device. The master device sends the high byte of the address for the location on the memory chip, followed by the low byte of the address. The master device waits for an acknowledgement from the slave device after every byte sent. When the master device receives the address acknowledgement from the slave device, it sends the data bytes to be stored at the location specified which is incremented by the slave device after each byte received. After the master device sends all the data to the slave device, the master device sends a stop byte to notify the slave device to end the connection. Figure 9 shows the flow chart for the I^2C communication.

The power switching subsystem was added to the system to terminate the power consumption when the system is not in use. The switching subsystem is composed of a micro-switch along with other electronic components to isolate the power source from the entire system when not in use. The switching subsystem uses the switching capabilities of transistors and the input/output pins on the microcontroller. The switching subsystem should be reliable and easy to use and implement.

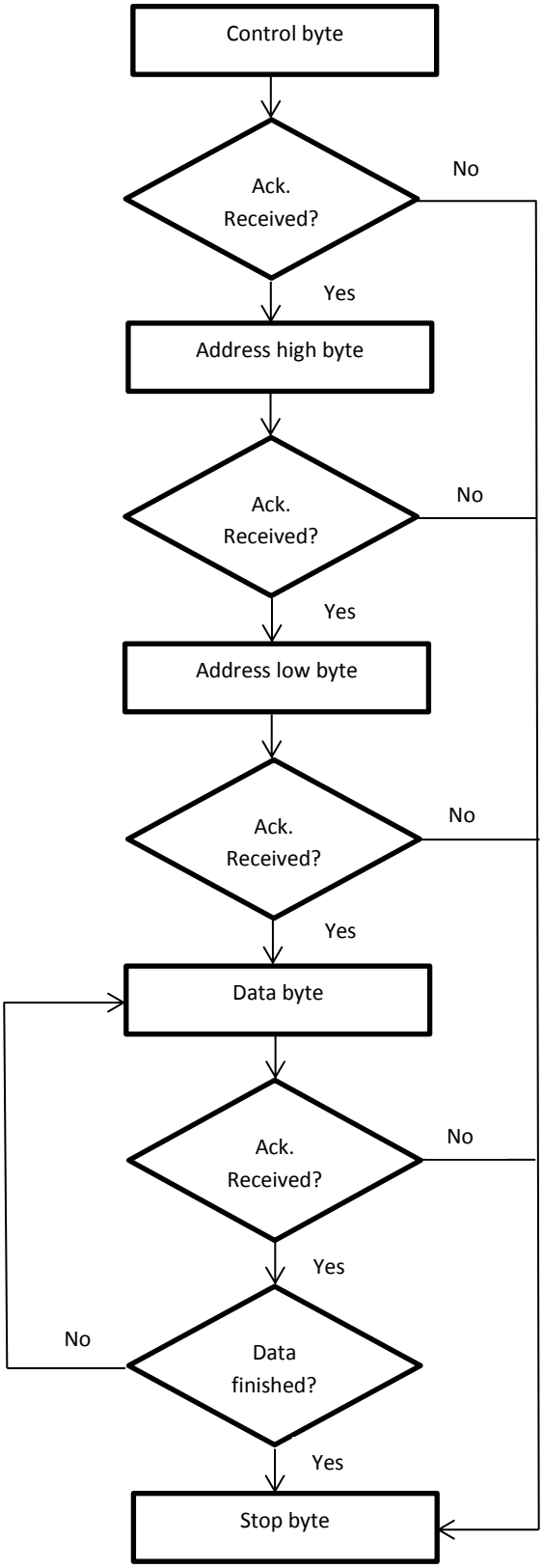

Figure 9: I^2C Interface Flow Chart

The switching circuit is composed of a mechanical (tactile) switch, two transistors, NPN and PNP, along with their biasing resistors, and two diodes. The concept of the switching circuit relies on pulling the base of the PNP transistor to the ground which turns on the PNP transistor to apply the supply voltage to the microcontroller. One output pin on the microcontroller is used to provide constant voltage when the microcontroller is turned on, which is applied to the base of the NPN transistor to turn on the NPN transistor. The NPN transistor pulls the base on the PNP transistor to the ground to keep the PNP transistor on. An input pin pulled to the positive voltage input on the microcontroller is used to detect the signal for initiating the switch off sequence which is pulled to the ground when the switch is pressed and initiates the switch off sequence. The power switching circuit schematic is presented in figure 10.

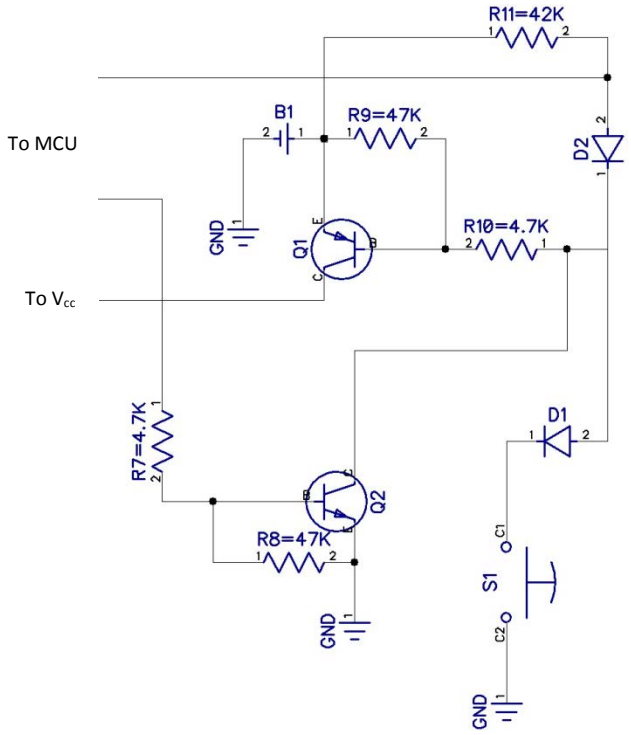

Figure 10: Power Switching Circuit

2-4- System Operation

The concept of operation of the system was designed to sense changes in a physical phenomenon due to changes in temperature, obtain these changes as analog input, convert the analog data into digital data, store the digital representation of the changes, retrieve the digital values from the storage location, and convert and process the digital values to represent the changes in temperature. The system can be switched on or off using a switching subsystem which is able to power the microcontroller to establish the link between the battery and the rest of the system and provide a constant reference voltage to the Wheatstone bridge. Each microcontroller cycle consists of several consecutive steps which are recording the voltage change in one side of the Wheatstone bridge, converting it into digital value, storing the digital value in the microcontroller RAM, and waiting for half of a second delay. The page write capability of the memory chip is used to reduce the power consumption during the communication and transfer of the data between the microcontroller and the memory chip. The memory chip has a page write of 64 bytes, which represents 32 conversions. After 32 conversions, the microcontroller initializes the I^2C communication to transfer 64 bytes to the external memory chip. The cycle of the microcontroller is repeated unless the memory chip is fully loaded. The system's operation flow chart is presented in figure 11.

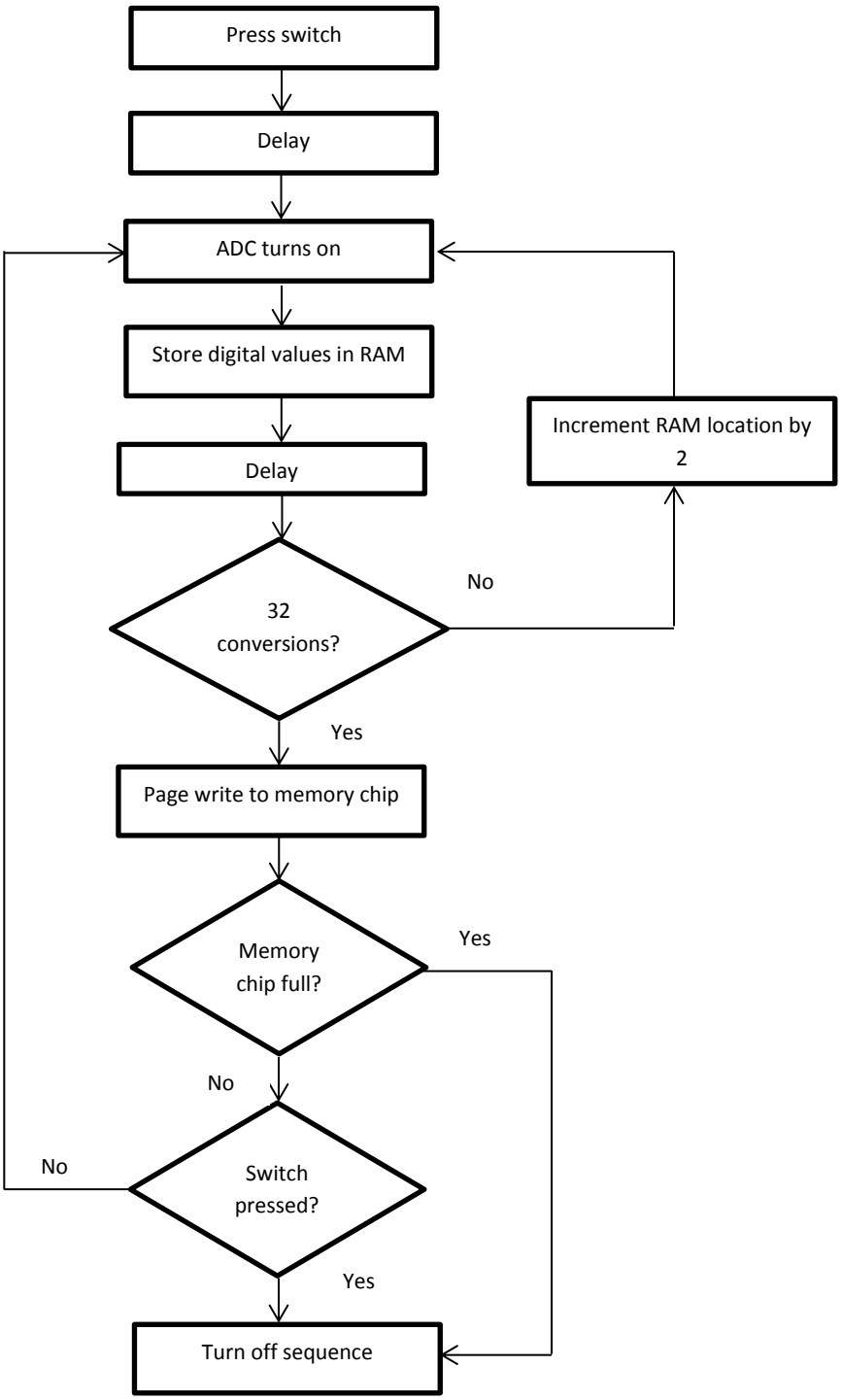

Figure 11: System's Operation Flow Chart

The system can be switched off using the switch to send a signal to the microcontroller to initialize the switching off sequence. The switch off sequence starts with a short delay, and then the microcontroller isolates the power source from the entire system which switches off all the components on the system. The switching off sequence can be initiated using the switch, and is initiated automatically when the memory chip is full, to avoid overwriting the data. The Light Emitting Diode (LED) is used to indicate the status of the system. The LED is turned on for about 1 second when the system starts, to indicate the initialization of the operation of the system. The switching off sequence flashes the LED during its delay cycle before switching off the entire system. The LED flashes with every communication cycle between the microcontroller and the memory chip to reflect the condition of the system. The microcontroller C code is presented in Appendix A.

The data can be retrieved once the system is turned off through the external unit using I^2C protocol. The external unit provides the power source to the memory chip, which is isolated from the rest of the circuit for proper communication and reliable connection. The external unit provides the clock source for the connection and opens the communication link for a total of 1024 bytes per cycle. The digital values are obtained from the memory chip in a hex decimal format which is sent to a processing software (e.g. Excel, MATLAB) to be converted to decimal values, and then converted to its analog equivalent value. The analog value represents the change in voltage at one side of the Wheatstone bridge and is used to compute the resistance value at each instance using equation 1. The temperature representation of each resistance value is computed using equation 2. The cycle is repeated until all the data in the memory is retrieved

which is equal to 32000 bytes. The data retrieving cycle flow chart through the external unit is presented in figure 12.

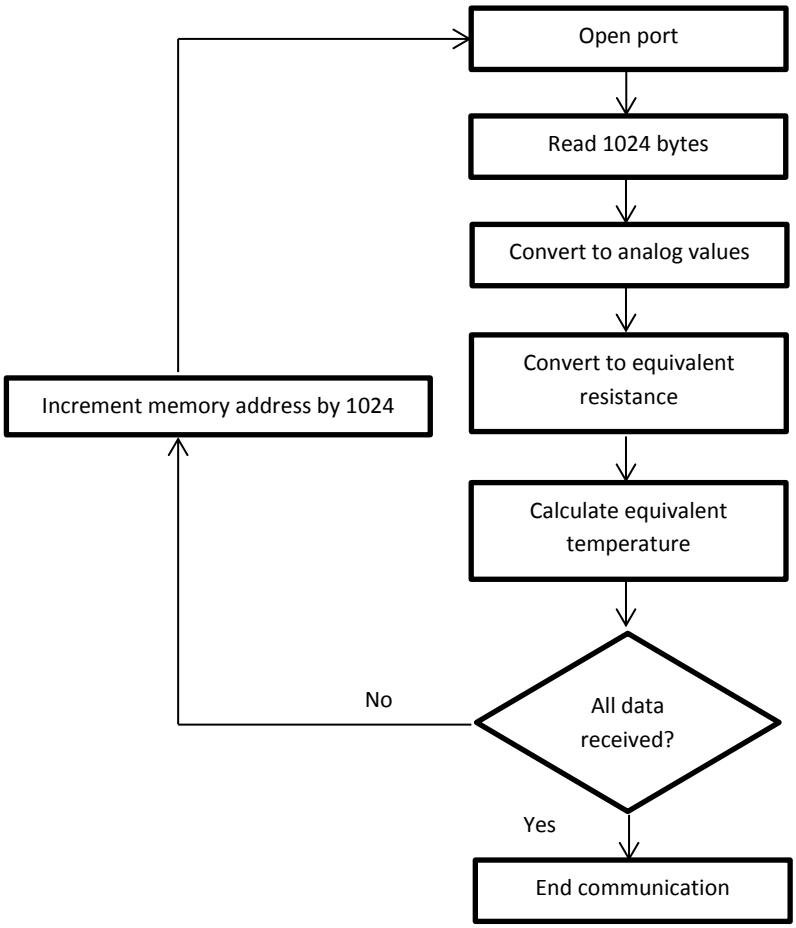

Figure 12: Data Retrieving Flow Chart

2-5- Circuit Design

The circuit design is the process of designing the proper integration between the circuit components based on the operation of the system and the components chosen. The main components of the systems were associated by electronic components which allow the proper operation of the system. The stability of the Wheatstone bridge increases as the difference between the associated resistors in the bridge decreases.

The resistors used in the Wheatstone bridge are 1 KΩ resistors, due to the use of the 1 KΩ RTD. The resistors chosen are surface mount device (SMD) resistors with a package size of 0603 to reduce the size of the Wheatstone bridge.

The switching subsystem should occupy a very limited space. For that reason, a transistor chip was used which contains a PNP transistor and a NPN transistor with the biasing resistors of value 47 KΩ and 4.7 KΩ. The ON semiconductor MUN5333DW1 transistor was used which is 2x2mm SOT−363 package. The switching off signal line had a pull up resistor of value 42 KΩ to reduce the current drawn in this line. A tactile switch was used which has a size of 3.5x0.5mm. An alternative switching mechanism was suggested which uses a magnetic reed switch instead of the tactile switch. The magnetic reed switch uses the same concept of switching using PNP and NPN transistors. The magnetic reed switch has more stable and reliable switching capabilities compared to the tactile switch. The magnetic reed switch has a higher cost compared to the tactile switch. The magnetic reed switch costs around $20 while the tactile switch costs around $1. The magnetic reed switch is suitable for applications with more mechanical contact or pressure and/or less desire for an economical device. The magnetic reed switch chosen to be considered for the device is the Redrock RR100. The Redrock RR100 has a 1.13mm^2 footprint with a wide temperature range.

The interface circuit consists of four pins for proper connection with the external unit which are V_{cc}, ground, SCL, and SDA. The interface circuit is responsible for isolating the power supply to the memory chip during the data retrieving from the microcontroller power supply. The SDA and SCL are connected to two pull-up resistors chosen as 10 KΩ to reduce the current drawn by the resistors while providing enough voltage to the

SDA and SCL lines. Table 7 shows a list of all the electronics used in the system and the purpose of each electronic component.

Table 7: System's Electronic Components

Electronics	Part chosen	Quantity	Purpose
Microcontroller	Texas Instruments MSP430F2012	1	Controlling the operation and synchronizing between different parts of the system
Memory	Microchip 24AA256	1	Data storage
RTD	Honeywell 785-701-02AAB-B00	1	Temperature sensing
1 KΩ resistor	Vishay 594-MCT0603MD1001BP1	3	Wheatstone bridge resistors
NPN and PNP Transistor	ON semiconductors MUN5333DW1T1G	1	Switching circuit transistors
42 KΩ resistor	Vishay 594-MCT0603MD4701BP1	2	One as a reset pull-up resistor on the microcontroller and the other as a pull-up resistor for the switching off signal
10 KΩ resistor	Vishay 594-MCT0603MD10001BP1	2	SDA and SCL line pull-up resistors
Switch	SKSWAHE010	1	Tactile switch for the switching circuit
LED	LOL296Q2S124Z	1	Indicating the status of the system
Diodes	BAV21WS-TP	4	Reduces the reverse power leakage
Battery	Panasonic CR1025	1	Power source for the system
Battery holder	534-3031	1	Holder for the coin battery

The system's schematic was developed to ensure the proper integration between the different functional blocks of the system and the associated components. The schematic illustrated the required connections between all the components in the system. Figure 13 shows the system's schematic diagram. The system's schematic was used to develop the printed circuit board (PCB) design. The PCB had the required dimensions of the system which is 16x16mm. The PCB's top side was used to place all the required components, while the bottom side was used for the battery connection. Figure 14 shows the top and the bottom side of the PCB. Figure 15 shows an illustrative example to demonstrate the size of the device.

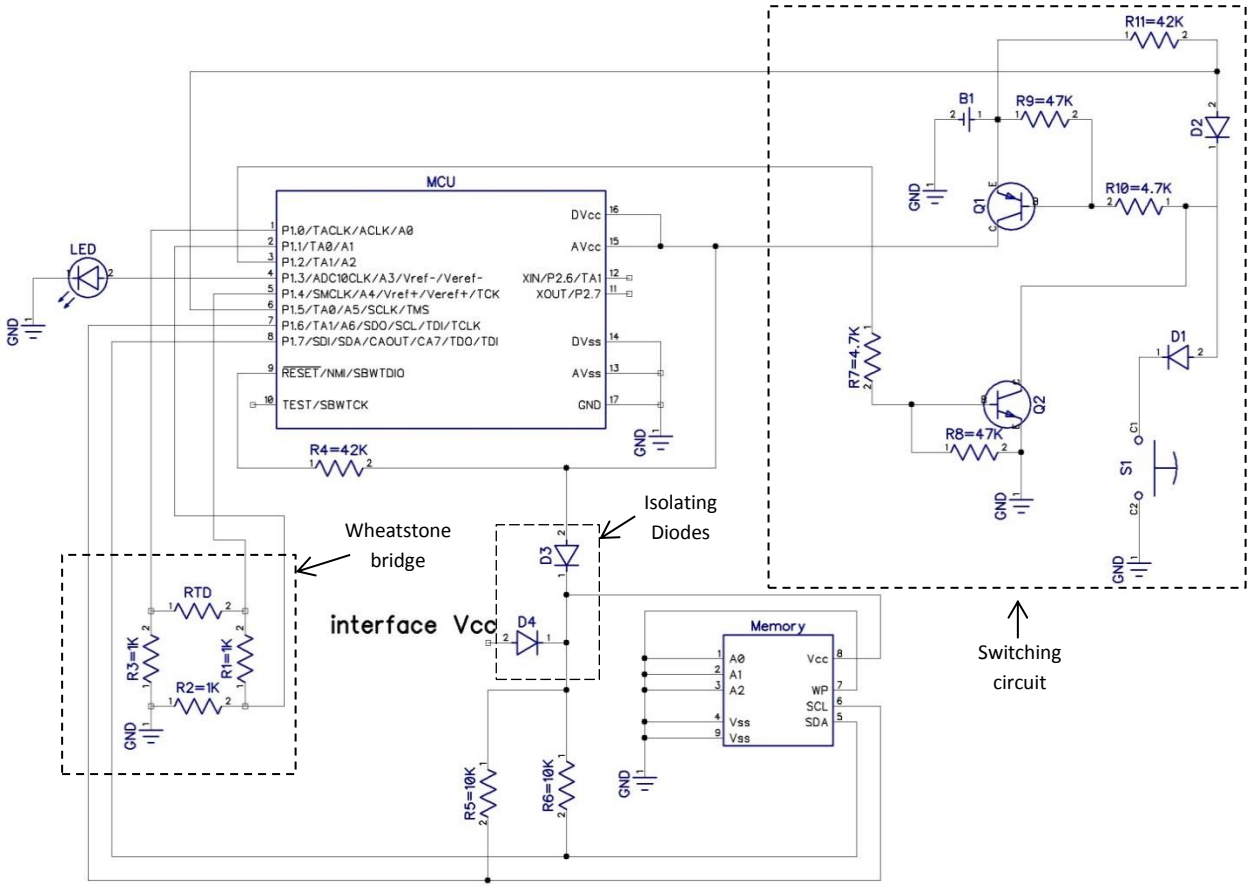

Figure 13: System Schematic

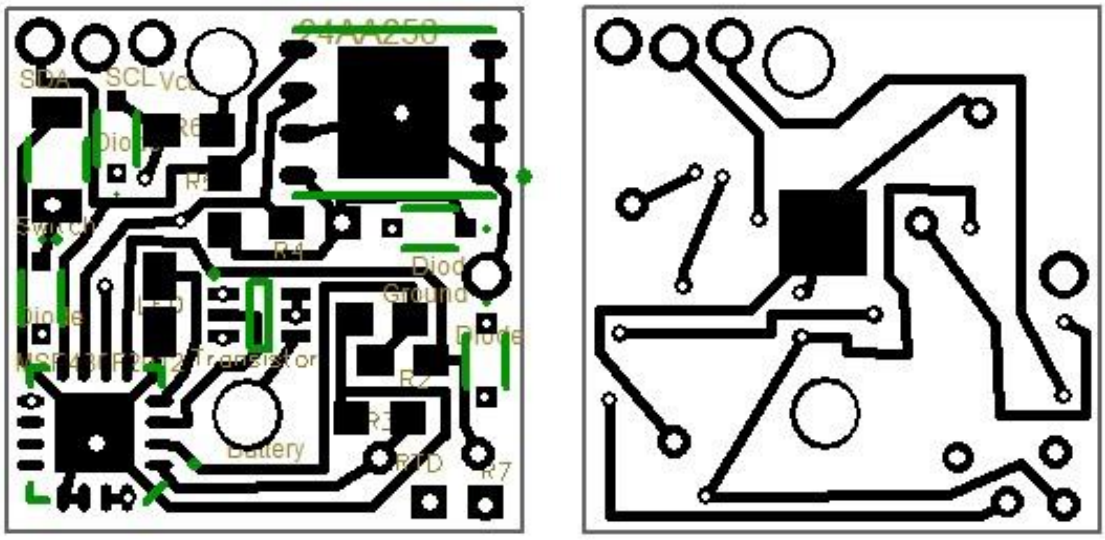

(a) (b)

Figure 14: PCB Design (a) Top Side (b) Bottom Side

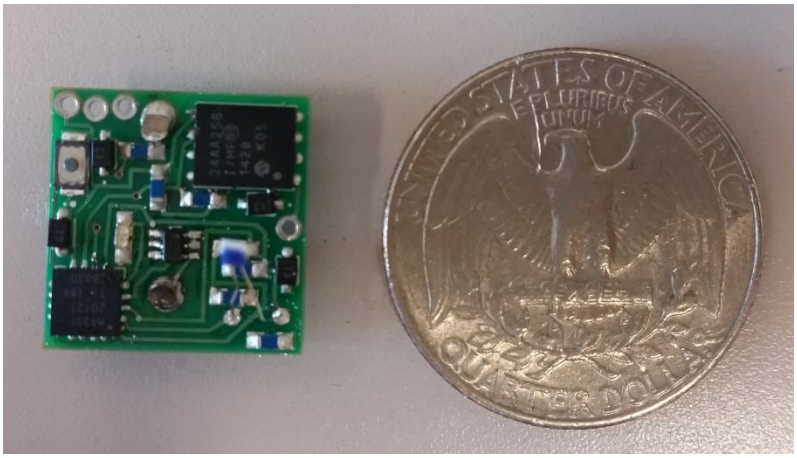

Figure 15: Illustrative Comparison of Size of Device

2-6- System Packaging

The system packaging is the process of encapsulating the device with an appropriate material to ensure its safety and proper operation in different environments. The packaging material was chosen based on its simple implementation, ability to allow an easy use of the encapsulated system, and allowing the encapsulated system to operate

in the intended environment. Materials considered for the use in packaging of the system were chosen based on their color, appearance, and thermal conductivity. The selected materials were tested to choose the appropriate material for the system.

The encapsulation materials were selected to be clear, flexible, with low viscosity, and compatible with the electronic components material. The material was chosen to be clear to observe the operation of the system after encapsulation, the LED in particular and flexible to provide soft encapsulation to be able to control the tactile switch in the encapsulated system. The material was selected with low viscosity to reduce trapped air while filling the mold for improved performance of the packaging. The material selected must be compatible with the electronic components and the PCB material to ensure adequate curing of the material. Different products were selected for testing from three different materials, epoxy adhesives, urethane, and silicone.

For the epoxy material, Loctite E60-NC, Hysol ES1901, and Hysol ES-40 were tested. The E60-NC is used for electrical components encapsulation, it has high electrical insulating ability, and it has black color appearance. The E60-NC showed good performance except for its dark appearance which makes it not suitable for the system. The ES1901 has medium viscosity, thermal insulating ability, clear appearance, and hard form after curing. The ES1901 was not chosen for this system due to its medium viscosity, and its hard form after curing which limits the access to the tactile switch. The ES-40 is a flexible, grey color epoxy with medium viscosity, and resistance to shock and vibration. The ES-40 had the best performance as an epoxy due to its flexible form after curing, but wasn’t chosen due to its grey color which blocks the LED emission and reduces the ability to monitor the operation of the system.

Two urethane encapsulation products were chosen, Loctite US-1152 and Loctite US-2651. The US-1152 is a flexible clear color urethane with low viscosity. The US-1152 didn't cure properly when added to the electronic components placed on the PCB, the US-1152 was not compatible with the electronic components and/or the PCB material. The US-2651 is a clear amber encapsulation with low viscosity used for the encapsulation and potting of electronic components. The US-2651 is a good encapsulation for electronic systems due to its flexible appearance and compatibility with electronic components, but unsuitable for this system due to its dark appearance after curing. Two silicone products were selected for testing, Nusil R-2615 and Nusil R-2188. The R-2615 is a clear silicone product with low viscosity, electrical stability, and provides protection against shock and vibrations. The R-2615 showed the best performance as an encapsulation material for this system. The R-2615 is composed of two parts with ratio 10:1 which required an inconvenient process for implementing the silicone to the system for curing. The R-2188 is a clear silicone product with low viscosity, and increased resistance to shock and vibrations. The R-2188 showed the same performance as the R-2615 as an encapsulation material for this system. Due to its composition of two parts with ratio 1:1, the R-2188 is easily implemented to the system. The Nusil R-2188 silicone encapsulation was chosen as the packaging material for the system. Table 8 summarizes the comparison between the selected encapsulation materials with the advantages and disadvantages of each one. Figure 16 shows the device after packaging.

Table 8: Encapsulation Material Selection

Material	Product	Advantages	Disadvantages
Epoxy	Hysol ES-1901	Clear, thermal insulating	Hard appearance after curing
	Hysol E60-NC	Encapsulating electrical components, electrical insulating	Dark appearance
	Loctite E-40	Flexible, resistance to shock and vibrations	Dark appearance
Urethane	Loctite US-1152	Flexible	Incompatible with electrical components
	Loctite US-2651	Clear amber, encapsulating electrical components	Dark appearance
Silicone	Nusil R-2615	Clear, electrical stability, protection from shock and vibrations	Difficult implementation
	Nusil R-2188	Clear, increased resistance to shock and vibrations	-

Figure 16: Encapsulated Device

2-7- Signal Processing

The developed system relies on measuring the change in the voltage through a Wheatstone bridge to measure the change in the temperature causing the voltage change. The system uses a 10-bit ADC to convert the voltage values into digital equivalent values for storage. The ADC resolution plays an important role in the accuracy and sensitivity of the system. To improve the sensitivity and the accuracy of the system, the values obtained should be processed properly using filtering techniques.

The ADC used in the microcontroller is a 10-bit ADC with a reference voltage of 1.5V. By considering the reference voltage and the number of bits of the ADC, the ADC resolution is 1.5mV based on the following calculations:

$$\Delta = \frac{Vref}{2^n}\text{ , n= number of ADC bits} \qquad (4)$$

The output voltage of the Wheatstone bridge equivalent to the temperature at room temperature (23^{o}C) and 100^{o}C are calculated using equation (1) and (2) to be 0.03V and 0.12V respectively, which represents the required range of the system as shown in table 9.

Table 9: Temperature Range Mapping

Temperature	Resistance (R_T)	Voltage (E_o)
23^{o}C	1083Ω	0.03V
100^{o}C	1381Ω	0.12V

Considering the range of the output voltage and the range of the equivalent temperature, since 0.03V represents temperature of 23^{o}C and 0.12V represents temperature of 100^{o}C, then a range of 77^{o}C is represented by a voltage range of about 0.1V, and every 1^{o}C change in temperature leads to about 1mV change in the output voltage.

Considering the resolution of the ADC and the change in the voltage due to the change in 1^{o}C change in temperature, the sensitivity of the system can be calculated. Since the ADC has 1mV resolution and the 1^{o}C causes 1.5mV change in voltage. The sensitivity of the system is ±1.5^{o}C.

Sensitivity = $\frac{1.5mV * 1\ degC}{1mV}$ = 1.5^{o}C

Due to the limitation of the ADC available in the microcontroller, the accuracy of the system can't go lower than ±1.5^{o}C which is higher than the required accuracy of the system. Signal filtering techniques were used to improve the fluctuation and the noise on the system's output which can improve its accuracy. Oversampling is one of the techniques used to improve the limitation due to the resolution of the ADC. Oversampling relies on collecting more samples than the sampling rate required for the system, and using the extra samples to filter the results of the system [23]. The memory chip used in the system had limited storage capabilities due to the temperature effect on the memory storage which imposed limitation on the available oversampling. The maximum oversampling allowed is two readings per second which is double the data rate required by the system. Low-pass filtering techniques were used to attenuate the noise and the fluctuation, and flatten the peaks in the output of the system. Low-pass

filters are implemented in signal processing by applying averaging techniques such as normal average and moving average. The normal average adds m samples and divides the results by m, while the moving average adds samples within window size m and divides the result by m, and then moves the window with a value n which is smaller than the window size m. The moving average reduces the noise and fluctuation in the output better than the normal averaging, but the disadvantage of the moving average is the time delay at the output. The interpolation method is used to improve the accuracy of the system and reduces the effect of noise, which utilizes oversampling and averaging techniques [23]. The filtering techniques were implemented to the results obtained during the system's bench-top testing to investigate the effect of each technique on the system's results and apply the suitable technique to the system.

2-8- Experimental Setup

The system testing was conducted in two stages, bench top experimental testing and manufacturing process production line testing. The first stage was conducted to validate the ability of the system to operate over the required temperature range with exposure to the chemicals specified in the requirements. The bench top testing investigated the accuracy and the sensitivity of the system, the data rate of the readings, power capabilities of the system, and the performance of the encapsulation material. The second stage was conducted in the production line of the target application industry to test the stability and the operation of the system inside the production line. The second testing investigated the mechanical effect of the production line on the system, and the reliability of the results. In each testing phase, a new device was built and used for the testing procedure to investigate the reproducibility of the system.

The first phase of testing was conducted in the laboratory inside a bench top Cole-Parmer gravity convection oven with an accuracy of ±1^{o}C using a PID controller [24]. The system was validated against a commercial temperature data-logger, PICO technology PT-104 data-logger. The PT-104 is a four-channel platinum resistance temperature measuring data-logger with certified calibrated accuracy of 0.015°C and temperature range from –200^{o}C to +800°C, calibration certificate presented in appendix B. The PT-104 uses 100Ω RTD stainless steel probe. The probe has accuracy of ±0.15^{o}C, and its size is 150mm in length and 6mm in diameter [25]. The probe used in the validation data-logger has a better accuracy compared to the calculated accuracy of the system. The probe can be used to validate the accuracy of the proposed system up to ±0.15^{o}C, which will represent the maximum accuracy to be validated for the proposed system.

The first stage of testing was conducted using three different testing phases. The first phase was conducted at room temperature to test the ability of the system to operate and monitor the temperature accurately. The first testing procedure investigated the accuracy of the readings and the effect of the signal processing techniques in reducing the noise in the system and improving its accuracy. The second phase was conducted inside the convection oven with exposure to heated air to investigate the operation of the system in heated environment. The second testing procedure studied the transient response of the system in increasing temperature environment and the steady state response in constant temperature environment. The third phase was conducted in exposure to three heated chemicals, PG, IPA, and de-ionized water, at different temperatures to investigate the operation of the system in exposure to the required

chemicals at the target temperatures. The third testing procedure studied the transient response of the system with exposure to the chemicals at increasing temperature, and its steady state response at constant temperature.

The second stage of testing was conducted inside the hydration line of a contact lens manufacturing process to investigate the operation of the system in its target application. The second stage of testing was conducted in several phases to study the mechanical effect of the hydration line on the operation of the system and applying the required improvements to the system. The results obtained from the second stage of testing were validated against the expected trend of temperature based on the operation of each hydration line, and the temperature of the chemicals used. The results obtained were used for statistical analysis of the temperature inside the hydration lines.

Chapter 3: Results and Analysis

In this chapter, the results obtained from the first and second stage of system testing are presented and discussed. The first section discusses the results obtained from the bench top testing conducted at room temperature. The signal processing and filtering techniques are discussed and implemented in this section to investigate the improvements applied to the results. The second section presents and discusses the performance of the system with exposure to heated air using a transient response and a steady state analysis. The third section presents and discusses the performance of the system in exposure to chemicals at the target temperature. The system performance in exposure to propylene glycol (PG), Isopropyl alcohol (IPA), and de-ionized water was investigated using transient response and steady state analysis for each case. The fourth section presents and discusses the results obtained from the online testing conducted inside the hydration lines of a contact lens manufacturing process.

3-1- Bench Top Testing

This section presents and discusses the results obtained from the bench top testing conducted in the laboratory to investigate the performance of the system. The testing was conducted using different testing profiles to study the success of the system in its target application.

3-1-1- Room temperature testing

The first phase of bench top testing was conducted at room temperature to monitor the operation of the system and investigate the results obtained. During this stage of testing two devices were built and tested at room temperature for the duration of one hour. The validation data-logger was setup to run for the same duration in the same location as the devices.

The data rate of the system was investigated using the results obtained from this stage of testing. The number of the data points obtained was compared to the duration of operation of the device. The data rate of the readings recorded matched the theoretical data rate with less than 1% error. The results obtained from the first device were plotted without implementing any filtering technique to record the raw data accuracy. The results represented the measurement taken every half a second due to the oversampling of the system. Figure 17 shows the raw data obtained from the system over duration of one hour. The results showed the ability of the system to represent the room temperature over its period of operation. The device took a short period at the beginning of its operation to adjust to the surrounding environment temperature. Figure 18 shows a zoomed in view of the raw data over duration of 5 minutes. The zoomed in view of the data showed the fluctuation of the data over a range close to $2^{o}C$, which is $0.5^{o}C$ higher than the theoretical value due to the added noise by the system. The duration taken by the device to adjust to the surrounding environment and the spikes observed in the results were studied and related to the hardware issues which added unexpected noise to the system.

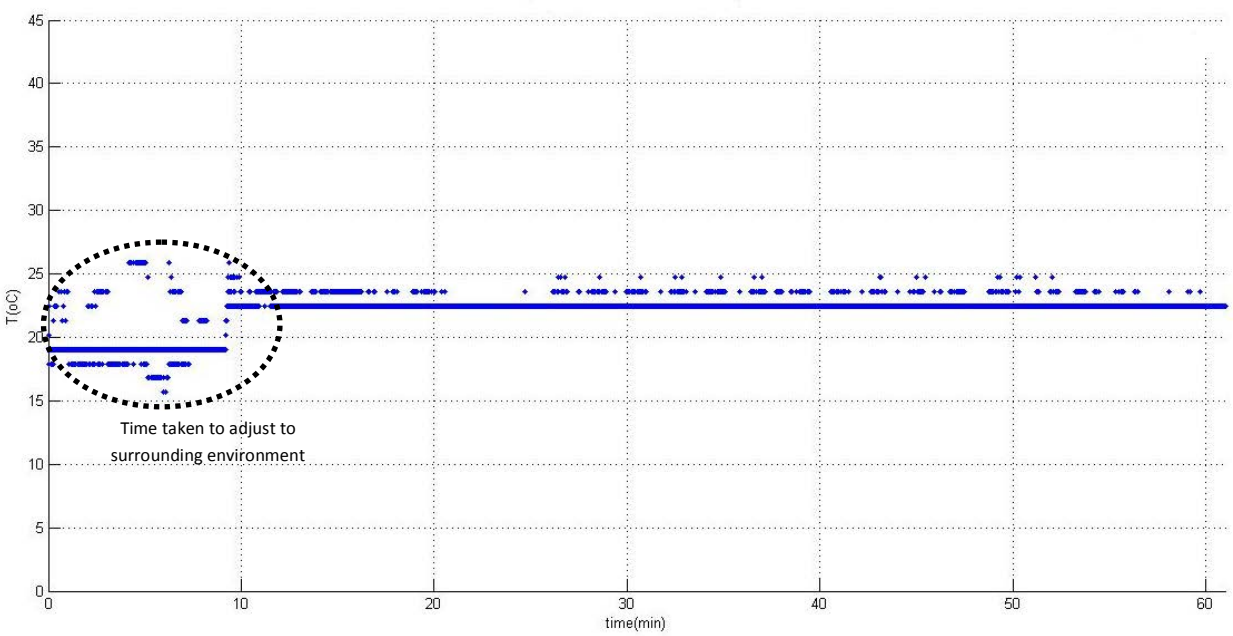

Figure 17: Raw Data at Room Temperature

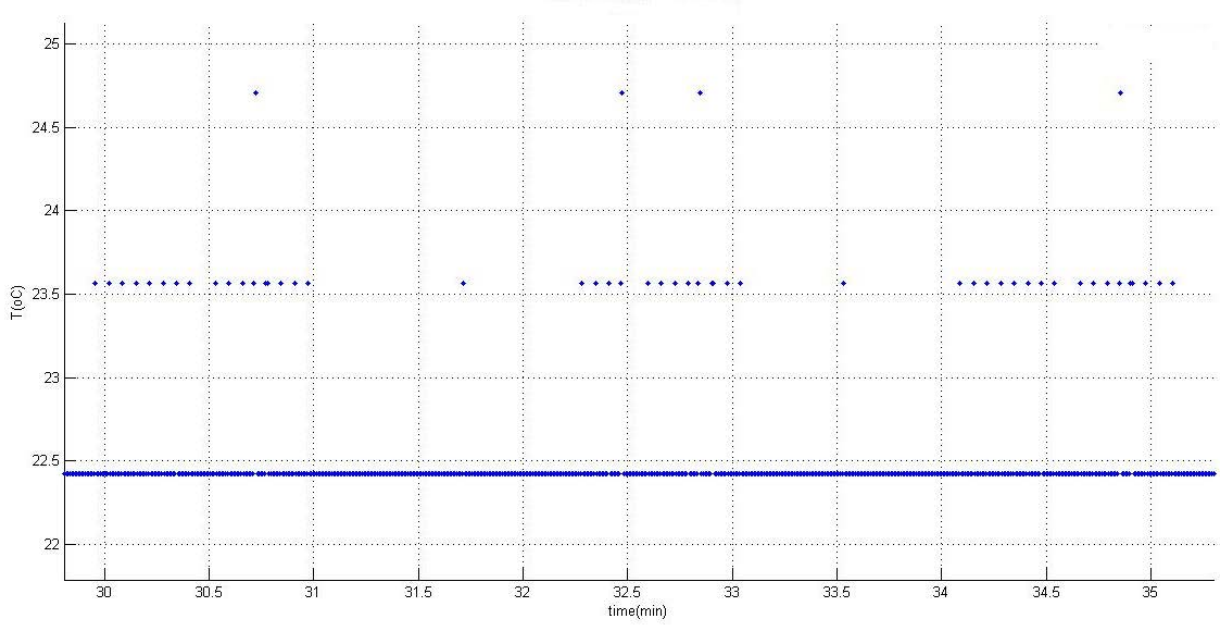

Figure 18: Zoomed In Raw Data from Minute 30 to Minute 35

The filtering techniques were implemented to the results of the system to improve the results' representation. The filtering techniques aim to reduce the fluctuation of the

results and improve the system's accuracy. The filtering process uses the oversampling of the data to apply a low-pass filter. The first filtering technique used was normal averaging with a window of size two to maintain the data rate required by the system. The normal filtering increased the interval between consecutive readings to one second. Figure 19 shows the output of the system after applying the normal average filtering technique. Figure 20 shows the output of the averaged results zoomed in over a period of five minutes. The normal average filtering technique reduced the fluctuation of the output. The output of the system after applying the normal averaging had fluctuations within range close to 1.5^{o}C.

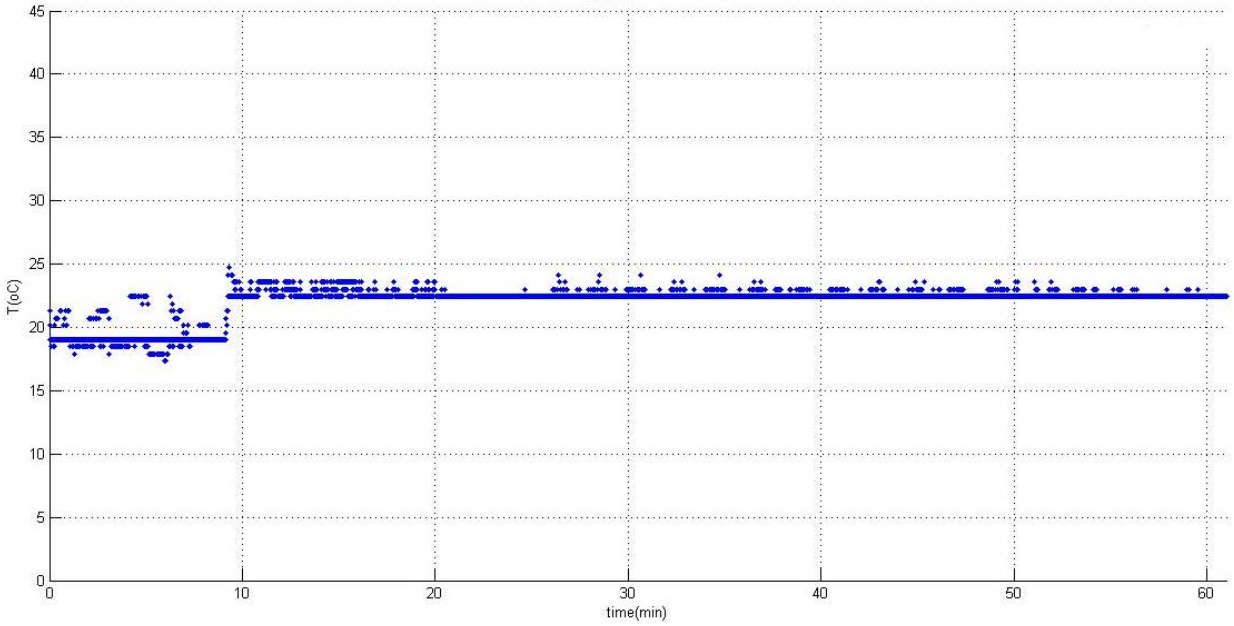

Figure 19: System Output with Normal Averaging Filtering Technique

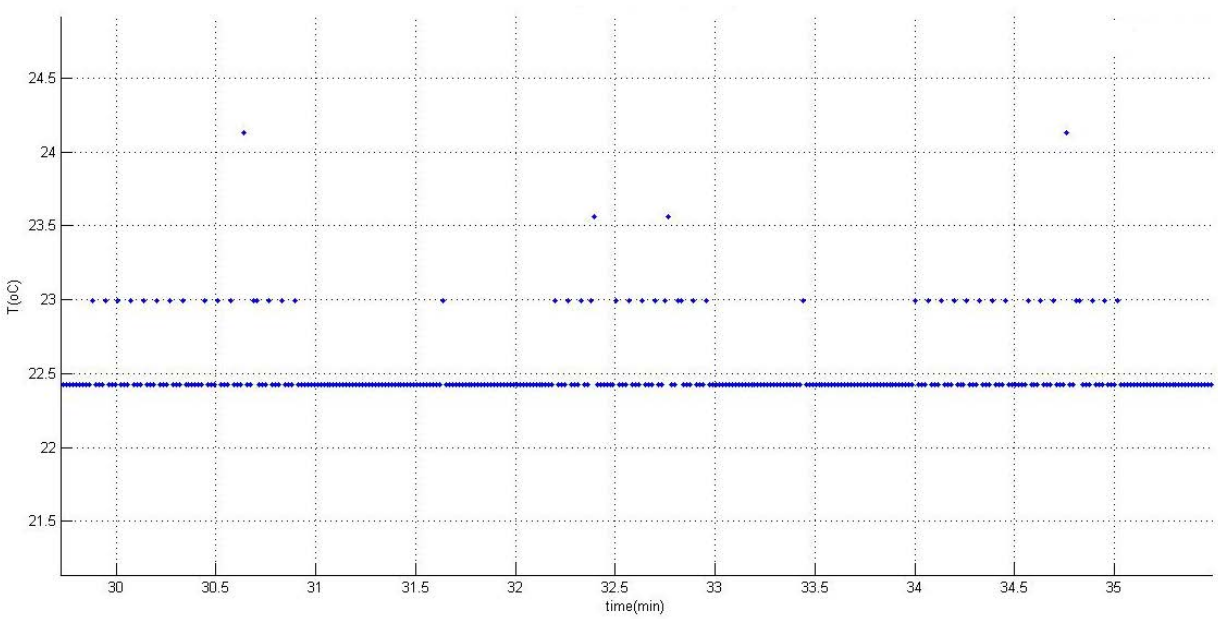

Figure 20: Zoomed In Normal Average Filtered Data from Minute 30 to Minute 35

The moving average was applied to the data obtained from the first device to improve its accuracy by flattening the peaks and reduce the fluctuations. The moving average had a window of size two and moving value of one to keep the data rate required while utilizing the oversampling of the data. The moving average caused a delay in each reading by half a second while the interval between consecutive readings remained at half a second due to oversampling. Figure 21 shows the output of the system after applying the moving average filtering technique. Figure 22 shows the output of the averaged results zoomed in over a period of five minutes. The moving average filtering technique reduced the fluctuation of the output within a range close to 1.5^{o}C.

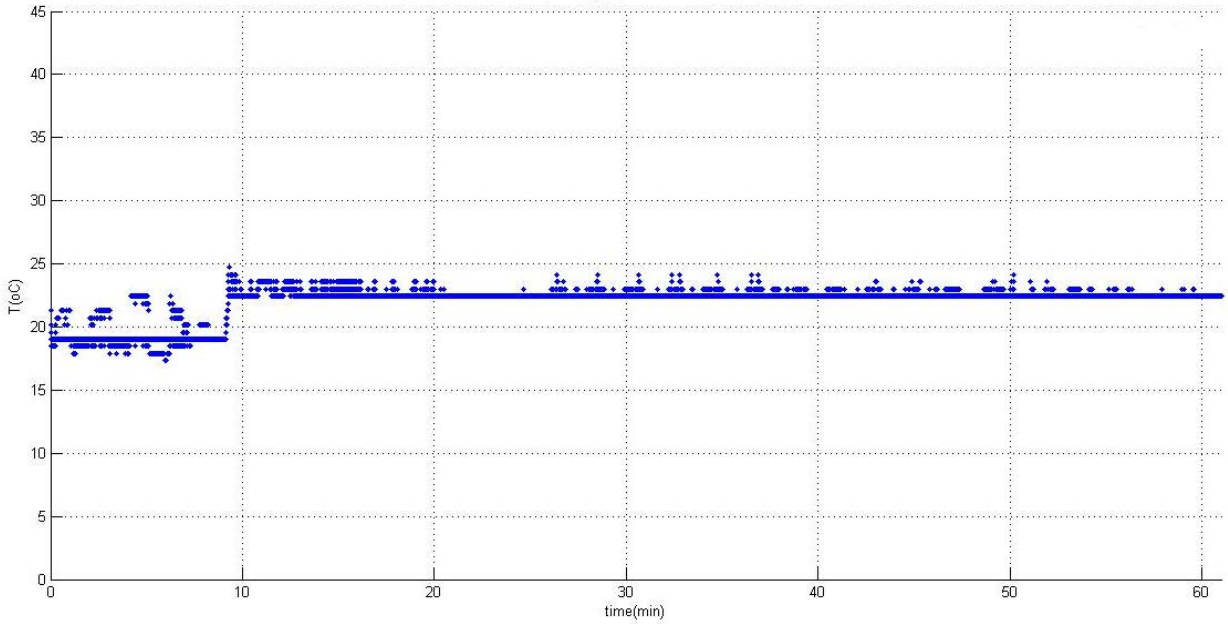

Figure 21: System Output with Moving Averaging Filtering Technique

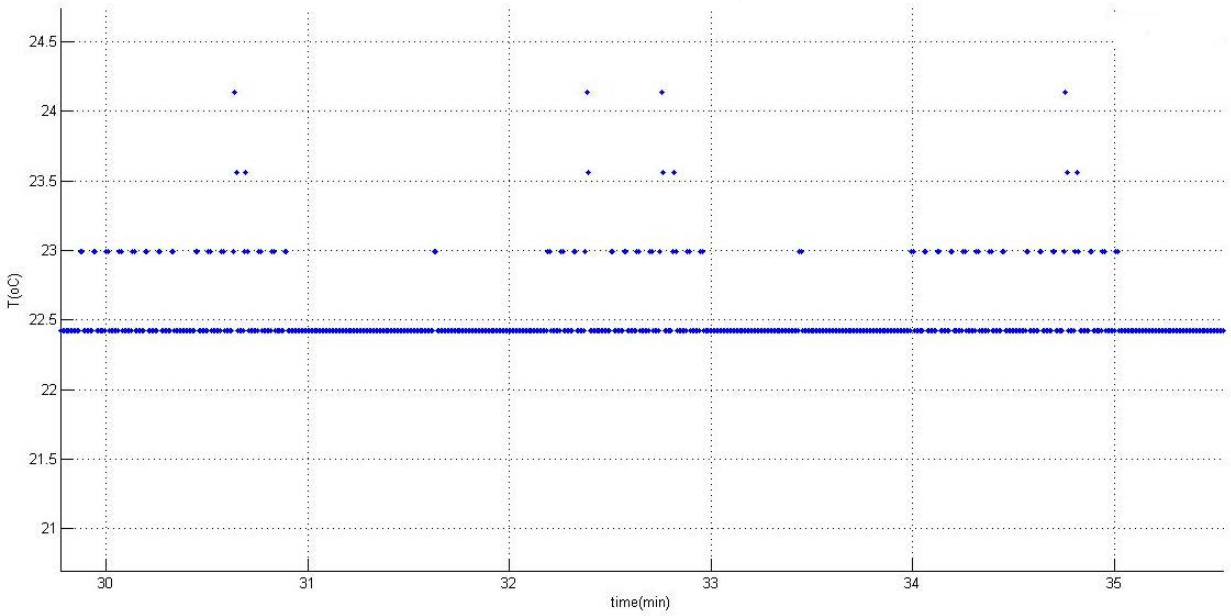

Figure 22: Zoomed In Moving Average Filtered Data from Minute 30 to Minute 35

The third filtering technique applied was the combination of the normal average and the moving average techniques. The combined technique uses the normal averaging with window of two to obtain the average value at one second interval. The averaged values

at one second interval are used to implement the moving average filter. The moving average caused a delay in the output of the system by half a second but the interval between consecutive readings was increased to one second. Figure 23 shows the output of the system after applying the normal average filtering followed by the moving average filtering techniques. Figure 24 shows the output of the combined average results zoomed in over a period of five minutes. The combined average filtering technique reduced the fluctuation of the output within a range less than 1^{o}C. The combined average filtering technique was chosen as the signal filtering technique for the system.

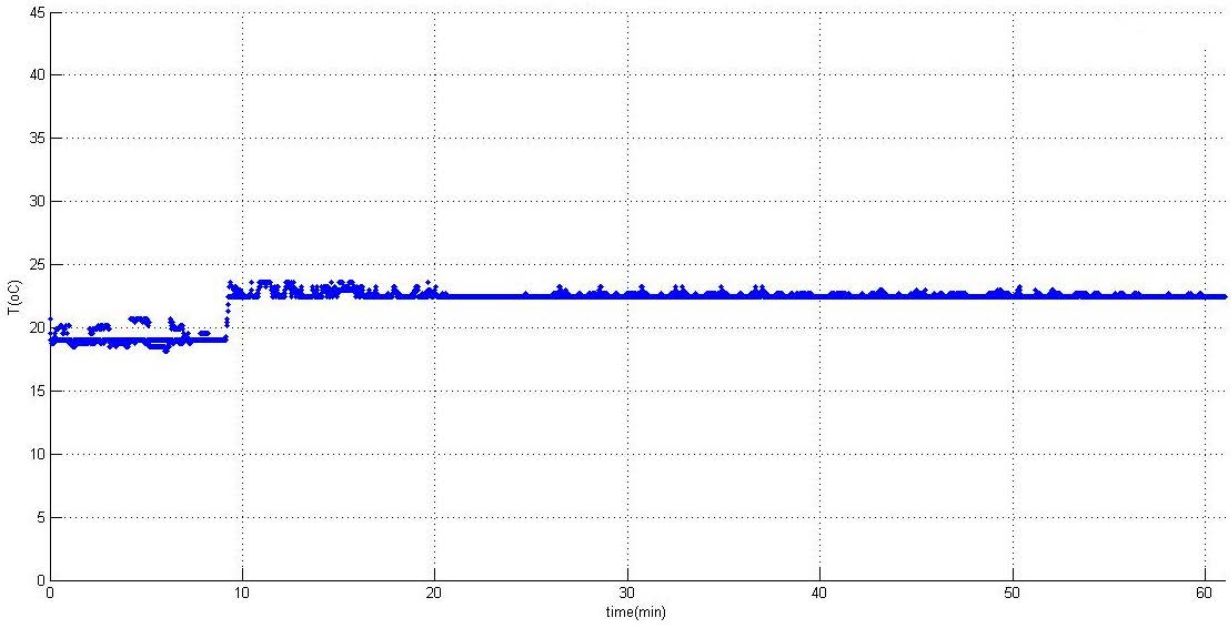

Figure 23: System Output with Combined Averaging Filtering Technique

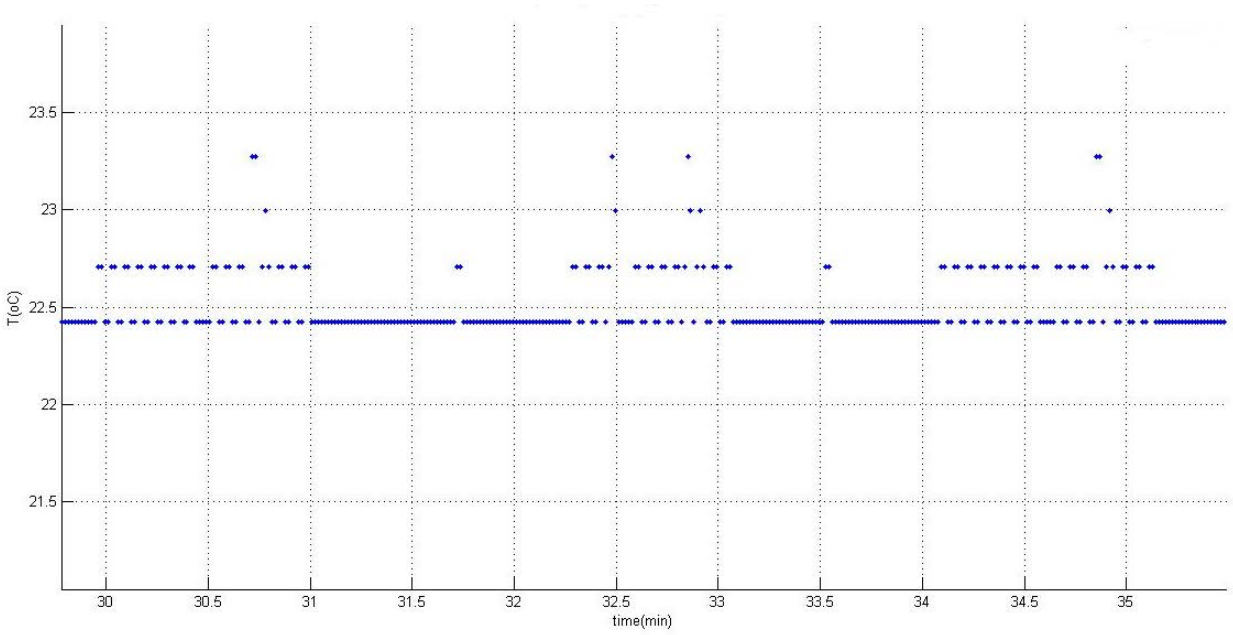

Figure 24: Zoomed In Combined Average Filtered Data from Minute 30 to Minute 35

The results obtained from the first device were processed using the combined average technique and plotted to be validated against the results obtained from the validation data-logger operated over the same time interval. Figure 25 shows the results obtained from the first device and the validation data-logger. The results showed the agreement between the system monitoring ability and the validation data-logger. The results were used to investigate the accuracy of the system based on the accuracy of the validation data-logger. Figure 26 shows the results obtained from the system and the validation data-logger zoomed in over duration of three minutes. The comparison graph between the readings from the system and the data-logger shows the accuracy of the system of $\pm 0.4^{o}C$. The accuracy of the probe of the validation data-logger has an effect on the accuracy of the device. The accuracy of the system after considering the accuracy of the probe is $\pm 0.5^{o}C$ at ambient conditions disregarding the added noise and fluctuations.

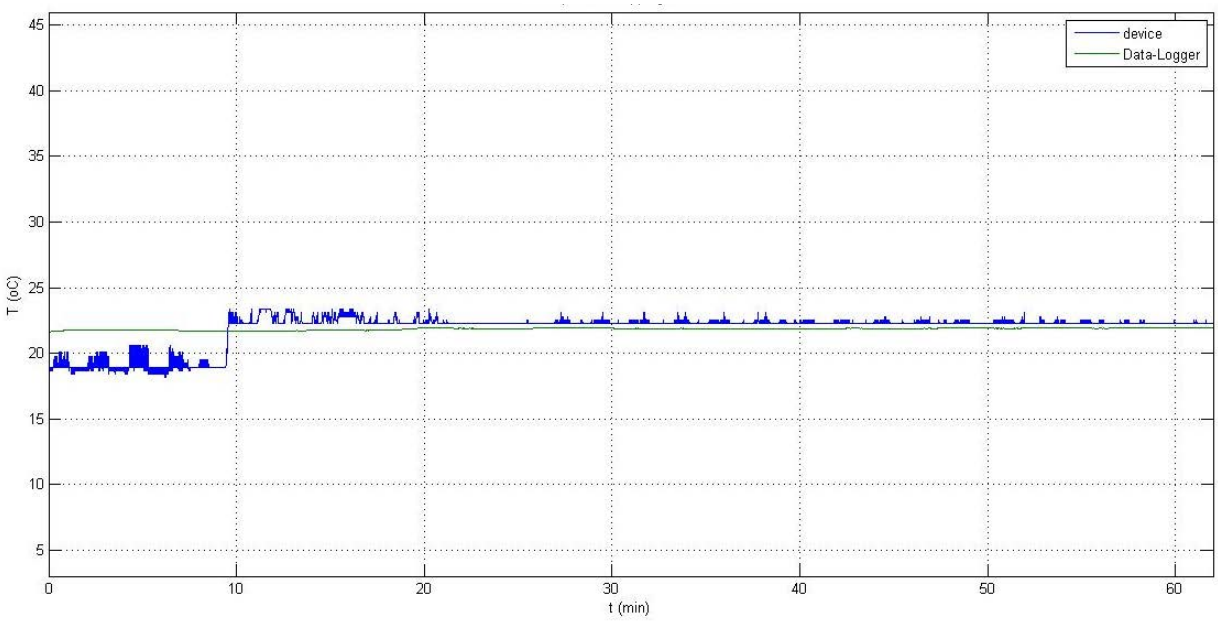

Figure 25: System Validation at Room Temperature

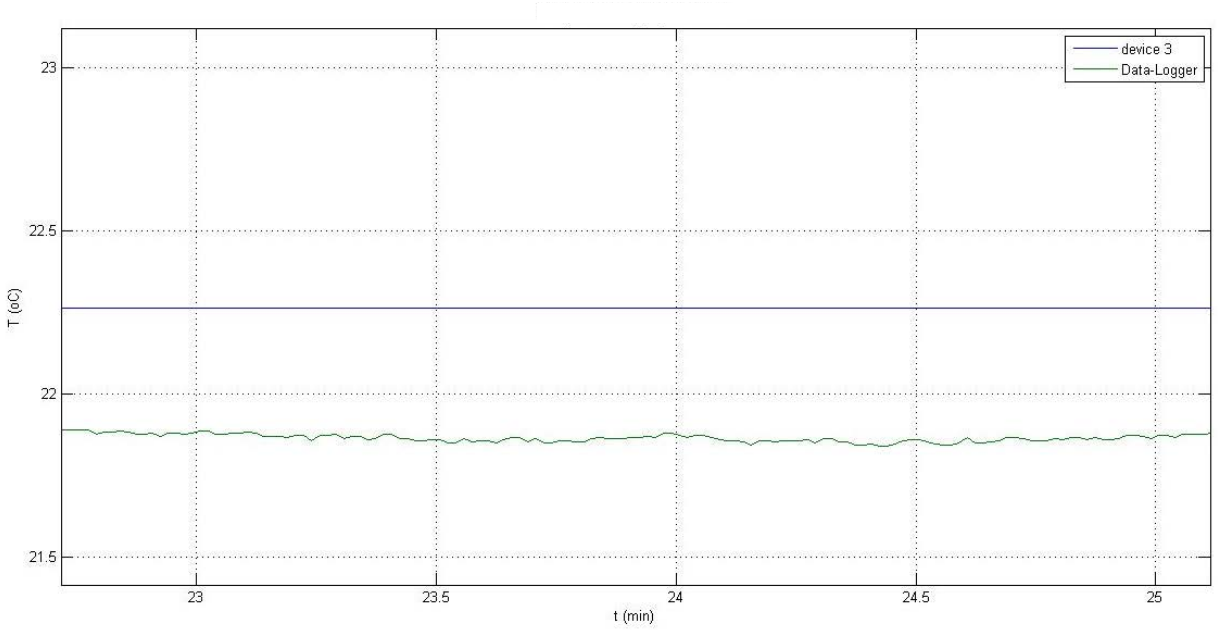

Figure 26: System Validation at Room Temperature Zoomed In from Minute 22 to Minute 25

The results obtained from the second device were processed using the combined filtering technique and plotted to be validated against the results obtained from the validation data-logger operating in the same environment at the same time interval. Figure 27 shows the results obtained from the second device and the validation data-logger. The device took a period close to ten minutes to stabilize and adjust to the environment. The device showed more fluctuation during the entire period of operation compared to the validation data-logger. The fluctuations were related to the possible hardware issues in the device such as added noise by certain components such as memory chip or RTD, improper connections and integration between components, capacitance discharge, or impedance mismatch which altered the device's output. The hardware issues focused investigation was moved to the following testing procedures to observe the trend and the consistency of the fluctuations. The results showed the high sensitivity of the device to the changes in the surrounding environment. The results can be better presented by applying a fit model to the results. The fit model is applied to each set of data individually to reduce the consistent trend of fluctuations in each case.

3-1-1- Exposure to heated air testing

The second phase of the first stage of testing was conducted inside the convection oven at different temperatures in exposure to heated air to investigate the effect of temperature on the system's operation and its ability to withstand heated environments, and to validate the results obtained by the system. The second phase was conducted using four different devices to study the performance of the transient response and the steady state response of the system. The validation data-logger was used to validate the results obtained in each case.

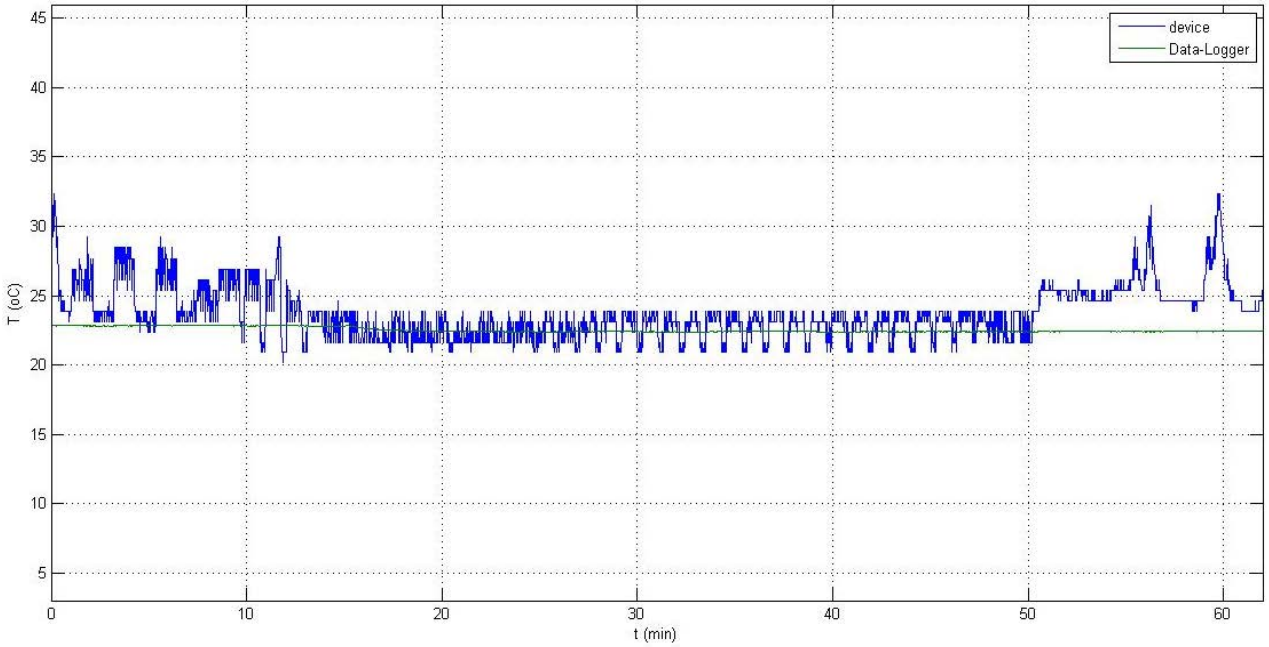

Figure 27: System Validation at Room Temperature, Second Trial

The first experiment was conducted by placing the device and the probe of the data-logger inside the convection oven at room temperature and gradually increasing the temperature up to 80^{o}C for total duration of two hours. The readings from the device were retrieved and processed using the conversion equations and the filtering technique. The results from the device and the data-logger were plotted as shown in figure 28. The results showed the device and the data-logger's reaction to the increase in temperature. The device showed faster response to the increase in temperature compared to the response of the data-logger. The difference in the response between the two systems is related to the difference in the thermal mass of the sensing element due to its size in each system. The developed system has the RTD as its sensing element which has a total size of 2x2mm while the validation data-logger has the stainless steel probe as its sensing element which has a size of 150x6mm. Due to the difference in the thermal mass of each sensing element, the response of each system to

the increase in temperature is different. The results showed more fluctuation in the device's results compared to the results from the validation data-logger which is related to the hardware issues as observed from the previous testing. The results showed the high sensitivity of the device to the changes in temperature which agreed with the observation developed during the first phase.

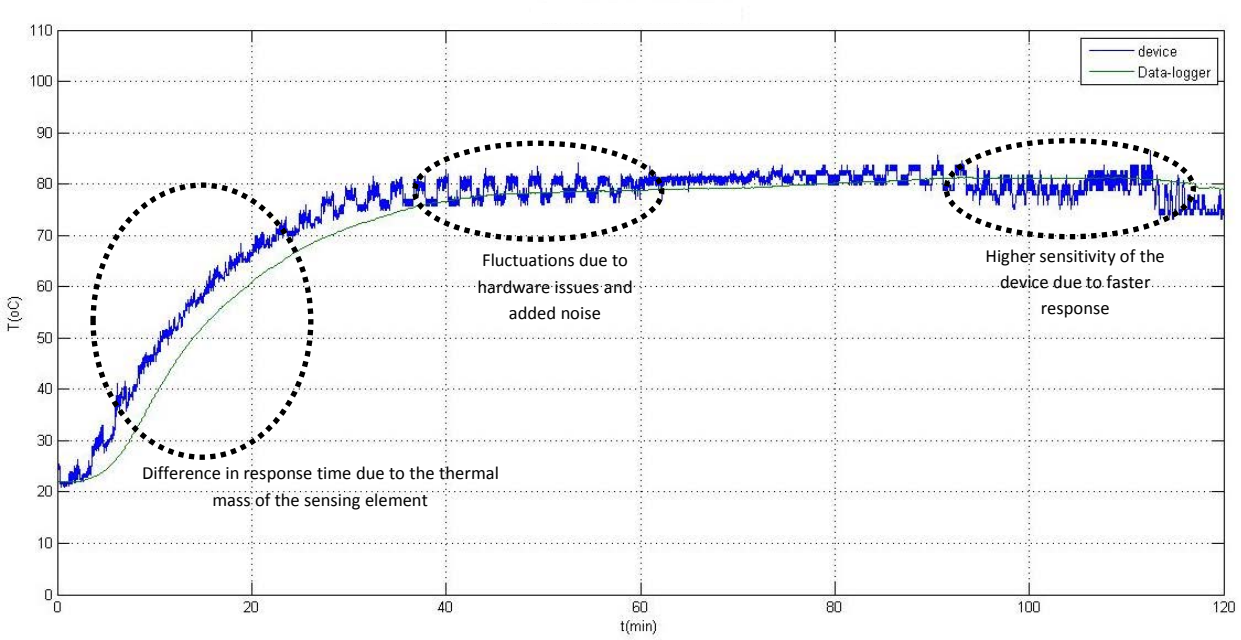

Figure 28: System's Transient Response in Exposure to Air Up to 80^{o}C

The second test was conducted by placing a device along with the probe of the data-logger inside the convection oven at room temperature and gradually increasing the temperature up to the required limit of the system which is 100^{o}C. The readings obtained from the device were processed and plotted against the readings obtained from the validation data-logger. The results from the second test are shown in figure 29. The results showed the response of the device and the data-logger as the temperature gradually increased in which the two systems were able to reflect the increase in temperature from room temperature up to 100^{o}C. The results showed the faster

response of the device compared to the data-logger but fewer fluctuations compared to the previous testing. The faster response of the device compared to the data-logger was related to the thermal mass of the sensing element in each system as observed in the previous testing.

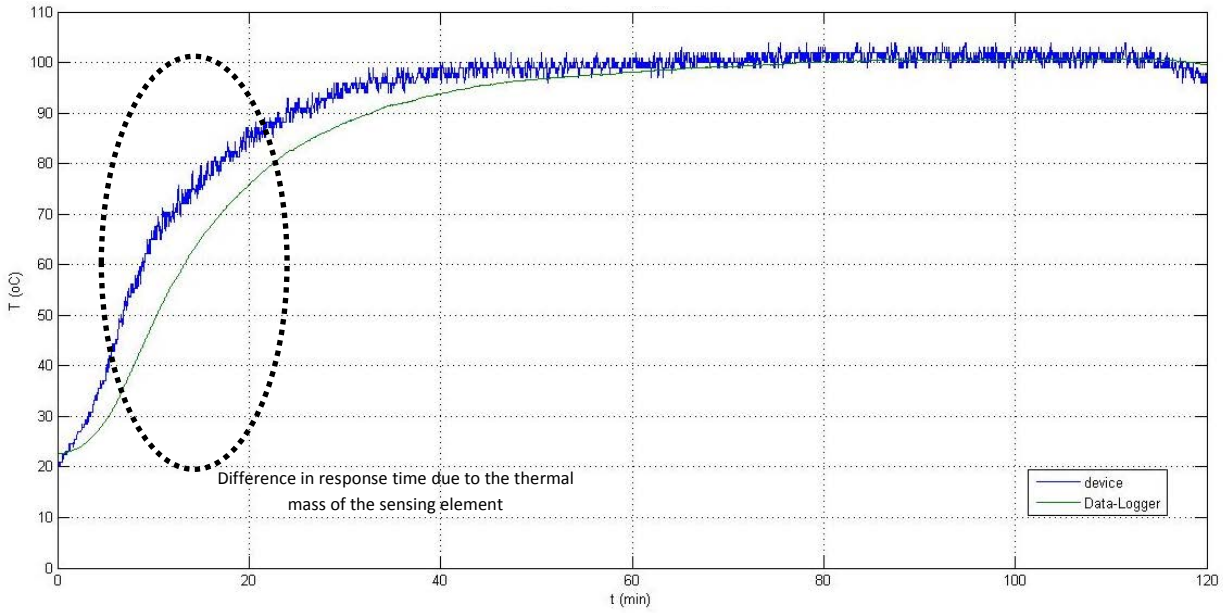

Figure 29: System's Transient Response in Exposure to Air Up to 100^{o}C

The third test was conducted to validate the steady state response of the system by placing the device and the probe of the data-logger inside the preheated convection oven for duration of two hours. The purpose of this test was to investigate the response of the device when placed into a heated environment to eliminate the effect of the thermal mass of the sensing element observed during the transient response of the device and the validation data-logger. Two devices were used by placing each device with the validation data-logger probe in the oven set at a stable temperature of 80^{o}C for duration of two hours. The readings from the two devices were retrieved, processed, and plotted with the readings of the validation data-logger at each case. Figure 30

shows the readings obtained from the first device. The readings showed the stability of the two systems after a period of time close to 10 minutes at temperature 80^{o}C due to the initializing conditions for each system. The device was turned on outside the oven and then placed inside the heated environment, while the data-logger probe is placed inside the oven when it is turned on. The readings from the two systems slightly increased over time. The readings from the two systems lied within the same range and followed the same trend over time. The results showed the higher sensitivity of the device to the changes in the surrounding environment compared to the validation data-logger.

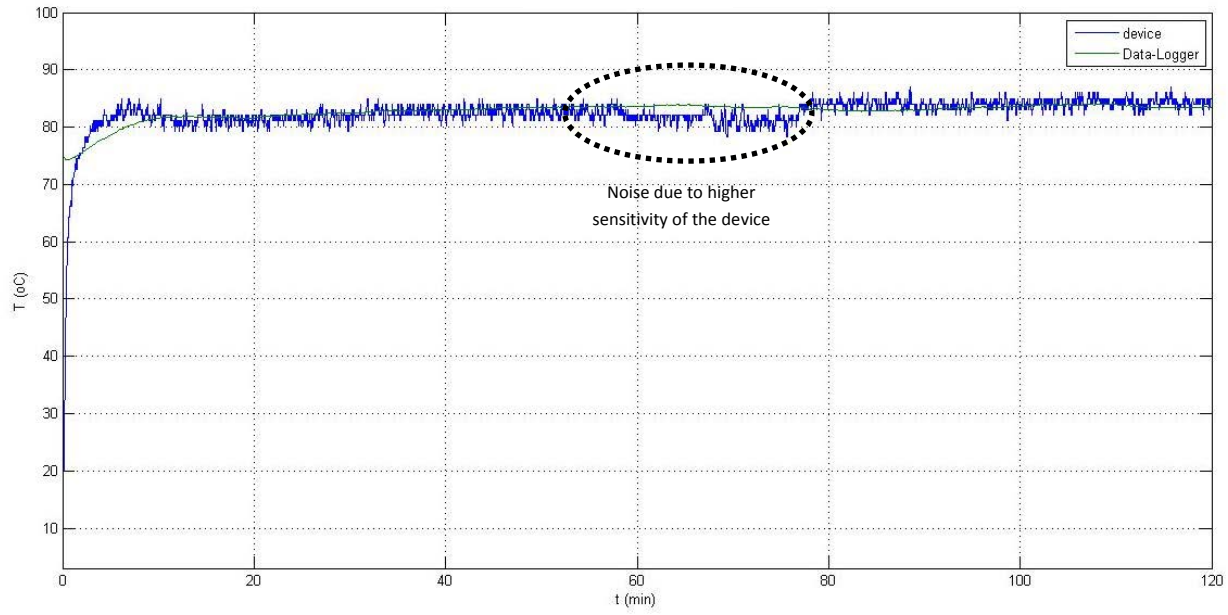

Figure 30: System's Steady State Response in Exposure to Air at 80^{o}C

The results obtained from the second device plotted with the data-logger readings obtained during the same time interval are shown in figure 31. The results showed the consistency of the readings from the device with the data-logger when it reached the steady state at the maximum temperature. The results from the second device proved

the high sensitivity of the device to the changes in the surrounding environment. The readings at the beginning of the duration differed between the data-logger and device due to the difference in the initializing conditions between the two devices.

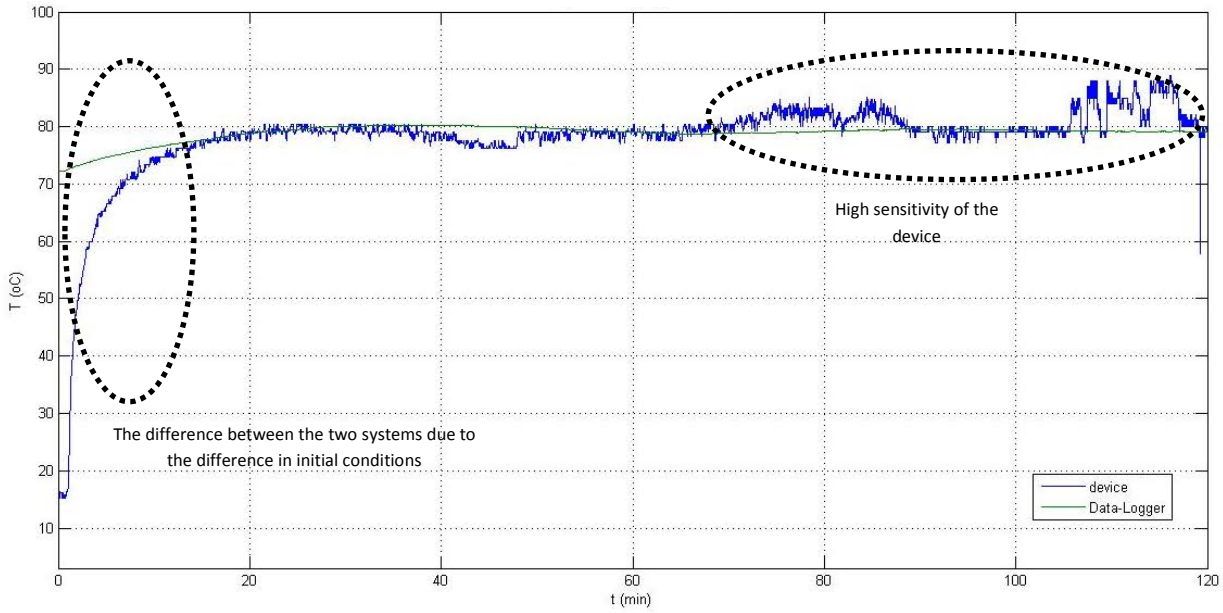

Figure 31: System's Steady State Response in Exposure to Air at 80°C, Second Trial

Accuracy validation procedure was conducted on the data collected during the heated air exposure testing to observe the accuracy at the high end of the temperature range. The maximum temperature recorded by the device was compared to the maximum value recorded by the validation data-logger in heated environments at temperatures of 80°C and 100°C to eliminate the effect of external noises or response time on the accuracy calculation. The maximum temperature recorded by the device at 80°C environment was 81.58°C while the maximum temperature recorded by the validation data-logger was 81.102°C, with a margin of about 0.5°C less than the device temperature. While at 100°C environment, the highest temperature recorded by the device is 101.6°C, and the validation data-logger had a maximum value of 100.9°C with

a margin of about 0.7°C less than the device temperature. The accuracy of the probe used by the validation data-logger was considered in the accuracy calculations which had a value of ±0.15°C. After considering the probe's accuracy, the accuracy reached by the device at 80°C is ±0.6°C, while the accuracy reached by the device at 100°C is ±0.8°C. The temperature range required by the system had an accuracy ranging from ±0.5°C at low level and ±0.8°C at high level. Table 10 shows the comparison between the device's output, the validation data-logger's output, and the accuracy at each case. Figure 32 shows the accuracy fit model between the readings recorded by the device and the validation data-logger.

Table 10: Output Accuracy Comparison

Environment temperature	Device output	Validation data-logger output	Accuracy
22°C	21.9°C	22.3°C	±0.5°C
80°C	81.102°C	81.58°C	±0.6°C
100°C	100.9°C	101.6°C	±0.8°C

The fourth test was conducted to study the operation of the system using a magnetic reed switch instead of the tactile switch. The magnetic reed switch was added to a new device, and tested over increasing temperature up to 90°C for duration of about one and a half hour. A strong magnet was used to turn on and turn off the device. The magnetic switch showed a reliable performance in controlling the device. The readings from the device were recorded and plotted as shown in figure 33.

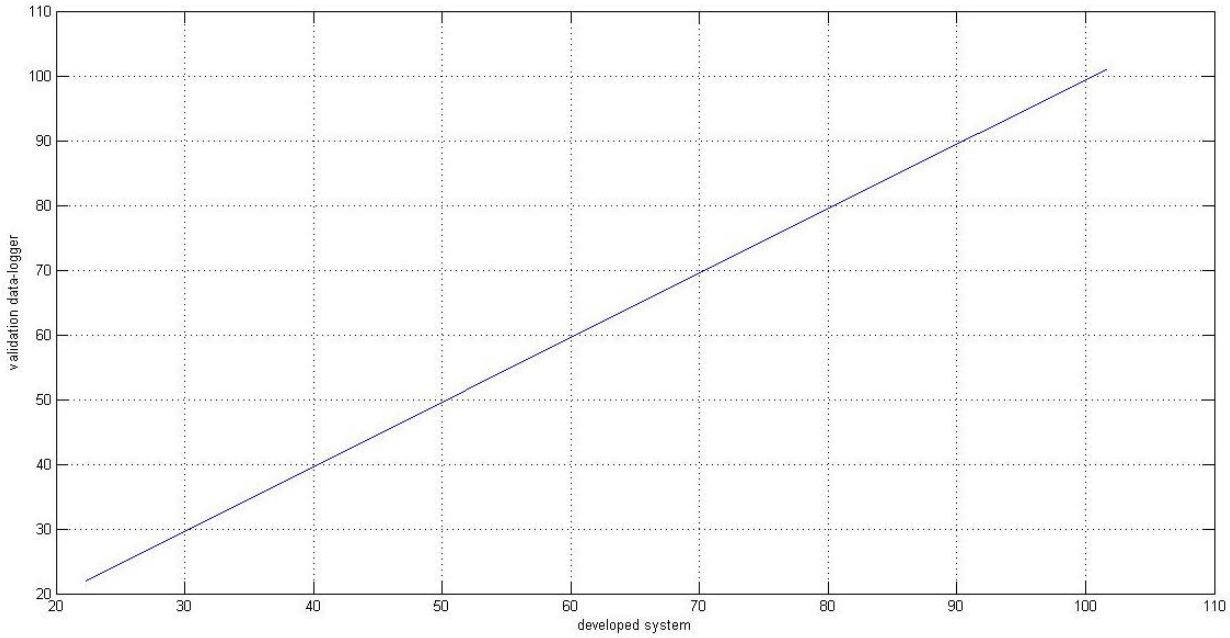

Figure 32: Output Accuracy Fit Model

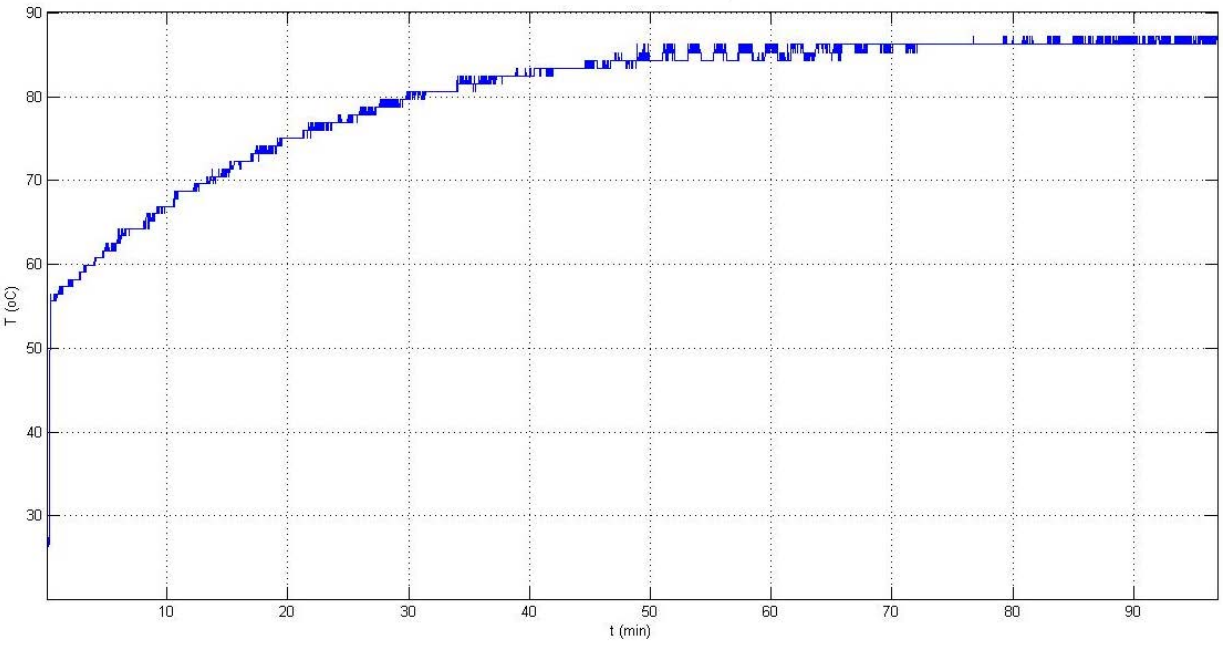

Figure 33: System Performance Using a Magnetic Reed Switch

3-1-2- Exposure to heated chemicals testing

The third stage of the first testing was conducted by exposing the system to different heated chemicals at different temperatures to investigate the ability of the system to operate properly and accurately in exposure to heated chemicals. The system was tested in exposure to three chemicals, Isopropyl Alcohol (IPA), Propylene Glycol (PG), and de-ionized water. The PG and de-ionized water were heated at temperatures up to 80^{o}C while the IPA was heated at temperatures up to 50^{o}C due to its low flashing point and to avoid any hazardous consequences from heating. The system's transient response and steady state response were tested and analyzed for each chemical. The results of the systems were validated using the validation data-logger with its immersion probe placed inside the chemicals in each case.

An initial testing was conducted to investigate the effect of the chemicals on the components of the system and the importance of the packaging material in protecting the system. The device was placed inside the three chemicals (PG, IPA, and de-ionized water) without encapsulation while heating the chemicals to the target temperature. The devices failed to operate for the entire duration inside the chemicals, and the data obtained did not represent the temperature in the respective environments. The devices used were encapsulated and reused in another testing. The encapsulated devices were able to operate for the entire duration of the testing, and accurately monitor the temperature in the respective environments. The testing showed the effect of the chemicals on the operation of the device during its exposure to those chemicals without damaging the components in the system. The testing proved the importance of the packaging material in protecting the devices.

The first chemical exposure testing was conducted in exposure to PG at temperature up to 80^{o}C by placing the device along with the probe of the data-logger inside a flask filled with PG. The flask containing the device and the probe was placed inside the oven at room temperature and gradually increasing the temperature up to 80^{o}C for duration of two hours. Figure 34 shows the transient response readings from the device along with the validation data-logger in exposure to PG. The readings from the two systems gradually increased to reach 80^{o}C by the end of the two hours. The results showed the faster response of the device compared to the data-logger. The faster response of the device was related to the difference in the thermal mass of the sensing element in each system as observed from the previous testing. The results showed the higher sensitivity of the device to the surrounding changes and noises as compared to the validation data-logger. The same testing procedure was conducted using another device along with the validation data-logger. The device and the probe from the data-logger were placed inside a flask containing PG at room temperature and gradually increased to reach 80^{o}C. The readings from the two systems were recorded and plotted. Figure 35 show the readings obtained from the device with the validation data-logger. The readings showed the gradual increase in temperature to reach 80^{o}C. The ability of the system to record the change in the temperature agreed with the readings recorded during the previous testing which showed the consistency of the system in similar environments.

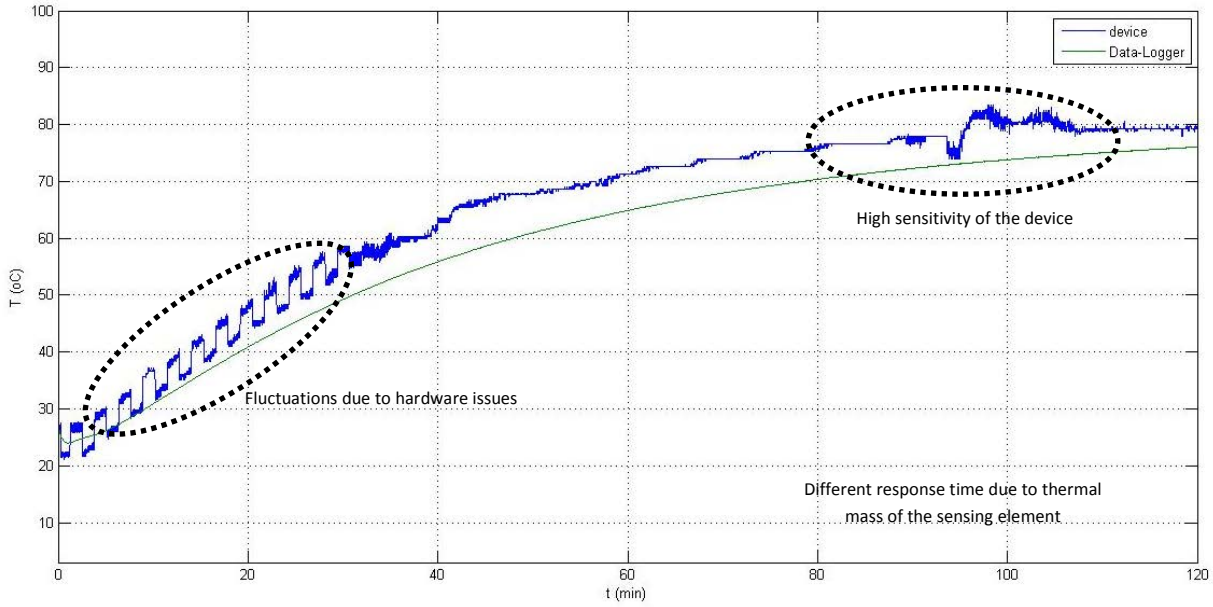

Figure 34: System's Transient Response in Exposure to PG at 80^{o}C

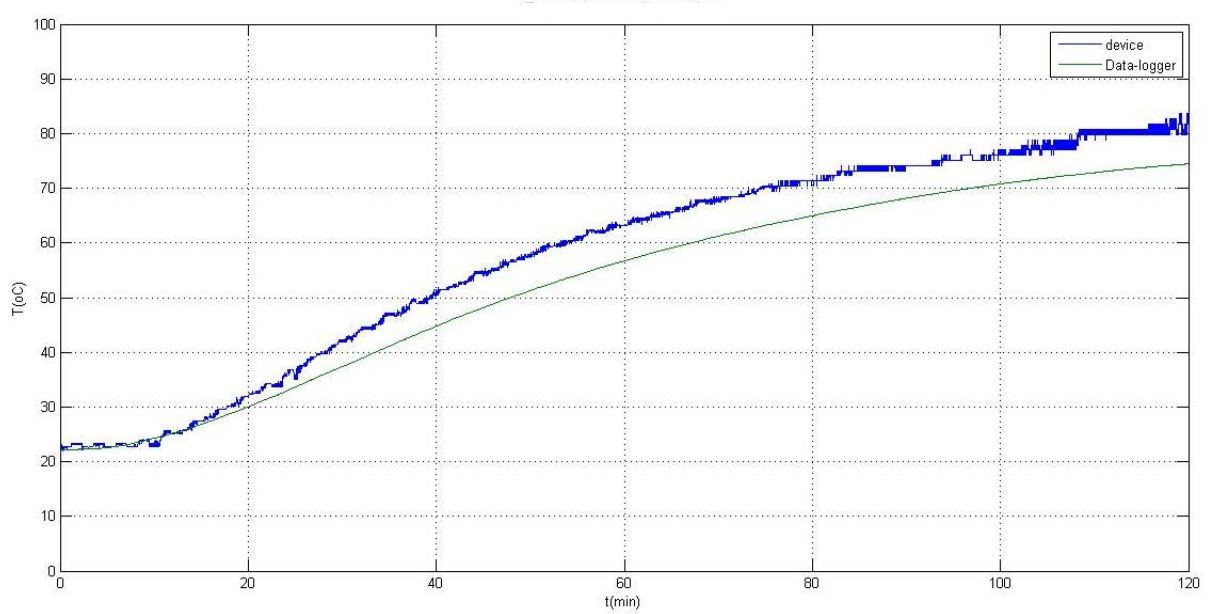

Figure 35: System's Transient Response in Exposure to PG at 80^{o}C, Second Trial

Further testing for the device's transient response with exposure to PG was conducted by placing another device in the same setting as the first testing. The device was placed in PG for duration of two hours in increasing temperature up to 80^{o}C and the results

were verified against the validation data-logger results. Figure 36 shows the readings obtained from the device and the validation data-logger operating in the same setting. The results showed the increasing temperature recorded by the two devices. The readings from the device showed its faster response to the change in temperature as compared to the data-logger. The faster response of the device proved the previous assumption considering the thermal mass of the sensing element form each device as the reason for the difference in the response time to the change in temperature.

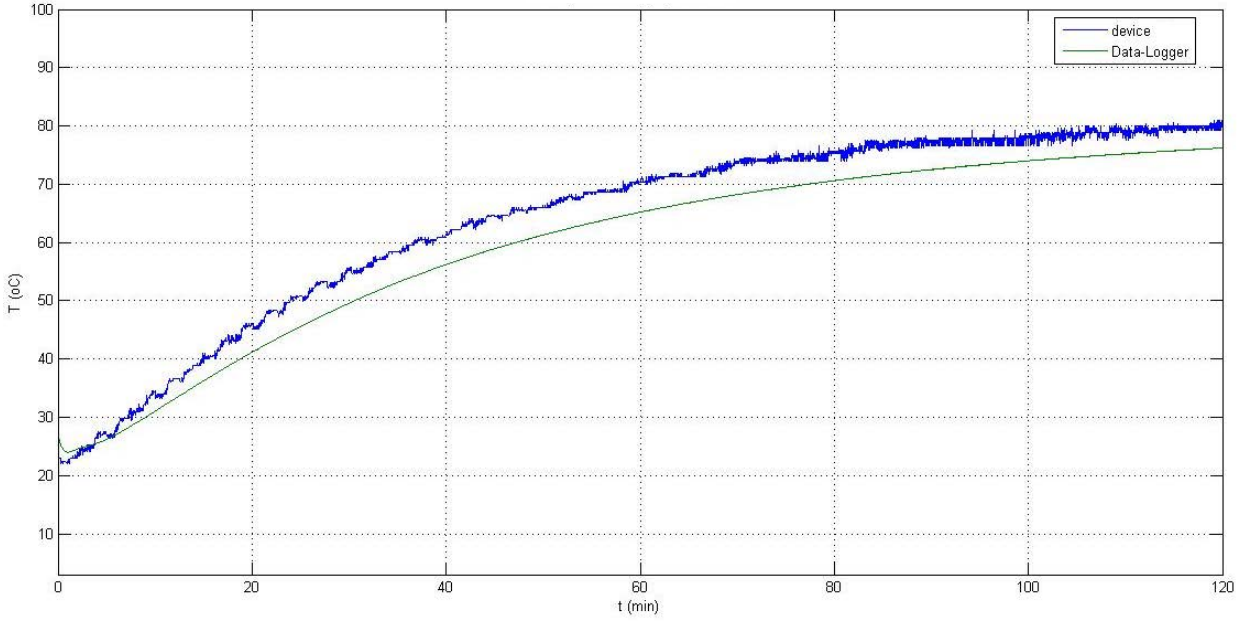

Figure 36: System's Transient Response in Exposure to PG at 80^{o}C, Third Trial

Another test was conducted to investigate the steady state response of the system when operating in exposure to heated PG to eliminate the thermal mass effect of the sensing element in each device on the results of the test. The test was conducted by placing the device in a flask containing PG preheated to temperature of 80^{o}C for duration of two hours while keeping the temperature steady for the entire duration. The results obtained were compared to the readings obtained from the validation data-

logger with its probe placed in the same environment. Figure 37 shows the readings obtained from the two system's steady state response. The results showed the agreement between the device and the validation data-logger in recording stable temperature. The results showed added noise at certain instances which was related to the higher sensitivity of the device to the changes in the temperature as compared to the validating data-logger or as a reason of the fluctuations due to the hardware issues.

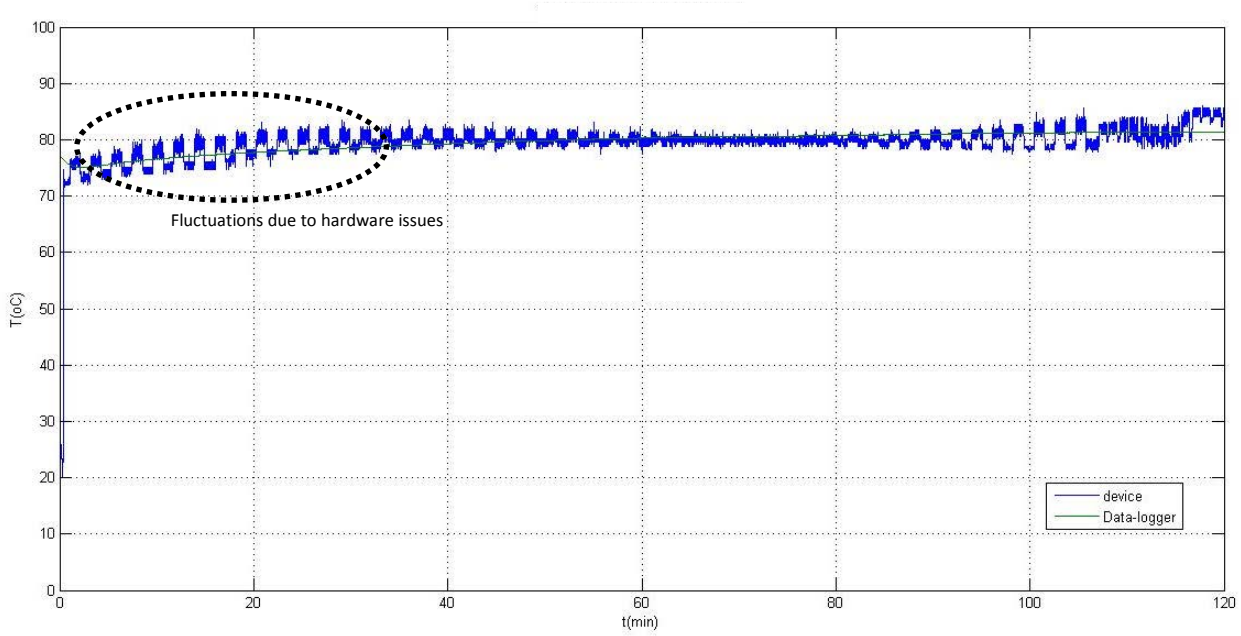

Figure 37: System's Steady State Response in Exposure to PG at 80^{o}C

The second chemical exposure testing was conducted with the device exposed to De-ionized water at temperature up to 80^{o}C. The first test was conducted by placing the device along with the probe of the data-logger inside a flask filled with de-ionized water. The flask containing the device and the probe was placed inside the convection oven at room temperature and gradually increasing the temperature up to 80^{o}C for duration of two hours. Figure 38 shows the transient response readings from the device along with the validation data-logger in exposure to de-ionized water. The readings from the two

systems were gradually increasing to reach 80°C with the device reaching 70°C at the end of the two hours while the validation data-logger reached 60°C at the end of the two hours which proved the faster response of the device compared to the validation data-logger. The faster response of the device was related to the difference in the thermal mass of the sensing element in each system as observed from the previous testing. The results showed the higher sensitivity of the device to the surrounding changes and noises compared to the validation data-logger. The de-ionized water testing showed higher sensitivity of the system than the sensitivity observed during the PG testing.

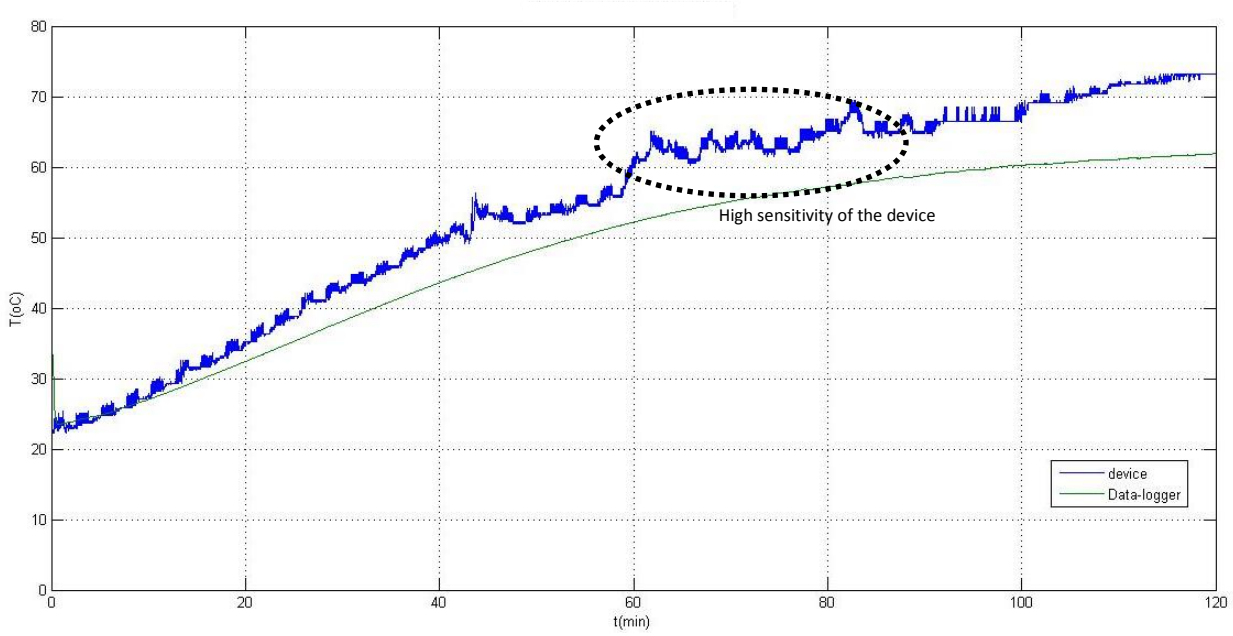

Figure 38: System's Transient Response in Exposure to De-ionized Water at 80°C

Another test was conducted using a device immersed in de-ionized and gradually increasing temperature to reach 80°C for duration of two hours. Figure 39 shows the readings obtained from the device along with the validation data-logger in exposure to de-ionized water. The readings from the two systems were gradually increasing to reach 80°C with the device reaching 70°C at the end of the two hours while the validation

data-logger reached 65^{o}C at the end of the two hours which proved the faster response of the device compared to the validation data-logger. The faster response of the device was related to the difference in the thermal mass of the sensing element in each system as observed from the previous testing. The results showed higher sensitivity of the device to the surrounding changes and noises compared to the validation data-logger. The results obtained agreed with the results obtained from the previous testing, which showed the consistency of the system.

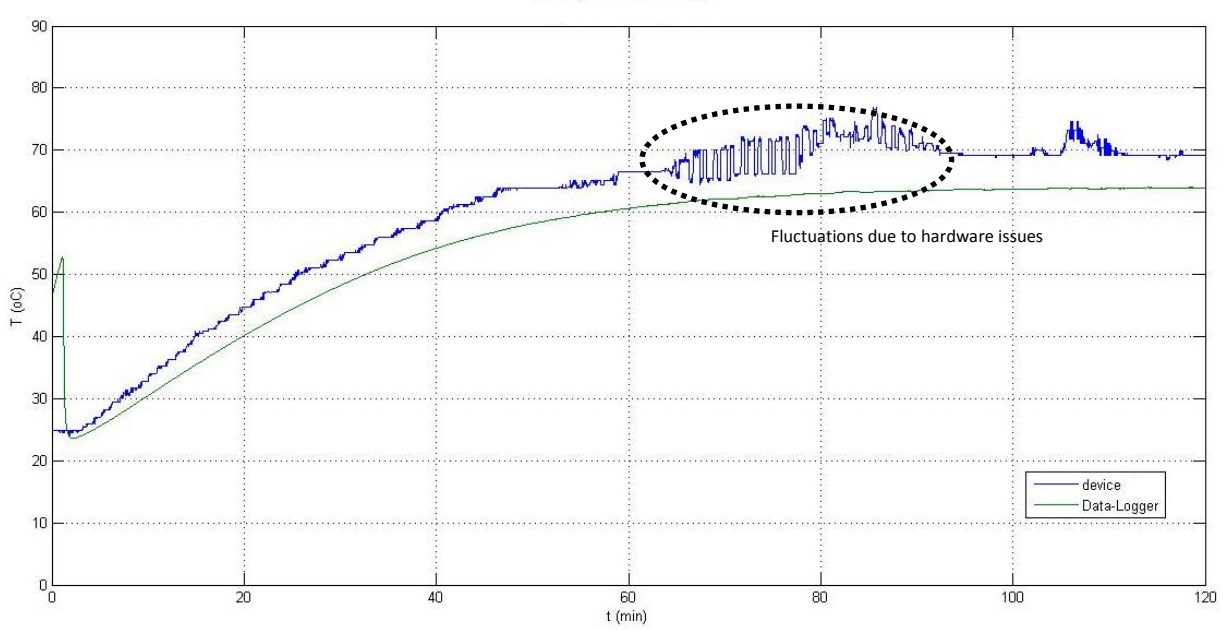

Figure 39: System's Transient Response in Exposure to De-ionized Water at 80^{o}C, Second Trial

Another test was conducted to investigate the steady state response of the system when operating in heated de-ionized water to eliminate the thermal mass effect of the sensing element in each device on the results. The test was conducted by placing the device in a flask containing de-ionized water preheated to temperature of 80^{o}C for duration of two hours while keeping the temperature steady for the entire duration. The

results obtained were compared to the readings obtained from the validation data-logger with its probe placed in the same environment. Figure 40 shows the readings obtained from the two system's steady state response. The results showed the agreement between the device and the validation data-logger in recording stable temperature. The results showed the same fluctuations in temperature observed by the device and the validating data-logger which was explained as the effect of the oven operation. The fluctuations were assumed as a result of the effect of the water vapor on the oven's controls. The readings from the two devices showed the temperature slightly varying around 70^{o}C but it didn't reach the maximum temperature of 80^{o}C. The results showed the higher sensitivity of the device to the changes in the temperature compared to the validation data-logger. The steady state testing in de-ionized water showed less sensitivity to the changes in temperature compared to the previous testing.

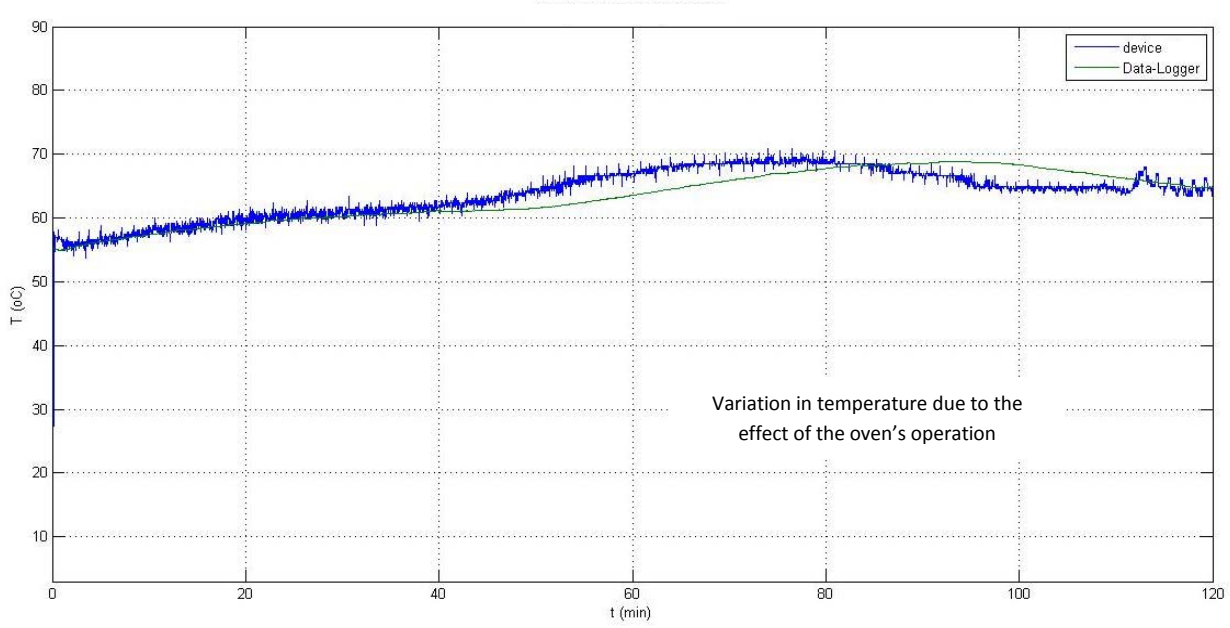

Figure 40: System's Steady State Response in Exposure to De-ionized Water at 80^{o}C

The third chemical exposure testing was conducted using isopropyl alcohol (IPA) at temperature up to 50^{o}C. The first test was conducted by placing the device along with the probe of the validation data-logger inside a flask filled with IPA. The flask containing the device and the probe was placed inside the oven at room temperature and gradually increasing the temperature up to 50^{o}C for duration of two hours. Figure 41 shows the transient response readings from the device along with the validation data-logger in exposure to IPA. The readings from the two systems gradually increased to reach 50^{o}C by the end of the two hours. The readings showed the faster response of the device as compared to the validation data-logger which was related to the difference in the thermal mass of the sensing element in each system as observed from the previous testing. The results showed wider fluctuations and higher sensitivity of the device to the surrounding changes and noises compared to the validation data-logger. The IPA testing showed higher sensitivity of the system than the sensitivity observed during the PG and de-ionized water testing.

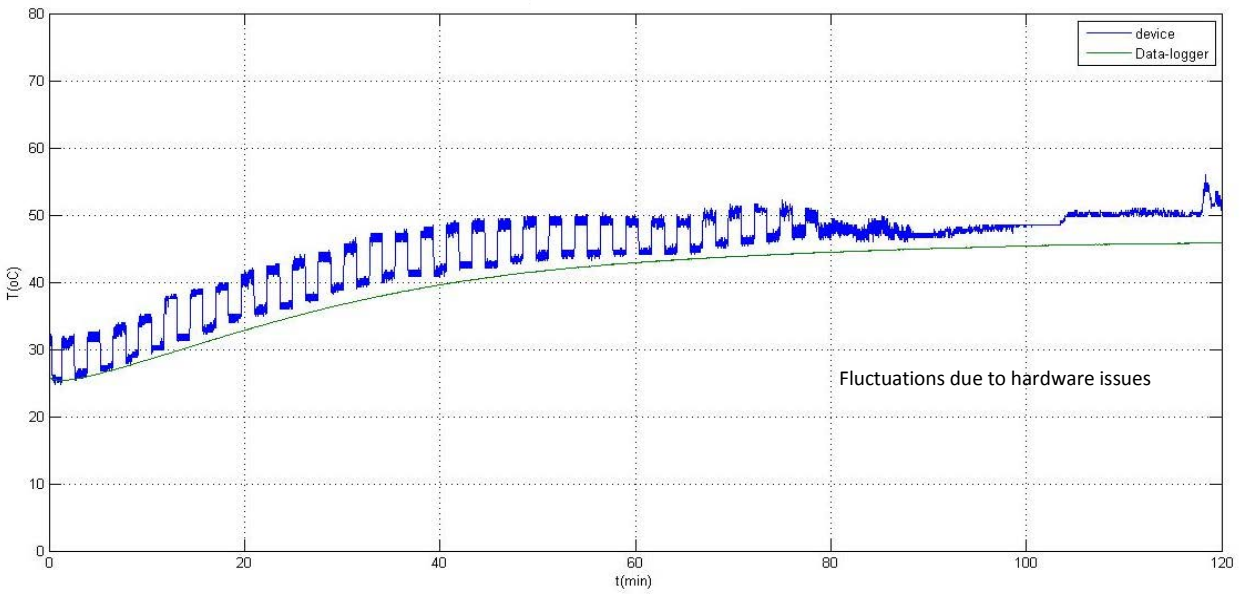

Figure 41: System's Transient Response in Exposure to IPA at 50^{o}C

Another test was conducted with the device immersed in IPA and gradually increasing the temperature up to 50^{o}C for duration of two hours. Figure 42 shows the transient response readings from the device along with the validation data-logger in exposure to IPA. The readings from the two systems gradually increased to reach 50^{o}C by the end of the two hours. The readings showed the faster response of the device compared to the validation data-logger which was related to the difference in the thermal mass of the sensing element in each system as observed from the previous testing. The results showed the higher sensitivity of the device to the surrounding changes and noises compared to the data-logger.

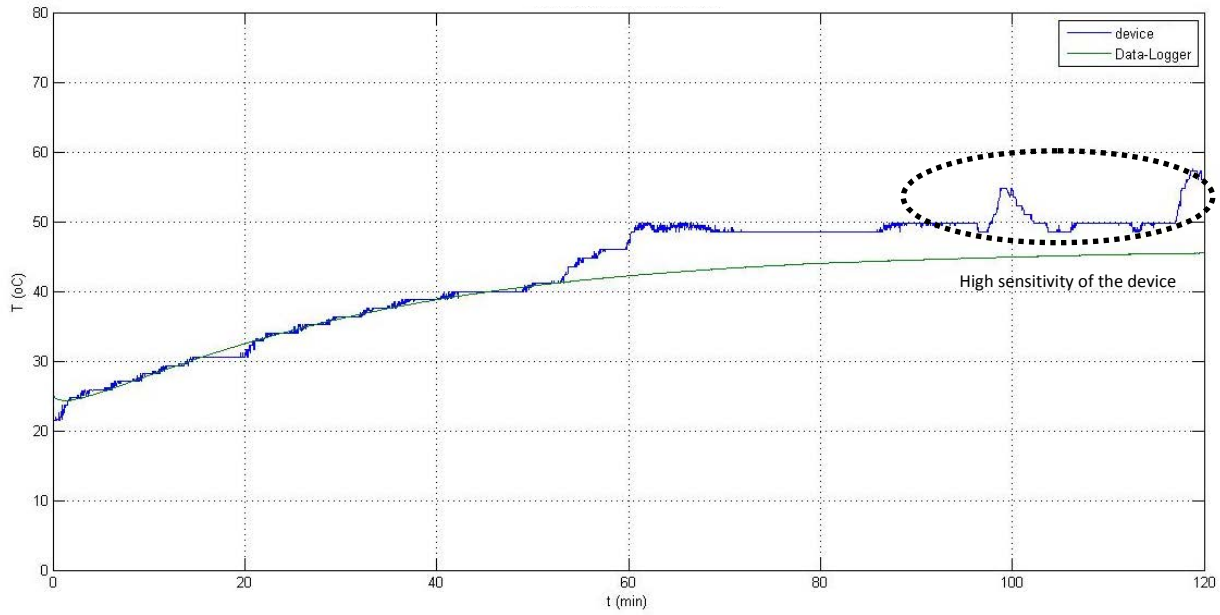

Figure 42: System's Transient Response in Exposure to IPA at 50^{o}C, Second Trial

A consistent trend was observed through all the transient response of the system with exposure to chemicals. The system output showed higher readings compared to the validation data-logger at the end of each cycle. The system's final temperature readings had a margin of about 5^{o}C higher than the temperature readings of the validation data-

logger, which was not observed in the steady state analysis of the system. Studying the response time of the two systems, the faster response of the device was suggested as one of the reason for the final temperature margin in which the device reached the temperature of the surrounding environment while the validation data-logger was in process of adjusting to the surrounding temperature. Another suggested explanation for the final temperature margin was related to the exposed leads connecting the RTD to the device which could be affected by the heated chemicals and led to the temperature shift observed in the system's output. The offset between the two systems could be as a result of the chemicals not reaching the thermal equilibrium, which varies the temperature of the liquid at different locations.

The unexpected fluctuations observed in few of the testing was studied and investigated. The noise added by the components in the system was suggested as a reason for these fluctuations. The noise added by the components could be a result of a manufacturing procedure which affected the connection between the components, the effect of the heated environment on the system or on certain components, the encapsulation failure in certain locations, or the exposed extension leads of the RTD. The fluctuations were observed in few devices in the early stages of the testing, and were improved in some of the latest testing. The fluctuations were reduced in the online testing by calibrating the devices before insertion in the target application.

3-2- Online Testing

The bench top testing was conducted to validate the operation concept and assumptions of the system which showed the feasibility of the system to be considered

for implementation in its target application. The system was tested on the hydration lines of a contact lens manufacturing process to validate its operation in its target environment and study the effect of the production line operation on the operation of the device. The online testing was conducted on three phases, in each phase the system's performance was evaluated and the required improvements were implemented to the system. The testing was conducted during the downtime for the production lines which enabled the implementation of the device to the hydration lines in different production lines. The results obtained were evaluated against the expected patterns of the temperature inside the towers based on their operation and the temperature of the dispensed liquids and chemicals.

3-2-1- PG line testing

The first online testing was conducted on the PG hydration line. The PG line consists of three towers, two of which uses PG, and the last tower uses de-ionized water. The temperature of the PG inside the two towers is about 87^{o}C and of the de-ionized water is about 40^{o}C, based on the temperature at the insertion head. Three devices were implemented to this line on the holder tray. Two devices were turned off when entered the hydration line and couldn't record any data, while one device was able to monitor the temperature inside the first tower. The operation of the devices inside the towers was studied and investigated. The reason for the shutdown of the devices in this testing procedure was related to the function of the components in the system, specially the tactile switch. The assembly mechanism of the components in the system was modified to ensure the proper operation of the components and electronics in the system in accordance with the operation conditions of the hydration process. Figure 43 shows the

readings obtained from the first tower. The temperature monitored showed room temperature for duration of about twelve minutes which reflected the duration between switching on the device and entering the first tower. The temperature gradually increased inside the tower to reach the maximum temperature of the dispensed liquid at the top of the tower.

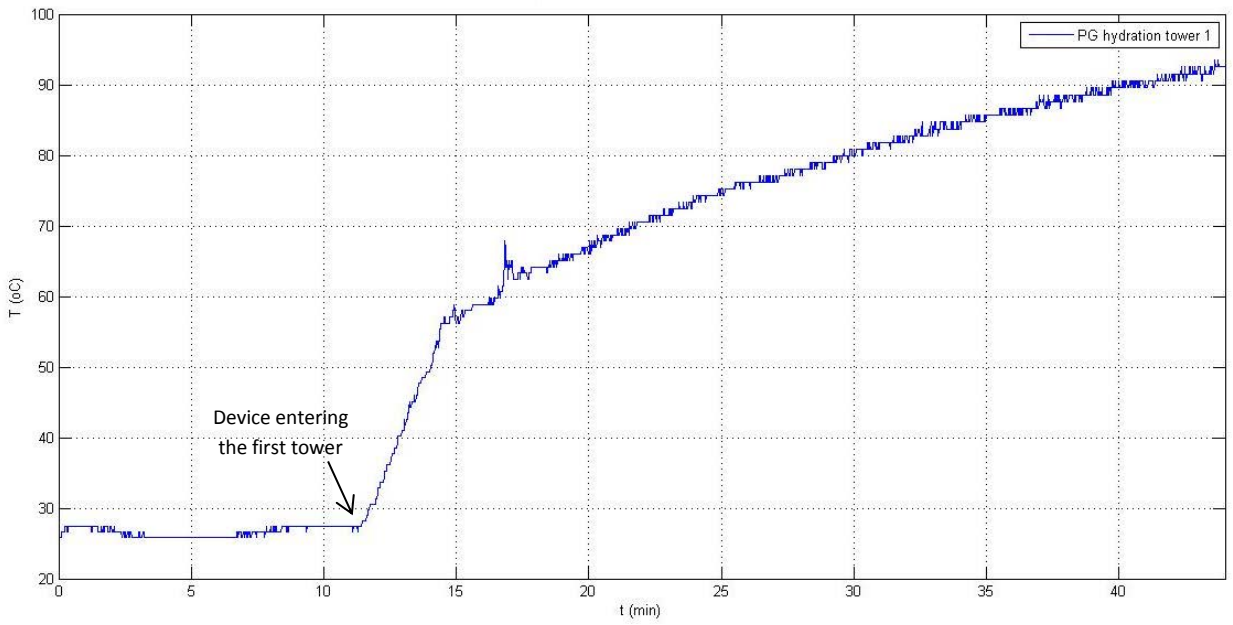

Figure 43: Temperature inside First Tower of PG Line

Further testing was conducted in the PG line after applying the improvements suggested from the previous testing. The device used was able to monitor the temperature inside the first two PG towers until it turned off after two hours. The line was shut down after seventy minutes due to an emergency shutdown in the production line. Figure 44 shows the readings obtained at the center of the PG line over duration of two hours. The readings showed room temperature for the first two minutes which represented the time before the device entered the first tower. The temperature gradually increased to reach the maximum temperature of PG in the first tower after

duration of forty five minutes which is longer than the typical time for one tower due to the maintenance stops. The transfer of the device from the first tower to the second tower showed a slight decrease in the temperature readings. As the device entered the second tower, the temperature increased back to the maximum temperature of PG. The production line was shut down after fifteen minutes which ceased the flow of PG in the hydration line. The readings showed a continuous decrease in temperature inside the hydration towers until the device was turned off after two hours.

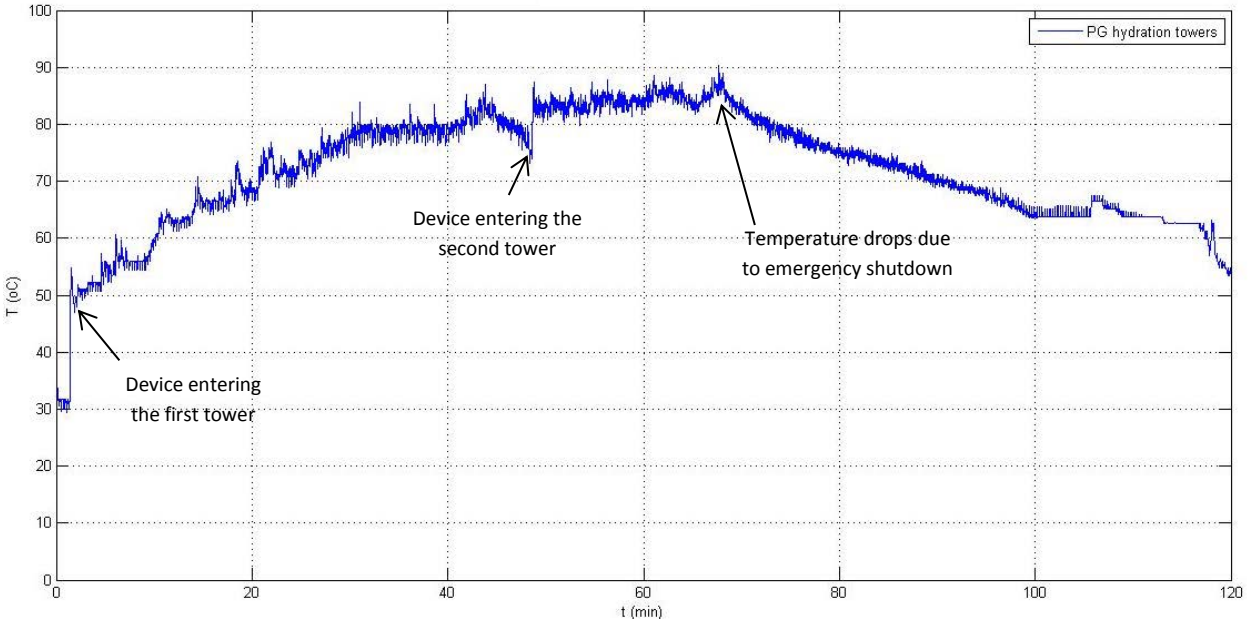

Figure 44: Temperature inside First Two Towers of PG Line

Another testing was conducted in the PG line to further investigate the operation of the system. Two devices were used which were placed at the center and the right side of one tray and were able to monitor the temperature for the entire duration of the hydration process including the two PG towers and the de-ionized water tower. The line was delayed due to some maintenance stops in the production line which increased the total duration of the hydration process to about one hour and forty minutes. Figure 45

shows the locations of the devices on the holder tray. Figure 46 shows the readings at the center of the PG line over its entire duration. The readings showed room temperature for the first couple minutes which represented the time before the device entered the first tower. The temperature immediately increased when the device entered the first tower. The temperature gradually increased to reach the maximum temperature of PG at the end of the first tower. The temperature slightly decreased as the device transferred from the first tower to the second tower. As the device entered the second tower, the temperature gradually increased back to the maximum temperature of PG in the second tower which is 89^{o}C. The temperature decreased as the device entered the third tower after around fifty minutes to reach the temperature of the de-ionized water which was dispensed at 47^{o}C. The de-ionized water is used to cool down the products before leaving the hydration process. The temperature dropped inside the third tower lower than 47^{o}C for a short duration which could be as a result of the tower operation. The readings obtained at the center of the PG line agreed with the readings obtained from the previous testing at the center of the PG line.

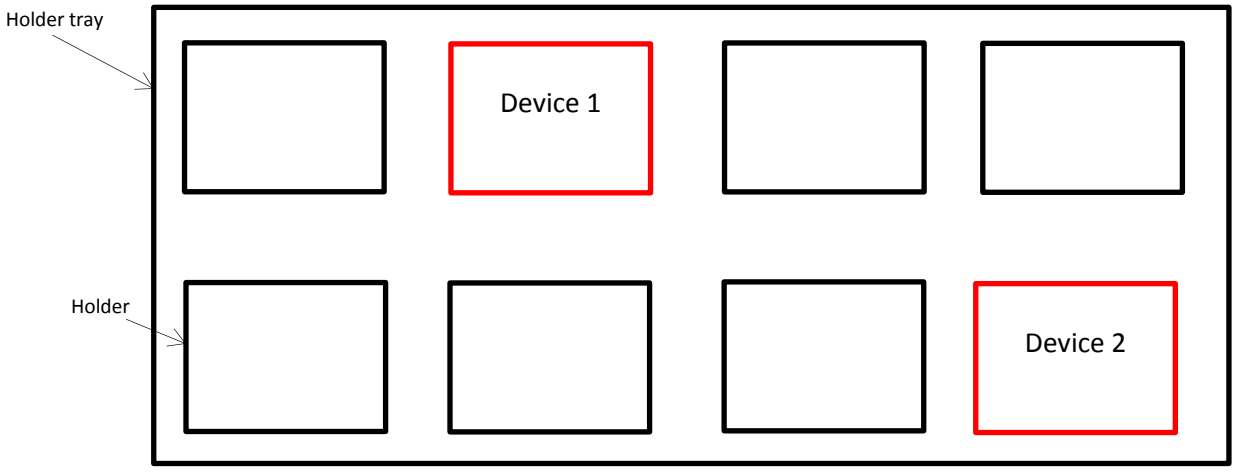

Figure 45: Devices Locations inside PG Line

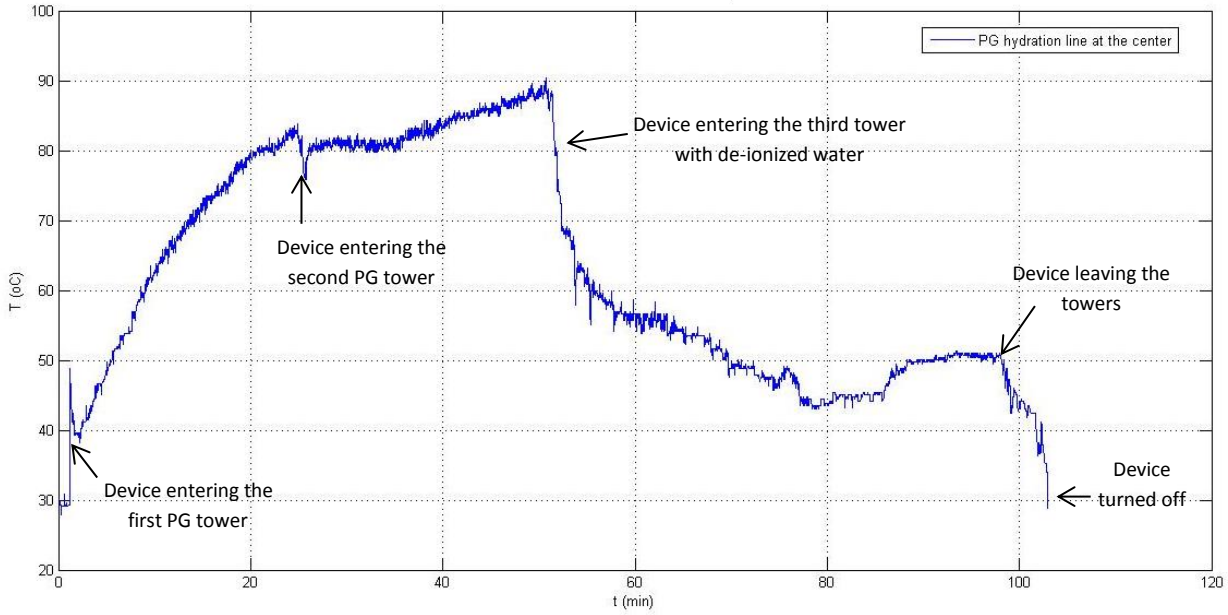

Figure 46: Temperature at Center of PG Line

Figure 47 shows the readings at the right side of the PG line over its entire duration. The readings showed room temperature for the first couple minutes which represented the time before the device entered the first tower. As the device entered the first tower, the temperature gradually increased to reach the maximum temperature of PG at the end of the first tower. As the device transferred from the first tower to the second tower, the temperature readings did not show significant change. As the device entered the second tower, the temperature gradually increased back to temperature 87^{o}C which is slightly less than the maximum temperature of PG in the second tower. The temperature decreased as the device entered the third tower after around fifty minutes to reach the temperature of the de-ionized water which was dispensed at 47^{o}C. The temperature at the center of the tower had a higher response time and higher values than the temperature at the sides of the tower due to the heat discharge at the sides of the tower. Figure 48 shows the comparison between the readings obtained at the center

of the hydration towers and the readings obtained at the right side of the towers which reflected the difference in temperature between different locations inside the tower.

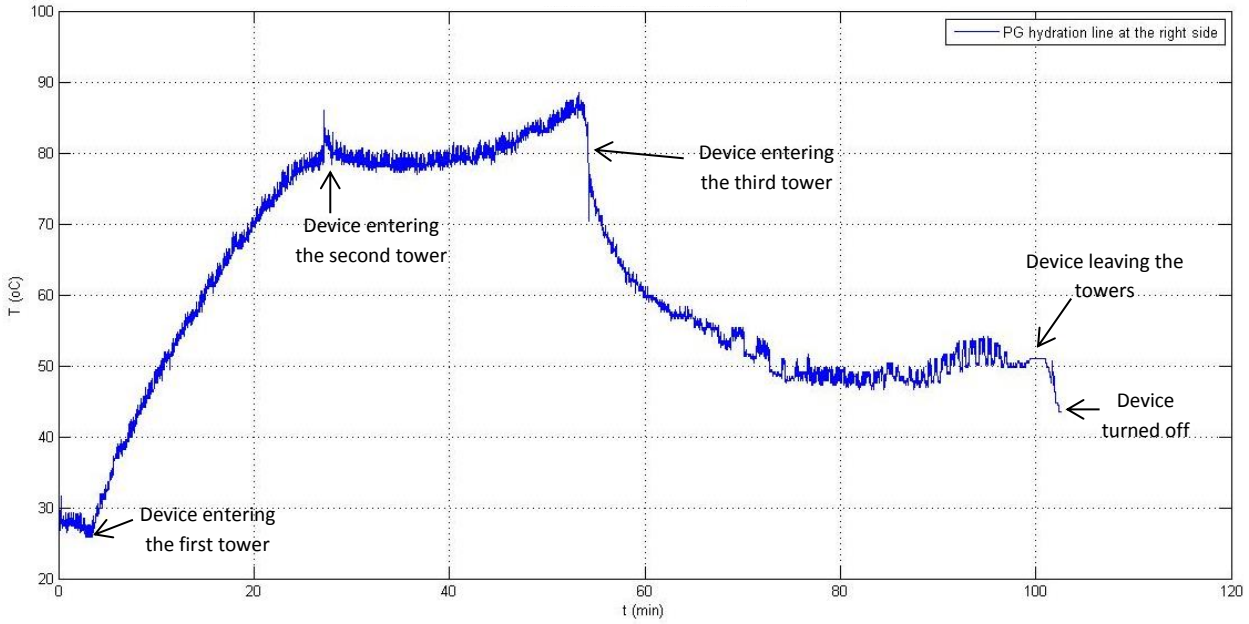

Figure 47: Temperature at Right Side of PG Line

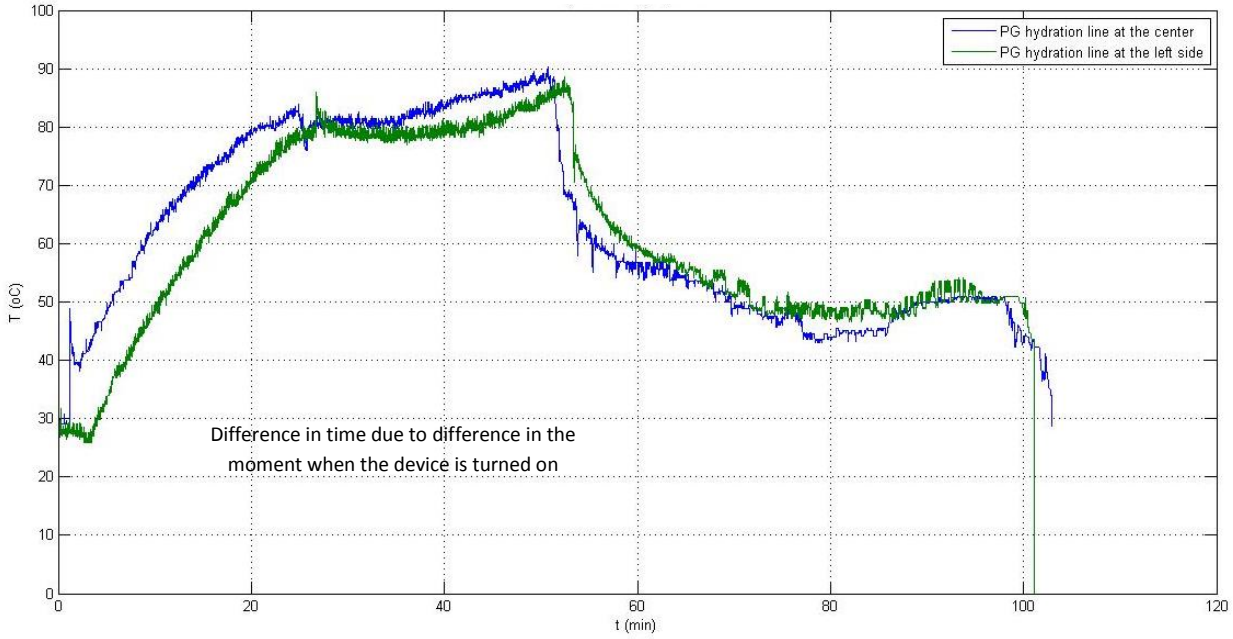

Figure 48: Comparison between Temperature at Center and Right Side of PG Line

3-2-2- IPA line testing

The second online testing was conducted on the IPA hydration line. The IPA line consists of three towers, two of which uses IPA, and the last tower uses de-ionized water. The temperature of the IPA inside the two towers is around 60^{o}C and the de-ionized water is around 40^{o}C, based on the temperature at the insertion head. Four devices were implemented to this line at different locations on the holder tray. Two devices were placed at the center and the right side of one tray, while the other two were placed in a different tray at the same locations. Figure 49 shows the locations of the devices on each holder tray. Two devices were switched off after a short period inside the tower and couldn't record any significant data, while two devices were able to monitor the temperature inside the first tower and were switched off after the first tower. The operation of the devices inside the towers was studied and investigated to identify the reasons for the unexpected stoppage of the device. The reason for the shutdown of the devices was suggested as a response to the failure of the encapsulation which led to the leakage of the liquid to the electronics in the system. Voids were observed in the encapsulation of all the failed devices, which was assumed to occur due to the nature of the operation inside the hydration towers or the surrounding environment effects. Figure 50 shows the encapsulation failure of the device from the IPA line. The packaging mechanism of the system was modified to ensure the proper encapsulation of all the components and electronics in the system.

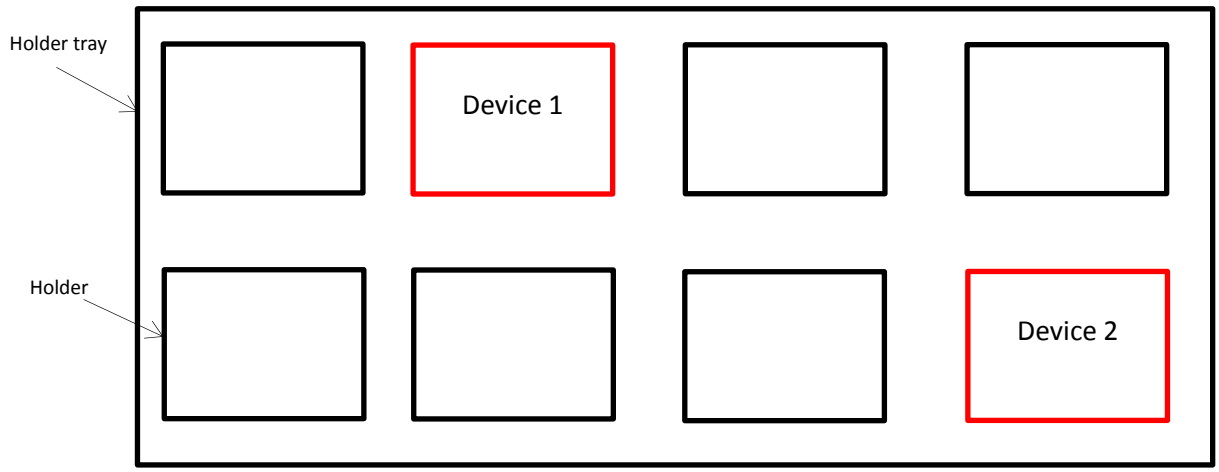

Figure 49: Devices Locations inside IPA Line

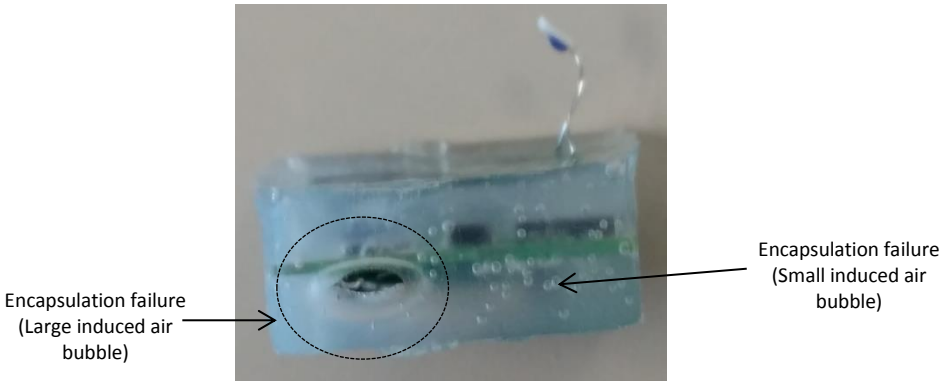

Figure 50: Encapsulation Failure

Figure 51 shows the readings obtained at the center of the first tower. The monitored temperature showed room temperature for duration of about four minutes which reflected the duration between switching on the device and entering the first tower. The temperature immediately increased to 42^{o}C when the device entered the tower and gradually increased to reach the maximum temperature 47^{o}C at the top of the tower after duration of about thirty minutes.

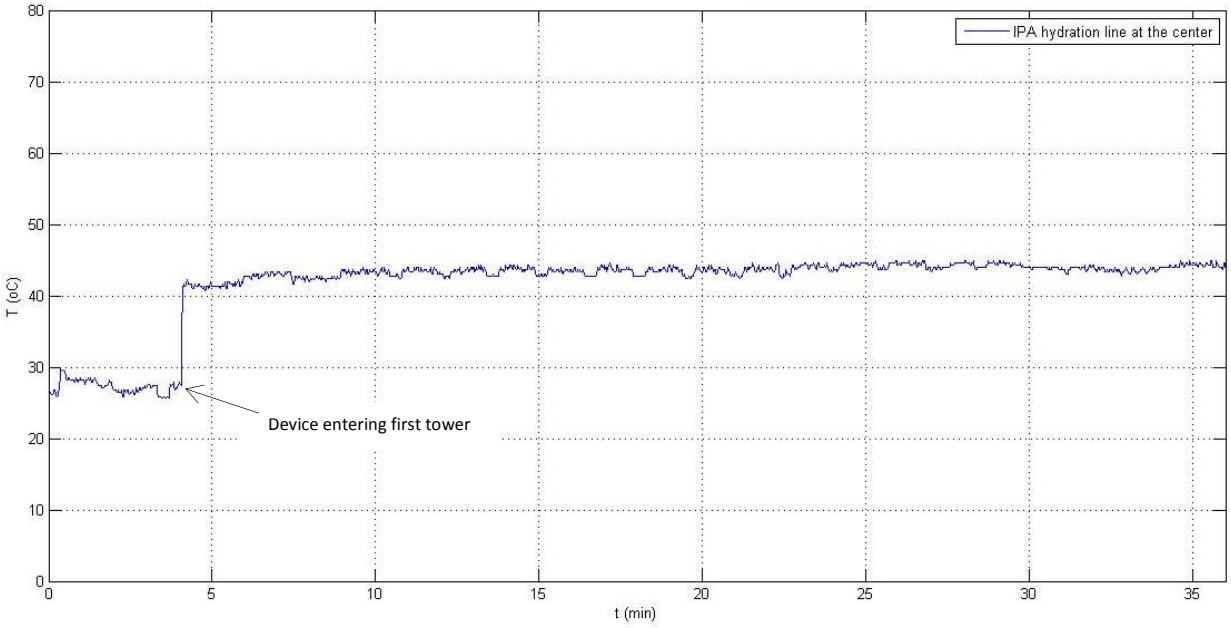

Figure 51: Temperature at Center of IPA Line

Figure 52 shows the readings obtained at the right side of the first tower. The monitored temperature showed room temperature for duration of about four minutes which reflected the duration between switching on the device and entering the first tower. The temperature immediately increased to 40^{o}C when the device entered the tower and gradually increased to reach the maximum temperature 42^{o}C at the top of the tower after duration of about thirty minutes. The readings obtained from the center of the hydration tower and the left side of the hydration tower showed the difference in temperature between different locations inside the towers. The temperature at the center of the tower had higher values than the temperature at the sides of the tower due to the heat discharge at the sides of the tower. Figure 53 shows the comparison between the readings obtained at the center of the hydration towers and the readings obtained at the right side of the towers.

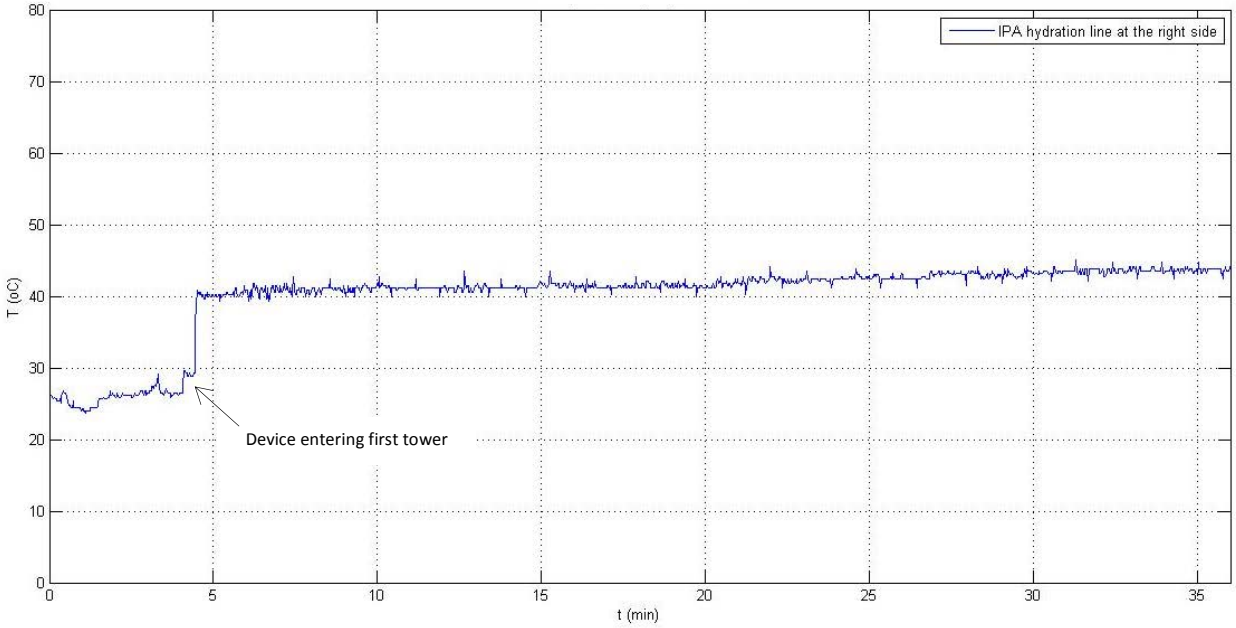

Figure 52: Temperature at Right Side of IPA Line

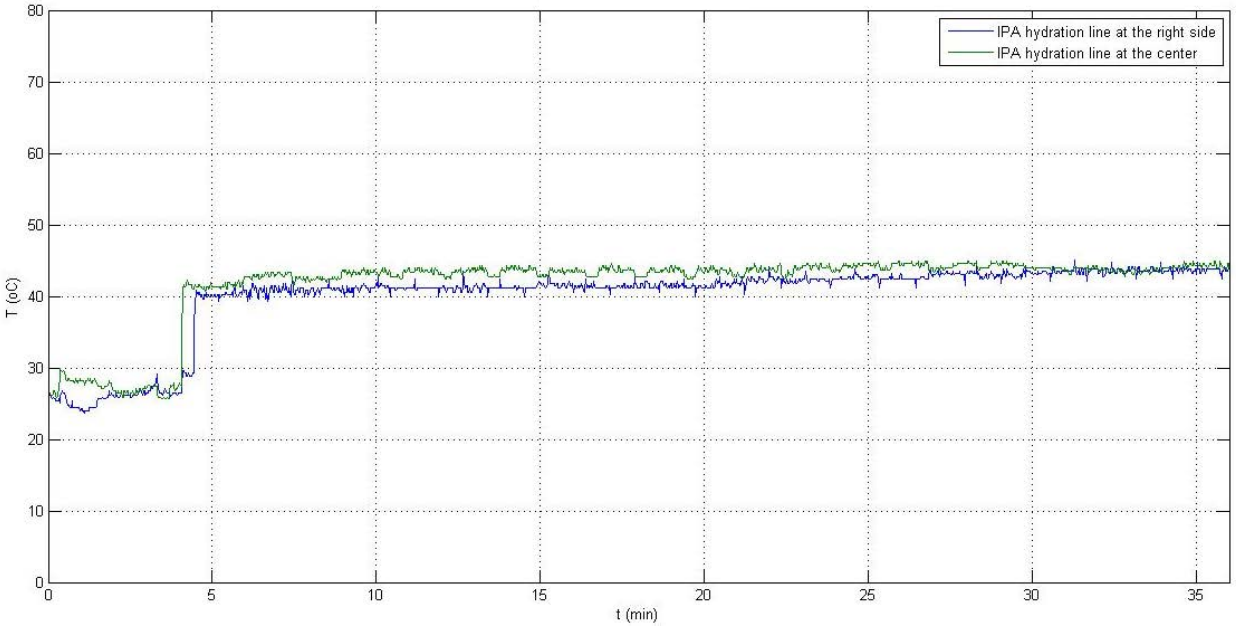

Figure 53: Comparison between Temperature at Center and Right Side of IPA Line

3-2-3- De-ionized water line testing

The third online testing was conducted on the de-ionized water hydration line. The de-ionized water line consists of one tower which has de-ionized water at temperature around 90^{o}C, based on the temperature at the insertion head. Two devices were placed at the center and the left side of one tray, while another two devices were placed at the same locations in a second tray which followed the first tray after a short period of couple minutes. Figure 54 shows the locations of the devices on the holder tray. The four devices were able to operate and record the temperature for the entire duration of the de-ionized water line. Figure 55 shows the readings collected at the center of the first tray. The monitored temperature showed room temperature for duration less than two minutes which reflected the duration between switching on the device and entering the first tower. The temperature immediately increased to 70^{o}C when the device entered the first tower. The temperature gradually increased inside the tower to reach 90^{o}C after duration of about two minutes. The temperature ranged between 90^{o}C and 100^{o}C for the entire duration of the hydration tower. The results obtained showed higher fluctuations when the temperature reaches its maximum value. The fluctuations observed can be related to the hardware issues faced by the system as observed from the bench-top testing.

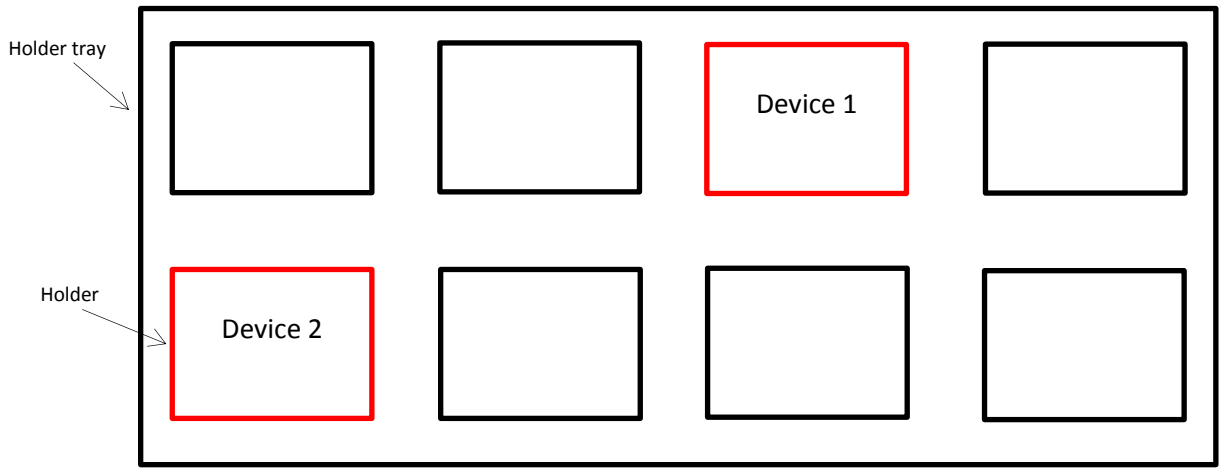

Figure 54: Devices Locations inside De-ionized Water Line

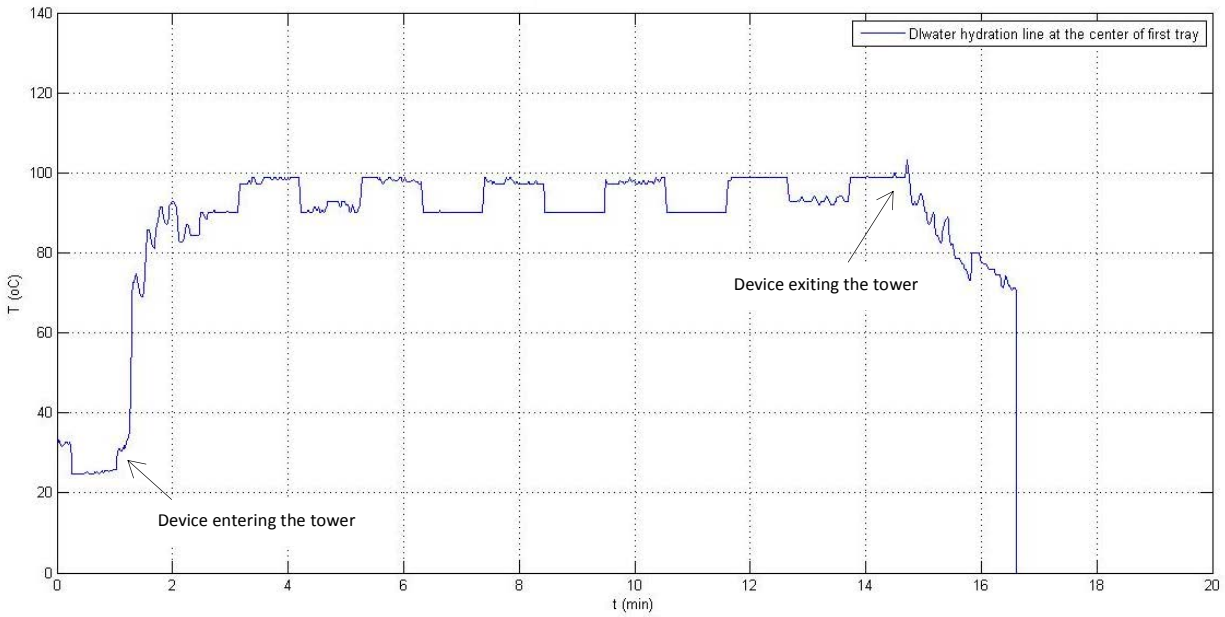

Figure 55: Temperature at Center of First Tray of De-ionized Water Line

Figure 56 shows the readings collected at the left side of the first tray. The monitored temperature showed room temperature for duration less than two minutes which reflected the duration between switching on the device and entering the first tower. The temperature immediately increased to 60^{o}C and then 70^{o}C when the device entered the first tower. The temperature gradually increased inside the tower to reach 90^{o}C after

duration of more than two minutes. The temperature slightly increased for the entire duration of the hydration tower to reach maximum temperature of 95^{o}C at the end of the line. The readings obtained at the center and the left side of the hydration tower showed the difference in temperature between different locations inside the towers. The temperature at the center of the tower had faster response and higher values than the temperature at the sides of the tower. The faster response and higher temperature values were related to the heat discharge at the sides of the tower. Figure 57 shows the comparison between the readings at the center and the left side of the first tray.

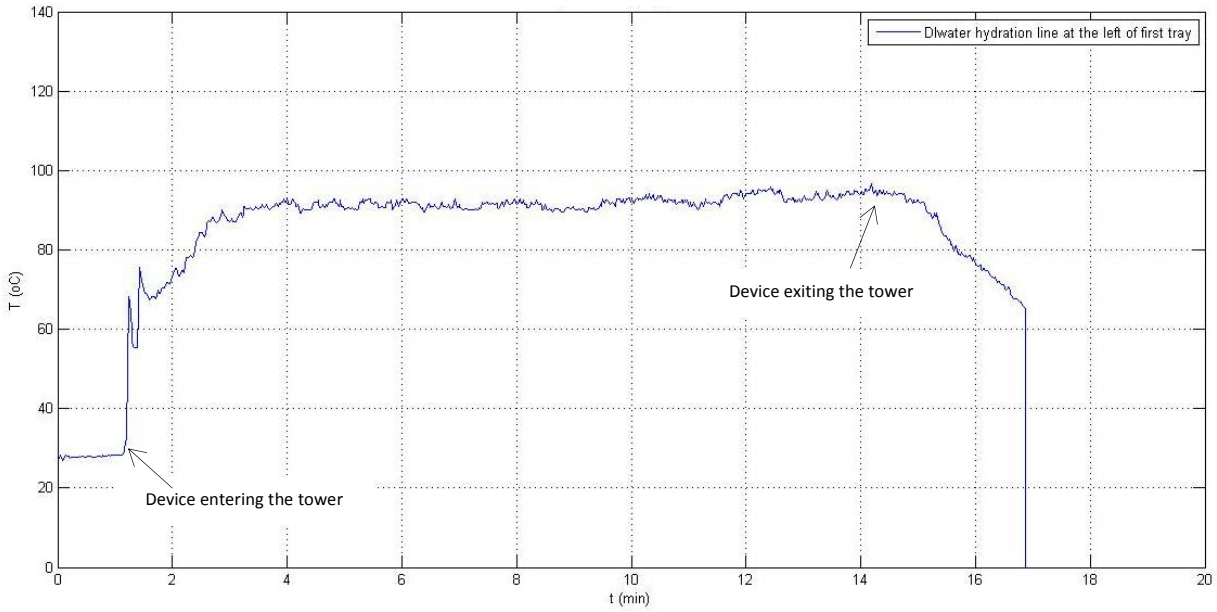

Figure 56: Temperature at Left Side of First Tray of De-ionized Water Line

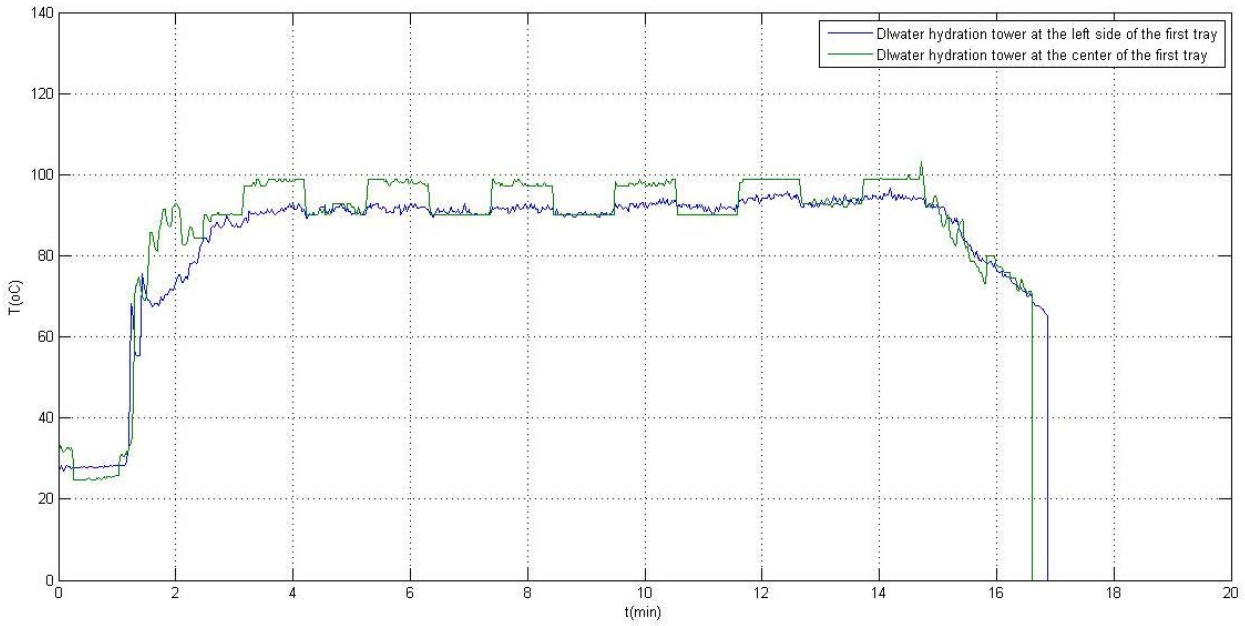

Figure 57: Temperature Comparison at Center and Left Side of First Tray of De-ionized Water Line

Figure 58 shows the readings collected at the center of the second tray. The monitored temperature showed room temperature for duration less than two minutes which reflected the duration between switching on the device and entering the first tower. The temperature immediately increased to 70^{o}C when the device entered the first tower. The temperature gradually increased inside the tower to reach 90^{o}C for the entire duration of the hydration tower. Figure 59 shows the readings collected at the left side of the first tray. The monitored temperature showed room temperature for duration less than two minutes which reflected the duration between switching on the device and entering the first tower. The temperature gradually increased inside the tower to reach 90^{o}C for the entire duration of the hydration tower. The readings obtained from the center of the hydration tower and the left side of the hydration tower showed the difference in temperature between different locations inside the towers. The temperature at the

center of the tower had faster transient response as compared to the transient response at the sides of the tower due to the heat discharge at the sides of the tower. Figure 60 shows the comparison between the readings at the center and the left side of the second tray. The temperature obtained from the two different trays followed the same trend of temperature difference between different locations in one tray, but showed the different trends in temperature between different trays inside the tower. Figure 61 shows the comparison between the four temperature readings obtained from the two trays at the same locations.

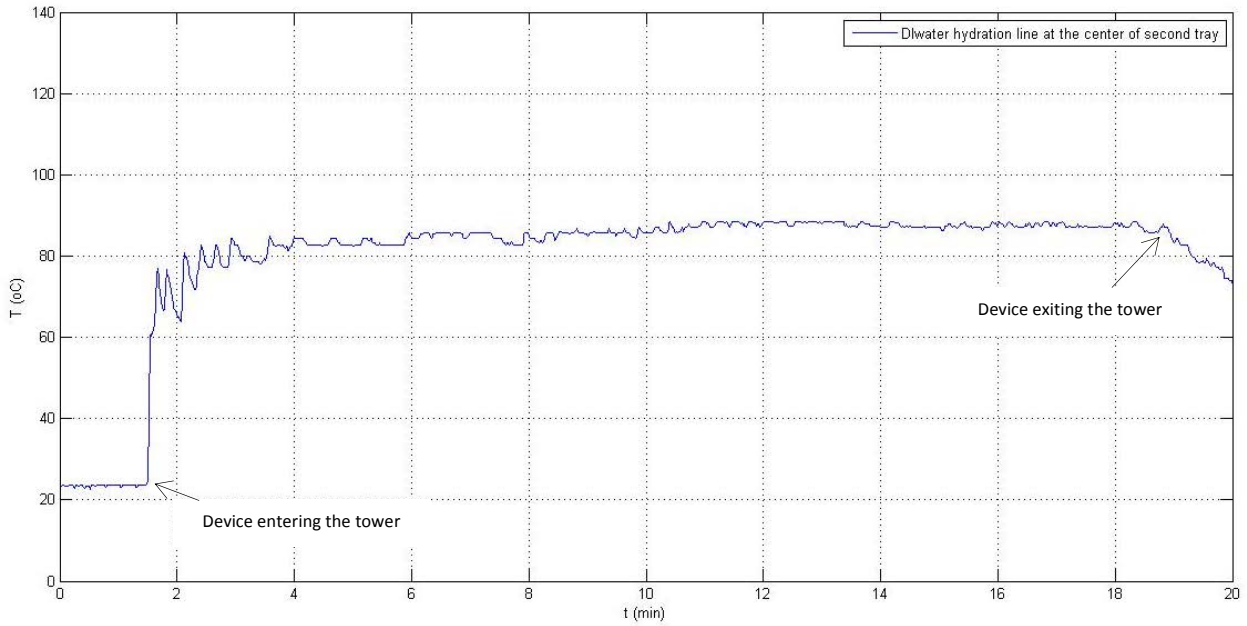

Figure 58: Temperature at Center of Second Tray of De-ionized Water Line

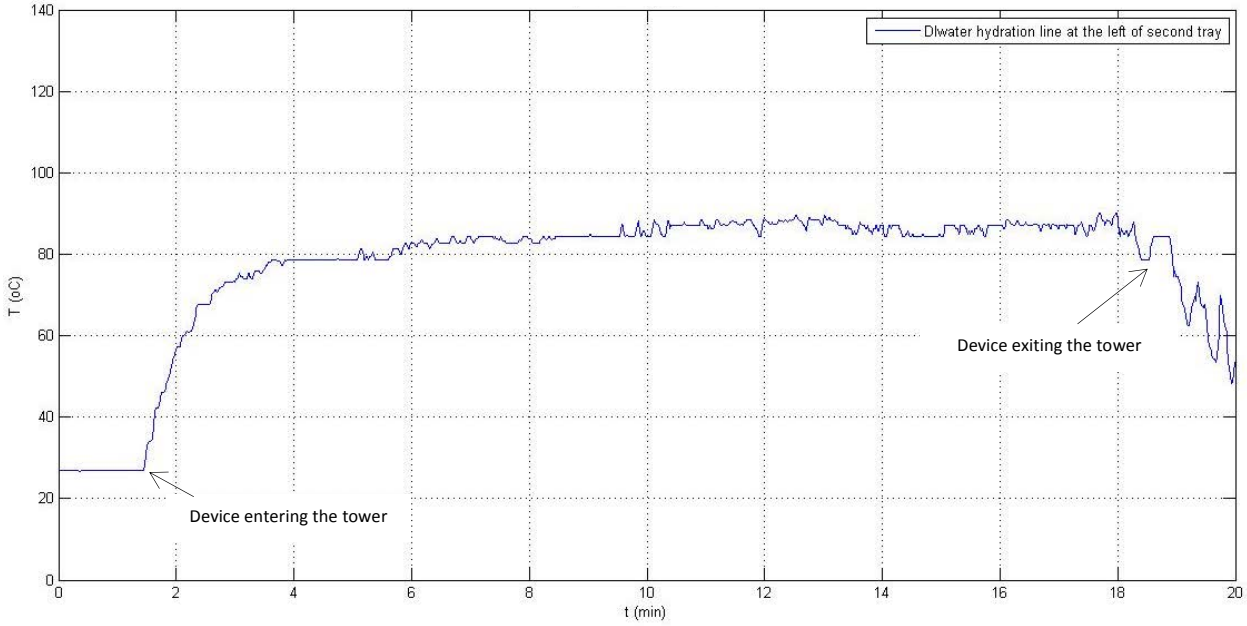

Figure 59: Temperature at Left Side of Second Tray of De-ionized Water Line

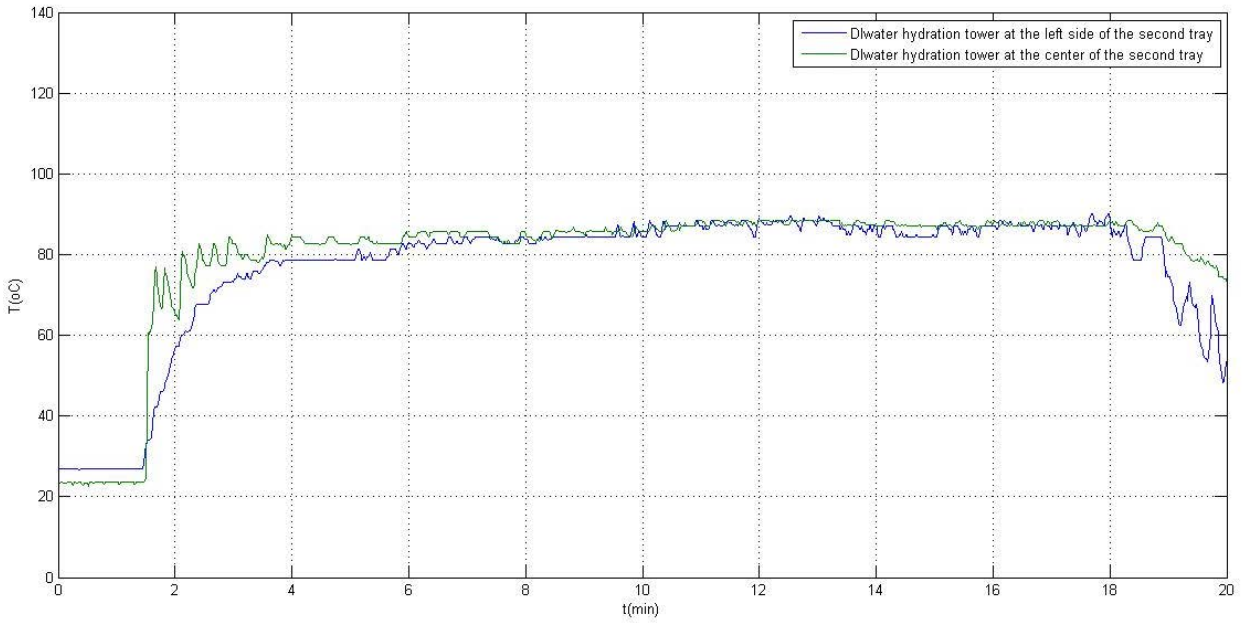

Figure 60: Temperature Comparison at Center and Left Side of Second Tray of De-ionized Water Line

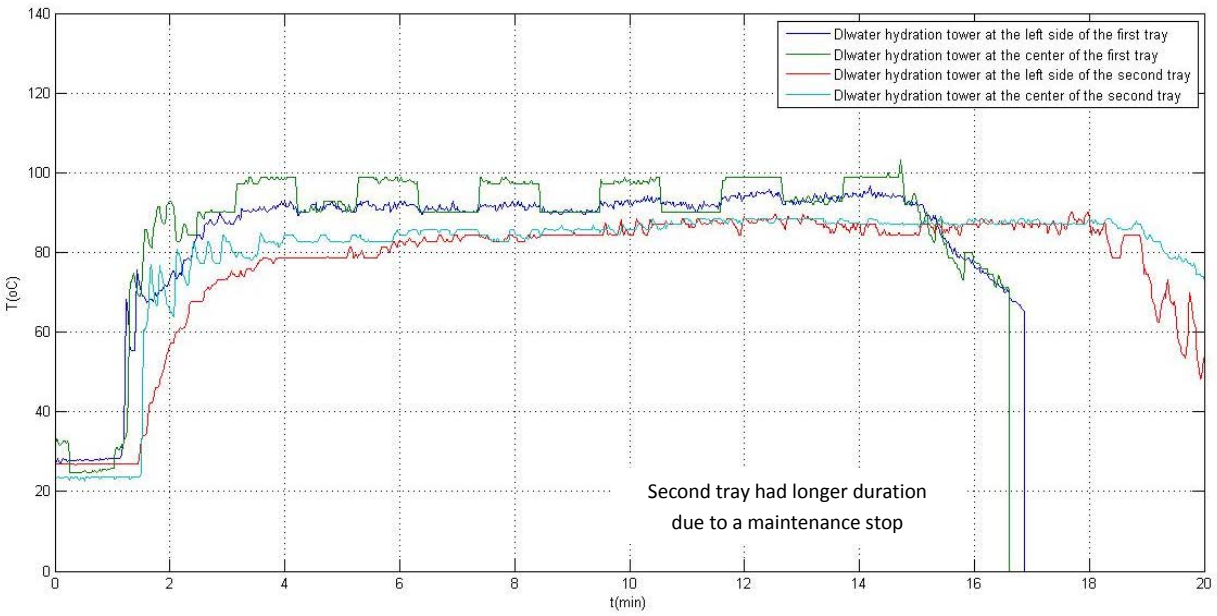

Figure 61: Temperature Comparison between Different Locations in De-ionized Water Line

Chapter 4: Conclusions and Recommendations

This chapter discusses the outcome of the system's design and testing, and the steps suggested for improved performance of the system. The conclusions obtained from the project are discussed, along with recommendations and suggested future work.

4-1- Conclusions

This work presented the development process of a small scale temperature data-logger that is economical and can operate when exposed to different chemicals and liquids. The data-logger requirements were developed based on a target testing application, the hydration process during the manufacturing of contact lenses. The developed system was tested using two testing procedures, bench top testing and online testing. The bench top testing setup was established to resemble the target application environment using a convection oven and set of chemicals. Different profiles for the system's performance were investigated for the success of the system in its intended use in the target application. The online testing was conducted inside different hydration lines through the contact lens production line. The system testing demonstrated the ability of the system to operate in its target application and meet most of the specified requirements.

The developed temperature data-logger met all the requirements indicated except the accuracy requirement. The system's requirements and their accomplishment are listed below:

1- Size: The overall size of the system after applying the packaging is 16.1x16.1x6mm. The size of the system stayed constant with a very slight variation over different devices due to designing and printing the PCB with the exact size and using molds for encapsulation with symmetrical shape and size. The PCB size was fixed at 16x16x0.5mm, while the mold had dimensions of 16.1x16.1x6mm, to ensure the proper encapsulation of all the components on the system including the battery.
2- Economical: The overall cost of the system was estimated to be $35. The prices of each component on the systems are MCU costs $3, memory costs $1.5, seven resistors cost $3.5, four diodes cost $0.8, transistor cost $0.5, switch costs $0.5, battery and holder cost $1.5, LED costs $0.2, RTD costs $10, PCB costs $10, and encapsulation for each device costs around $5. Table 11 summarizes the price of each component in the system and the total cost for producing a new device.
3- Temperature range: The system was able to monitor temperature from room temperature (23^{o}C) up to 100^{o}C during bench top testing. The system was able to record the entire temperature range inside the hydration towers.
4- Duration: The system was able to operate for the entire duration of two hours. The developed system was able to monitor the temperature during the entire hydration process including maintenance stops.

Table 11: Components Prices and Total Cost of System

Component	Quantity	Price (each) ($)	Price (total) ($)
MCU	1	3	3
Memory	1	1.5	1.5
Resistor	7	0.5	3.5
Diodes	4	0.2	0.8
Transistor	1	0.5	0.5
Switch	1	0.5	0.5
Battery and holder	1	1.5	1.5
LED	1	0.2	0.2
RTD	1	10	10
PCB	1	10	10
Encapsulation	1	5	5
Total			$36.5

5- Chemical exposure: The system was able to operate in exposure to the chemicals and liquids present inside the hydration towers (PG, IPA, and de-ionized water). The system had consistent and reliable operation during the bench top and online testing with exposure to these chemicals.

6- Power efficient: The developed system was able to operate reliably and independently using the battery power source during its intended duration. The data-logger was able to operate consistently and provide reliable readings for the entire duration of two hours.

7- Accuracy and data rate: The system was able to operate with the data rate of one reading per second with less than 1% error in the time representation. The steady state accuracy achieved by the current system ranged between ±0.5^{o}C at ambient conditions and ±0.8^{o}C at 100^{o}C, with disregard to the added noise and fluctuations. The accuracy required by the system which is ±0.1^{o}C could not be achieved.

The concept of developing a small scale autonomous temperature data-logger is demonstrated in this work. The system developed is a platform that can be used for monitoring different parameters for various applications. The development process illustrated in this work can be used as a base to develop the “best fit” monitoring system for different applications. The recommendations suggested for improving the operation and performance of the system can be used to develop an enhanced and reliable data-logger.

4-2- Recommendations and Future Work

Recommendations for improved performance of the system were suggested during the system design and testing to achieve the requirements of the system. The recommendations were implemented based on the priority of the requirement addressed. The higher priority recommendations were implemented during different phases of developing and testing the system while the less prioritized recommendations were discussed, studied, and suggested as a future work for the next phase of the project. The suggested recommendations were divided into two subsections, system enhancements and encapsulation improvement.

4-2-1- System enhancements

The system enhancements recommendations focused on improving the operation of the system in monitoring temperature readings. The first recommendation focused on improving the accuracy of the system by adding a signal amplification subsystem to the system design. Signal amplification can be used to improve the resolution of the ADC by adding an instrumentation amplifier to the system to amplify the output voltage from the Wheatstone bridge before entering the ADC in order to increase the voltage range equivalent to the temperature range required by the system. The amplifier should have a gain of 12 to reach the accuracy of ±0.1^{o}C required by the system, based on these calculations:

$$\Delta \text{ (required)} = 1.5\text{mV} = 0.1^{o}\text{C}$$

Based on the required accuracy and the ADC resolution, one degree change in temperature is presented by 15mV change in voltage, and the required temperature range of 77^{o}C is presented by around 1.2V change in voltage

Since temperature range before amplification is presented by 0.1V voltage change, the gain of the amplifier G = $\frac{1.2V}{0.1V} \approx 12$

Using the chosen amplifier gain, the voltage equivalent to 23^{o}C will be 0.03V * 12 = 0.36V, and the voltage equivalent to 100^{o}C will be 0.12V * 12 = 1.44V. The ADC used by the microcontroller has a 1.5V reference voltage, limiting the maximum input voltage to the ADC to this value. Since the voltage equivalent to 100^{o}C is very close to the maximum input voltage allowed by the ADC, the gain of the amplifier should be reduced to allow voltage range within the allowed voltage range of the ADC.

The gain of the amplifier is chosen to be 10. The amplifier with gain 10, will lead to voltage range from 0.3V to 1.2V, representing the required temperature range. The amplifier chosen reduces the accuracy of the system to ±0.15^{o}C, according to the following calculations:

Since 0.3 V represents temperature of 23^{o}C and 1.2V represents temperature of 100^{o}C, then the temperature range of 77^{o}C is represented by a voltage range of about 1V, and one degree change in temperature presented around 10mV change in voltage.

Accuracy obtained by the 1.5mV resolution of the ADC = $\frac{1.5mV * 1\ degC}{10mV}$ = 0.15^{o}C

The achieved accuracy after the amplification process is higher than the accuracy required by the system and can be obtained using the interpolation and filtering techniques. The most suitable available instrumentation amplifier with gain of 10 for the system is Maximum MAX4461. MAX4461 has size 3x3mm and requires supply voltage in the range of 2.85V and 5.25V [26].

Due to the size requirement and the power limitation of the system, adding a small scale amplifier to the system will be a challenge. The amplifier chosen for this application has a relatively big size compared to the total available space in the system. The amplifier requires power supply close to the maximum voltage supplied by the power supply of the system, affecting the ability of the system to operate for the entire duration. The amplification process was not implemented to the system due to the size constraints and the power limitations.

A proper and focused study needs to be conducted to choose an appropriate amplifier for the developed system. The amplifier should be smaller in size to be suitable for the required dimensions, and have lower power ratings. The system design needs to be modified to accommodate the amplifier into the current design and integrate its function to the system's operation. Further testing is required to investigate the effect of the input amplification on temperature accuracy.

Preliminary testing was conducted to investigate the effect of the signal amplification on the system's operation. Due to the size and power constraints, the testing was conducted using traditional wiring connections and through hole components to represent different subsystems of the system, and a bench-top power supply. The traditional wiring connections and the noisy components used increased the overall noise in the system. Figure 62 shows the functional blocks diagram illustrating the amplification block added to the system's design. Figure 63 shows the results obtained from the improved system's preliminary testing at room temperature with the results obtained from the validation data-logger in the same setting. The results showed the improved performance of the system with less sensitivity to change in temperature and less fluctuations in the system's output. The results obtained can be used as a base for further investigation of implementing the amplification technique.

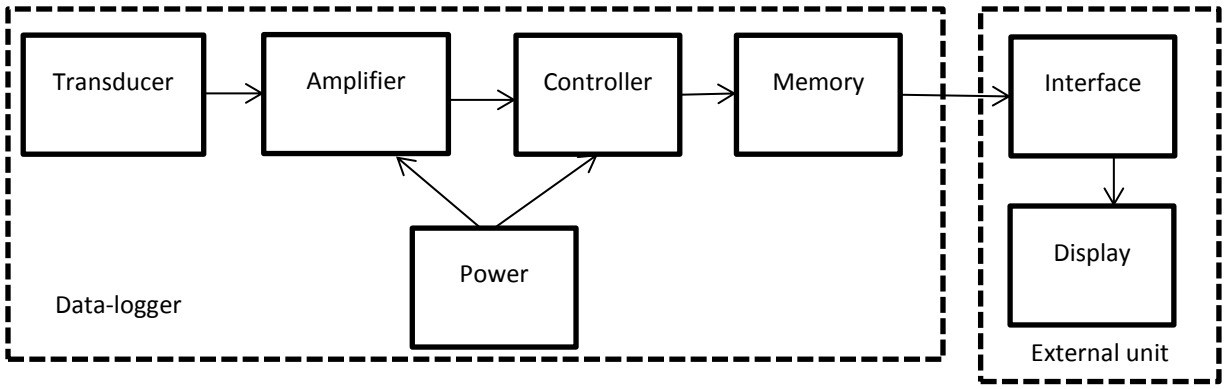

Figure 62: System's Functional Blocks with Amplification Subsystem

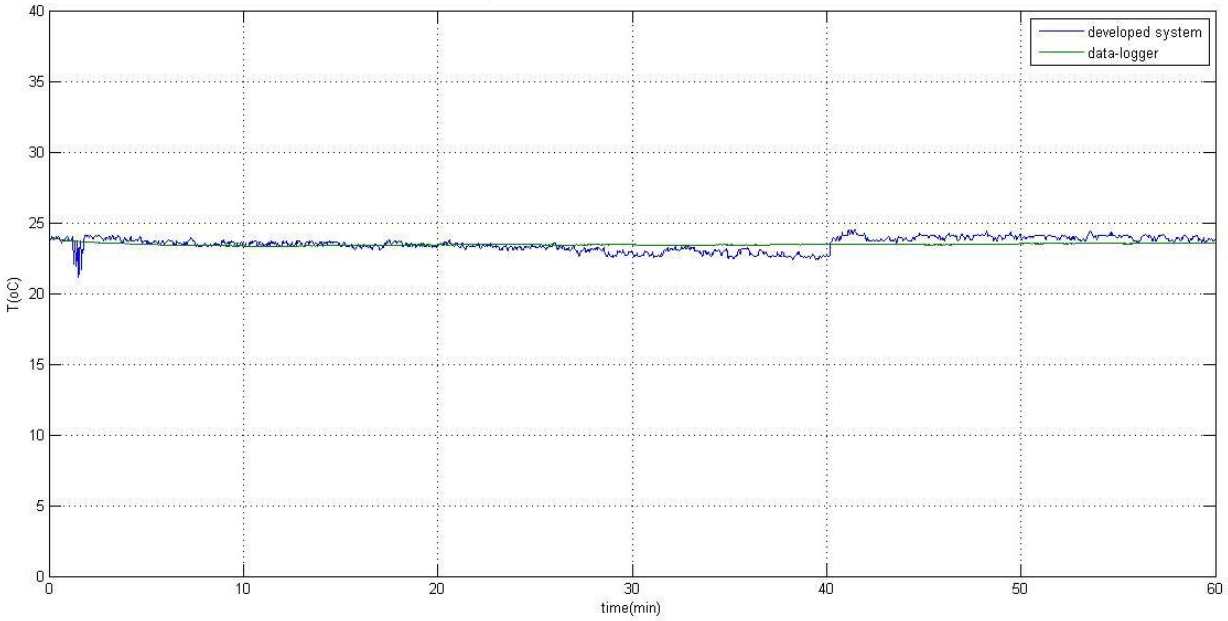

Figure 63: Amplification Circuit Preliminary Results

Other approaches can be implemented to improve the accuracy of the system which might violate other requirements of the system. The microcontroller used in the system can be changed into an advanced microcontroller with a higher bit ADC, to improve the resolution of the microcontroller and the sensitivity of the system. The microcontrollers with higher bit ADC studied during component selection were characterized by bigger size and higher power rating compared to the selected ones and violated the size and

power requirements of the system. The size and power requirements represented high priority requirements in this development process in comparison to the accuracy requirements. The higher bit ADC microcontroller was not implemented in this system but can be applied to different applications. Another approach relies on improved signal processing, oversampling in particular, to improve the system's output. The suggested approach is implemented by widening the window size of the averaging techniques to increase the samples used in each averaging step. Widening the window size will affect the data rate of the system by increasing the interval between consecutive readings, or might lead to a sampling rate slower than the rate of change in temperature of the surrounding environment, leading to misrepresentation of temperature in certain instances. The window size can be increased without violating the data rate of the system by increasing the oversampling, requiring a higher capacity memory chip. The higher capacity memory chip is characterized by less temperature rating, violating the temperature range requirement of the system. The approach of increased oversampling was not implemented in this system due to the violation of the temperature range requirement which represented a high priority requirement in this application.

The bench-top testing showed unexpected spikes and fluctuations in the temperature readings recorded by a few of the devices used, which were related to the hardware noise caused by the components and electronics used in the system. The hardware issues can be a reason of unmatched impedance between certain components, capacitor discharge, improper connections and integration between components, or noise added by the one or more components. A preliminary investigation was conducted to study the source of the irregularities in these few devices operation. The

components of the devices with irregularities were tested separately, and an initial observation related the irregularities to the RTD and its connections to the system, in particular the exposed RTD leads. Another observation of the trend of the irregularities, however, suggested the output fluctuation as a result of the communication cycles between the microcontroller and the memory chip. Further testing is required to focus on studying the reasons for the irregularities, and the effects of the hardware noise on the outcome of the system. Further testing should be conducted to focus on the reliability and the repeatability of the system. The reliability testing should investigate the performance of the system in the same testing profile multiple times to build confidence intervals for the temperature readings.

4-2-2- Encapsulation improvement

The encapsulation improvement recommendations focused on improving the performance of the system in monitoring temperature readings in the target application. The system packaging was able to protect the system and ensures its operation in the target environments during bench top testing, and most of the target application testing, but failed in providing the required protection in some of the target application testing. The packaging failure was related to the encapsulation process, which induced air bubbles into the packaging of the system in some cases. The process of encapsulating the system requires further improvements to ensure the absence of entrapped air bubbles inside the system.

Another issue affecting the current packaging of the system is the process of changing the battery. The current packaging material hinders the process of changing the battery in the system due to its consistent hard form, causing the system to be considered a

disposable device after one or two runs. The improvements in the packaging of the system should count for the battery changing process. The packaging should have mechanical flexibility to allow the changing of the battery without the need to completely remove the packaging and re-encapsulate the system. Economic analysis of the cost of the new replacement process for the non-rechargeable battery against the cost and the life cycle of the rechargeable one needs to be conducted.

References

1- Rinaldi, F. & Najafi, B. (2013). Temperature Measurement in WTE Boilers Using Suction Pyrometers. *Sensors*, *13*(11), 15633-15655.

2- Ivenso, I. & Wejinya, U. C. (2012, May). Automation of temperature system for formed meat products: A simulation approach. In *Cyber Technology in Automation, Control, and Intelligent Systems (CYBER), 2012 IEEE International Conference on* (pp. 86-91). IEEE.

3- Peters, L. S., Brackmann, E. J., & Park, W. T. (1987). Future Directions in Automation and Robotics for Manufacturing. *Aerospace and Electronic Systems Magazine, IEEE*, *2*(2), 12-16.

4- Agrawal, R. & Mohan, S. (2012, September). Complete industrial solution for automation in temperature and humidity monitoring using labview. In *Wireless and Optical Communications Networks (WOCN), 2012 Ninth International Conference on* (pp. 1-5). IEEE.

5- Wang, Y., Jia, Y., Chen, Q., & Wang, Y. (2008). A passive wireless temperature sensor for harsh environment applications. Sensors, 8(12), 7982-7995.

6- Knobloch, A. J., Ahmad, F. R., Sexton, D. W., & Vernooy, D. W. (2013). Remote Driven and Read MEMS Sensors for Harsh Environments. *Sensors*, *13*(10), 14175-14188.

7- Tarapata, G., Weremczuk, J., Jachowicz, R., Shan, X. C., & Shi, C. W. P. (2009). Construction of wireless sensor for harsh environment operation. *Procedia Chemistry*, *1*(1), 465-468.

8- Mouli, C. & Srinivasan, K. (2004, May). Intel automation and its role in process development and high volume manufacturing. In *Advanced Semiconductor Manufacturing, 2004. ASMC'04. IEEE Conference and Workshop* (pp. 313-320). IEEE.

9- Tortissier, G., Blanc, L., Tetelin, A., Lachaud, J. L., Benoit, M., Conédéra, V., & Rebière, D. (2011). Langasite based surface acoustic wave sensors for high temperature chemical detection in harsh environment: Design of the transducers and packaging. *Sensors and Actuators B: Chemical*, *156*(2), 510-516.

10- Boufouss, E. H., Francis, L. A., Kilchytska, V., Gérard, P., Simon, P., & Flandre, D. (2013). Ultra-Low Power High Temperature and Radiation Hard Complementary Metal-Oxide-Semiconductor (CMOS) Silicon-on-Insulator (SOI) Voltage Reference. *Sensors*, *13*(12), 17265-17280.

11- Tangirala, P., Heath, J. R., Radun, A., & Conners, T. (2008, October). A hand-held programmable-Logic-Device based temperature and relative-humidity sensor, processor and display system platform for automation and control of industry processes. In *Industry Applications Society Annual Meeting, 2008. IAS'08. IEEE* (pp. 1-8). IEEE.

12- Dalola, S., Ferrari, V., Guizzetti, M., Marioli, D., Sardini, E., Serpelloni, M., & Taroni, A. (2009). Autonomous sensor system with power harvesting for telemetric temperature measurements of pipes. *Instrumentation and Measurement, IEEE Transactions on*, *58*(5), 1471-1478.

13- Jingwei, Y., Rongxia, S., Na, J., Lei, L., & Zhangle, C. (2009, December). The Portable Temperature and Humidity Monitor Based on Intelligent Sensor. In

Information Science and Engineering (ICISE), 2009 1st International Conference on (pp. 5245-5247). IEEE.

14- Doebelin, E. O., (1990). Measurement Systems: Application and Design, fourth edition, Nueva York, EUA: McGraw-Hill.

15- Conversation with Olga Kostrubsky, Staff Process Engineer, VISTAKON®, a division of Johnson & Johnson Vision Care, Inc. September 2014.

16- Andersen, F. T., Bjerre, K., Christensen, S., Keene, D. S., Kindt-Larsen, T., Newton, T. P., & Widman, M. F. (1997). U.S. Patent No. 5,690,866. Washington, DC: U.S. Patent and Trademark Office.

17- Kindt-Larsen, T. (1992). U.S. Patent No. 5,080,839. Washington, DC: U.S. Patent and Trademark Office.

18- Mixed Signal Microcontroller, SLAS491I Application Note –AUGUST 2005, Texas Instruments, www.ti.com.

19- Criteria for Temperature Sensor Selection of T/C and RTD Sensor Types, A Comparison of Thermocouple and RTD Temperature Sensors Part 3 of 3, 8500-906-A10L000 – July 2011, Acromag, www.acromag.com.

20- Tiny Temperature Sensors for Remote Systems, SNIA009 Application note – 2011, Texas Instruments, www.ti.com

21- 700 series platinum RTDs temperature sensors, 009018-3-EN Datasheet – April 2010, Honeywell, www.honeywell.com

22- 256K I2C™ CMOS Serial EEPROM, DS20001203T Datasheet– 2013, Microchip, www.microchip.com.

23- Enhancing, A. D. C. resolution by oversampling, AVR121 Application Note, Rev. 8003A-AVR- September 2015, www. atmel. com.

24- Economy Gravity Convection Oven 3.5 cu.ft; 120VAC. (n.d.). Retrieved January, 2015, from http://www.coleparmer.com/Product/Economy_Gravity_Convection_Oven_3_5_cu_ft_120VAC/EW-52402-84#Specs

25- PT-104 Data Logger, MM000-2 Datasheet - 2012, Pico technology, www.picotech.com

26- SOT23, 3V/5V, Single-Supply, Rail-to-Rail Instrumentation Amplifiers, 19-2279 Datasheet – March 2006, Maxim Integrated Products, www.maximintegrated.com

```
#include <msp430.h>

void Data_TX (void);
char *MST_Data = (char*) 0x20A;
static volatile int I2C_State = 0;                    // State variable
static volatile char mem_highaddr = 0x00;            // high byte memory location
static volatile char mem_lowaddr = 0x00;             // low byte memory location
static volatile int  transmit = 0;                       // transmit byte counter

int main(void)
{      WDTCTL = WDTPW + WDTHOLD;                 // Stop WDT
   if (CALBC1_1MHZ==0xFF)                  // If calibration constants erased
            {
              while(1);                            // do not load, trap CPU!!
            }
  volatile int i, j;
  int index = 0;
  volatile int ram = 0x20A;           //RAM location for intermediate storage

 P1DIR = 0xCC;                        // port 1 pins as outputs
 P1OUT = 0xCC;
 P2OUT = 0;
 P2DIR = 0xFF;                        // port 2 pins as outputs
 TACCTL1 = 0;                         // CCR0 interrupt enabled

  ADC10CTL0 = ADC10SHT_1 + SREF_1 + REFON + REFOUT + ADC10ON + ADC10IE;
                                          // 1.5 Vref, ADC on
  ADC10DTC1 = 0x01;                      // 1 conversions
  ADC10AE0 |= 0x01;                      // P1.0 ADC10 option select
  DCOCTL = 0;                            // Select lowest DCOx and MODx settings
      BCSCTL1 = CALBC1_1MHZ;              // Set DCO
      DCOCTL = CALDCO_1MHZ;

      P1REN |= 0xC0;                                // P1.6 & P1.7 Pullups
      USICTL0 = USIPE6+USIPE7+USIMST+USISWRST;    // Port & USI mode setup
      USICTL1 = USII2C+USIIE;                    // Enable I2C mode & USI interrupt
      USICKCTL = USIDIV_3+USISSEL_2+USICKPL;
                                          // Setup USI clocks: SCL = SMCLK/8 (~125kHz)
      USICNT |= USIIFGCC;                          // Disable automatic clear control
      USICTL0 &= ~USISWRST;                       // Enable USI
      USICTL1 &= ~USIIFG;                         // Clear pending flag
      __enable_interrupt();
 // delay to indicate the system is on
      CCTL0 = CCIE;                               // CCR0 interrupt enabled
         TACTL = TASSEL_2 + MC_2 ;                    // SMCLK,
       __bis_SR_register(LPM0 + GIE);       // Enter LPM0 w/ interrupt
           TACTL = TASSEL_2 + MC_2 ;                    // SMCLK,
       __bis_SR_register(LPM0 + GIE);       // Enter LPM0 w/ interrupt
           TACTL = TASSEL_2 + MC_2 ;                    // SMCLK,
        __bis_SR_register(LPM0 + GIE);       // Enter LPM0 w/ interrupt
           TACTL = TASSEL_2 + MC_2 ;                    // SMCLK,
```

```
        __bis_SR_register(LPM0 + GIE);       // Enter LPM0 w/ interrupt
           TACTL = TASSEL_2 + MC_2 ;                  // SMCLK,
        __bis_SR_register(LPM0 + GIE);       // Enter LPM0 w/ interrupt
           TACTL = TASSEL_2 + MC_2 ;                  // SMCLK,
        __bis_SR_register(LPM0 + GIE);       // Enter LPM0 w/ interrupt

     P1OUT &= ~0x08;                         // P1.3 = 0

for(;;){
  if ( P1IN &= 0x20)
  {
        if (mem_highaddr == 0x7D )                    // If memory is full
                          {
         P1OUT = 0x00;                          // P1.3 = 0, turn off battery
                          }
    ADC10CTL0 &= ~ENC;
    while (ADC10CTL1 & BUSY);               // Wait if ADC10 core is active
   ADC10SA = ram;                          // Data buffer start
    ADC10CTL0 |= ENC + ADC10SC;             // Sampling and conversion start
    __bis_SR_register(CPUOFF + GIE);        // LPM0, ADC10_ISR will force exit
   index = index +1;
   if (index == 32)                   // 32 conversions , 64 bytes, 16 seconds
   {
         P1OUT |= 0x08;           // LED on: sequence start
         USICTL1 |= USIIFG;                 // Set flag and start communication
         LPM0;                              // CPU off, await USI interrupt
        __no_operation();
        index = 0;                          //reset counters
        transmit = 0;
        MST_Data = (char*) 0x20A;
                if ( mem_lowaddr == 0xC0)   // check for 256 bytes sent
            { mem_lowaddr = 0x00;
            mem_highaddr = mem_highaddr + 0x01;
            }
                else{
                mem_lowaddr = mem_lowaddr + 0x40;}   // increment address by 64

         P1OUT &= ~0x08;                         // P1.4 = 0
         ram= 0x20A;                            //reset RAM
         // delay to reach 0.5 sec between readings
         TACTL = TASSEL_2 + MC_2 ;                  // SMCLK,
      __bis_SR_register(LPM0 + GIE);       // Enter LPM0 w/ interrupt
         TACTL = TASSEL_2 + MC_2 ;                  // SMCLK,
      __bis_SR_register(LPM0 + GIE);       // Enter LPM0 w/ interrupt
         TACTL = TASSEL_2 + MC_2 ;                  // SMCLK,
      __bis_SR_register(LPM0 + GIE);       // Enter LPM0 w/ interrupt
         TACTL = TASSEL_2 + MC_2 ;                  // SMCLK,
      __bis_SR_register(LPM0 + GIE);       // Enter LPM0 w/ interrupt

   }
   else{
         // dealy to reach 0.5 sec between readings
         TACTL = TASSEL_2 + MC_2 ;                  // SMCLK,
   __bis_SR_register(LPM0 + GIE);       // Enter LPM0 w/ interrupt
          TACTL = TASSEL_2 + MC_2 ;                  // SMCLK,
```

```
   __bis_SR_register(LPM0 + GIE);       // Enter LPM0 w/ interrupt
          TACTL = TASSEL_2 + MC_2 ;                  // SMCLK,
   __bis_SR_register(LPM0 + GIE);       // Enter LPM0 w/ interrupt
          TACTL = TASSEL_2 + MC_2 ;                  // SMCLK,
   __bis_SR_register(LPM0 + GIE);       // Enter LPM0 w/ interrupt
         ram = ram + 2;
  }
  }
  else  {    //switch off sequence
  for (i = 0;i < 20;i++)
  {P1OUT ^= 0x08;
  for ( j = 0;j < 3000;j++); }
  P1OUT = 0x00;                          // P1.3 = 0, turn off battery
}
}
}
// Timer A0 interrupt service routine
#if defined(__TI_COMPILER_VERSION__) || defined(__IAR_SYSTEMS_ICC__)
#pragma vector=TIMERA0_VECTOR
__interrupt void Timer_A (void)
#elif defined(__GNUC__)
void __attribute__ ((interrupt(TIMERA0_VECTOR))) Timer_A (void)
#else
#error Compiler not supported!
#endif
{

      __bic_SR_register_on_exit(LPM0_bits);

}

// ADC10 interrupt service routine
#if defined(__TI_COMPILER_VERSION__) || defined(__IAR_SYSTEMS_ICC__)
#pragma vector=ADC10_VECTOR
__interrupt void ADC10_ISR(void)
#elif defined(__GNUC__)
void __attribute__ ((interrupt(ADC10_VECTOR))) ADC10_ISR (void)
#else
#error Compiler not supported!
#endif
{
  __bic_SR_register_on_exit(CPUOFF);        // Clear CPUOFF bit from 0(SR)
}
/*******************************************************
// USI interrupt service routine
*******************************************************/
#if defined(__TI_COMPILER_VERSION__) || defined(__IAR_SYSTEMS_ICC__)
#pragma vector = USI_VECTOR
__interrupt void USI_TXRX (void)
#elif defined(__GNUC__)
void __attribute__ ((interrupt(USI_VECTOR))) USI_TXRX (void)
#else
#error Compiler not supported!
#endif
{ static volatile char SLV_Addr = 0xA0;                  // slave Address
```

```
  switch(I2C_State)
    {
      case 0: // Generate Start Condition & send control byte to slave
              USISRL = 0x00;           // Generate Start Condition...
              USICTL0 |= USIGE+USIOE;
              USICTL0 &= ~USIGE;
              USISRL = SLV_Addr;       // ... and transmit address, R/W = 0
              USICNT = (USICNT & 0xE0) + 0x08; // Bit counter = 8, TX Address
              I2C_State = 1;           // Go to next state: receive address (N)Ack
              break;

      case 1: // Receive control byte Ack/Nack bit
              USICTL0 &= ~USIOE;       // SDA = input
              USICNT |= 0x01;          // Bit counter = 1, receive (N)Ack bit
              I2C_State = 2;           // Go to next state: check (N)Ack
              break;
      case 2: // Process control byte Ack/Nack & handle address high TX
                  USICTL0 |= USIOE;        // SDA = output
                  if (USISRL & 0x01)       // If Nack received...
                  { // Send stop...
                    USISRL = 0x00;
                    USICNT |=  0x01;       // Bit counter = 1, SCL high, SDA low
                    I2C_State = 10;        // Go to next state: generate Stop
                  }
                  else
                  { // Ack received, TX address high to slave...
                     USISRL = mem_highaddr;     // Load data byte
                     USICNT |=  0x08;       // Bit counter = 8, start TX
                     I2C_State = 3;         // Go to next state: receive (N)Ack
                   }
                  break;
      case 3: // Receive address high byte Ack/Nack bit
                    USICTL0 &= ~USIOE;       // SDA = input
                    USICNT |= 0x01;          // Bit counter = 1, receive (N)Ack bit
                    I2C_State = 4;           // Go to next state: check (N)Ack
                    break;
      case 4: // Process control byte Ack/Nack & handle address low TX
                        USICTL0 |= USIOE;        // SDA = output
                        if (USISRL & 0x01)       // If Nack received...
                        { // Send stop...
                          USISRL = 0x00;
                          USICNT |=  0x01;       // Bit counter = 1, SCL high, SDA low
                          I2C_State = 10;        // Go to next state: generate Stop
                        }
                        else
                        { // Ack received, TX address low to slave...
                           USISRL = mem_lowaddr;     // Load data byte
                           USICNT |=  0x08;       // Bit counter = 8, start TX
                           I2C_State = 5;         // Go to next state: receive (N)Ack
                         }
                        break;
      case 5: // Receive address low byte Ack/Nack bit
                          USICTL0 &= ~USIOE;       // SDA = input
                          USICNT |= 0x01;          // Bit counter = 1, receive (N)Ack
bit
```

```
                  I2C_State = 6;           // Go to next state: check (N)Ack
                  break;
case 6: // Process Address Ack/Nack & handle data TX
        USICTL0 |= USIOE;         // SDA = output
        if (USISRL & 0x01)        // If Nack received...
        { // Send stop...
          USISRL = 0x00;
          USICNT |=  0x01;        // Bit counter = 1, SCL high, SDA low
          I2C_State = 10;         // Go to next state: generate Stop
        }
        else
        { // Ack received, TX data to slave...
       USISRL = *MST_Data;     // Load data byte
          USICNT |=  0x08;        // Bit counter = 8, start TX
          transmit ++;
          MST_Data ++;
          I2C_State = 7;          // Go to next state: receive data (N)Ack
          }
        break;

case 7: // Receive Data Ack/Nack bit
//  USICNT &= ~USI16B;
  USICTL0 &= ~USIOE;        // SDA = input
        USICNT |= 0x01;           // Bit counter = 1, receive (N)Ack bit
        I2C_State = 8;            // Go to next state: check (N)Ack
        break;

case 8: // Process Data Ack/Nack & send Stop
        USICTL0 |= USIOE;
        if (USISRL & 0x01)        // If Nack received...
          // Send stop...
        {USISRL = 0x00;
        USICNT |=  0x01;          // Bit counter = 1, SCL high, SDA low
        I2C_State = 10;           // Go to next state: generate Stop
        } else                      // Ack received
  if (transmit == 64)           // 64 bytes transmitted
     // Send stop...
    {USISRL = 0x00;
     USICNT |=  0x01;          // Bit counter = 1, SCL high, SDA low
     I2C_State = 10;           // Go to next state: generate Stop
    }else
    {
         Data_TX ();         // send next byte

    }
        break;

case 10:// Generate Stop Condition
        USISRL = 0x0FF;           // USISRL = 1 to release SDA
        USICTL0 |= USIGE;         // Transparent latch enabled
        USICTL0 &= ~(USIGE+USIOE);// Latch/SDA output disabled
        I2C_State = 0;            // Reset state machine for next transmission
        LPM0_EXIT;                // Exit active for next transfer

        break;
```

```
}
  USICTL1 &= ~USIIFG;                       // Clear pending flag
}

 void Data_TX (void){
       USISRL = *MST_Data;      // Load data byte
       USICNT |=  0x08;        // Bit counter = 8, start TX
       transmit ++;
       MST_Data ++;
       I2C_State = 7;          // Go to next state: receive data (N)Ack
}
```

Appendix B: Validation Data-logger Calibration Certificate

pico Technology

James House,Colmworth Business Park,
Eaton Socon,St Neots,Cambs,PE19 8YP
Tel: 01480 396395 Fax: 01480 396296

Certificate of Calibration

Certificate number: 10973
Calibration Date: 20th February 2015
Model: USB PT104
Serial Number: CT599/112
Invoice/Report No: 92195/25150
Pico Calibration Reference: TH03 DSR54/194 channel 1
EL015 TEST0164
Wilkins Standard Resistor 100 ohm Type 5685A No.279379 Certificate No: 0344521
Ambient Temperature: 23.87°C.... (23°C±0.5°C)

Accreditations & Procedure

The following measurements were carried out using working standards which are periodically verified, and are traceable to National Standards where these exist.

Measurement Results

PT104 Channel	PT104 Resistence Reading (ohms)	Error (ohms)	Max Allowable Error (ohms)
1	99.9999	-0.0001	0.0075
2	99.9991	-0.0009	0.0075
3	100.0016	0.0016	0.0075
4	99.9990	-0.0010	0.0075

PT104 resistance readings are given as an average of 30 measurements.
The uncertainties of the PT104 under test includes those that are attributable to the standards used together with those contributed by personnel, procedures and environment and are estimated not to exceed +/- 3ppm.

Signature Deleted

Calibrated Signature:

Signature Deleted

Checked Signature:

Authorised Signature: Alan Tong ☐ Jane Percy ☐ Paul Knight ☑

VITA

Ahmed Tawfik is an Egyptian graduate student at University of North Florida. Ahmed graduated with Bachelor degree in Electrical and Electronics Engineering from Universiti Teknologi PETRONAS, Malaysia in 2013. He specialized in control and instrumentation with minor in business management. During summer and fall 2012, Ahmed joined University of North Florida, as a research intern. In January 2014, he joined University of North Florida as a graduate electrical engineering student with the expectation to graduate with a master's degree in electrical engineering on July 2015.

Publications:

- A. Gamal, A. ElSafty and G. Merckel, "New System of Structural Health Monitoring," Open Journal of Civil Engineering, Vol. 3 No. 1, 2013, pp. 19-28. doi: 10.4236/ojce.2013.31004.
- A. ElSafty, A. Gamal, P. Kreidl and G. Merckel, "Structural Health Monitoring: Alarming System" Wireless Sensor Network, Vol. 5 No. 5, 2013, pp. 105-115. doi: 10.4236/wsn.2013.55013.
- "Health Monitoring Systems for Infrastructure", EGYPTIAN-AMERICAN SCIENTISTS ASSOCIATION - Annual Conference, December 2012.